Project Title:	ECOPOTENTIAL: IMPROVING FUTURE ECOSYSTEM BENEFITS THROUGH EARTH OBSERVATIONS
Project number:	641762
Project Acronym:	ECOPOTENTIAL
Proposal full title:	IMPROVING FUTURE ECOSYSTEM BENEFITS THROUGH EARTH OBSERVATIONS
Type:	Research and innovation actions
Work program topics addressed:	SC5-16-2014: "Making Earth Observation and Monitoring Data usable for ecosystem modelling and services"

Deliverable D8.4: Assessment of future ecosystems and ecosystem services

Due date of deliverable:	30th September 2018
Actual submission date:	10th January 2019
Version:	v1
Main Authors:	Ariane Walz, Rebecca Noebel, Elisa Palazzi, Lenny Smith, Simona Imperio, Jonathan Giezendanner, Damino Pasetto, Kristina Steinmar, Claudia Carvalho-Santos, Georg Umgiesser, Arturas Razinkovas-Baziukas, Samuel Bosch, Bénédicte Madon, Alex Ziemba, Ghada El´Serafy, Ricardo Moreno, Domingo Alcaraz-Segura, Carl Beierkuhnlein, Samuel Hoffmann, Maik Billing, Kirsten Thonicke, Yoni Gavis, Guy Ziv, Brigitte Poulin, Gaetan Lefebvre, and more co-authors listed in individual studies.

This project has received funding from the *European Union's Horizon 2020 research and innovation programme* under grant agreement No 641762

Project ref. number	**641762**
Project title	**ECOPOTENTIAL: IMPROVING FUTURE ECOSYSTEM BENEFITS THROUGH EARTH OBSERVATIONS**

Deliverable title	Assessment of future ecosystems and ecosystem services
Deliverable number	D8.4
Deliverable version	V1
Contractual date of delivery	30th September 2018
Actual date of delivery	10th January 2019
Document status	Final
Document version	V1
Online access	http://www.ecopotential-project.eu/products/deliverables.html
Diffusion	Public
Nature of deliverable	Report
Workpackage	WP8
Partner responsible	UP
Author(s)	Ariane Walz, Rebecca Noebel, Elisa Palazzi, Lenny Smith, Simona Imperio, Jonathan Giezendanner, Damino Pasetto, Kristina Steinmar, Claudia Carvalho-Santos, Georg Umgiesser, Arturas Razinkovas-Baziukas, Samuel Bosch, Bénédicte Madon, Alex Ziemba, Ghada El´Serafy, Ricardo Moreno, Domingo Alcaraz-Segura, Carl Beierkuhnlein, Samuel Hoffmann, Maik Billing, Kirsten Thonicke, Yoni Gavis, Guy Ziv, Brigitte Poulin, Gaetan Lefebvre, and more co-authors listed in individual studies.
Editor	
Approved by	
EC Project Officer	Gaëlle Le Bouler

Abstract	Europe's marine and terrestrial ecosystems are currently facing a multitude of challenges. Besides intense land management and land use pressures, ecosystem persistence, its biodiversity and ecosystem services are threatened by the change in climatic conditions. Climate impact assessments based on ecosystem models can help to understand and anticipate possible dynamics and potentially profound changes in ecosystems. But even with advanced simulation options, model-based predictions of future ecosystem states are subject to a high level of uncertainty. Deliverable 8.4 therefore presents a selection of ECOPOTENTIAL future modelling studies at

This project has received funding from the *European Union's Horizon 2020 research and innovation programme* under grant agreement No 641762

	individual PA scale and at large-scale. On the basis of these studies we further analyse the handling of uncertainty and propose how systematic integration of uncertainty assessment could be promoted in the future.
Keywords	Future simulations, uncertainty quantification, protected areas, large-scale assessment

This project has received funding from the *European Union's Horizon 2020 research and innovation programme* under grant agreement No 641762

Co-funded by the European Union

Table of Contents

Co-funded by the European Union

List of Figures

List of Tables

Abbreviations

AGB	Above Ground Biomass
AUC	Area under the (ROC) curve
B-NL	Boreal needle-leaved
BBN	Bayesian Belief Network
BL-E	Broad-leaved Evergreen
BL-S	Broad-leaved Summergreen
CC	Climate Change
CDDA	Common Database on Designated Areas
CMIP5	Coupled Model Intercomparison Project Phase 5
CORDEX	Coordinated Regional Climate Downscaling Experiment
CSI	Cross-scale Interactions
ESS	Ecosystem Services
ESDAC	European Soil Data Centre
FAO	Food and Agriculture Organization of the United Nations
FRich	Functional Richness
FVC	Fractional Vegetation Cover
GCM	General Circulation Model
GLM	Generalized Linear Model
GPNP	Gran Paradiso National Park
GPP	Gross Primary Production
IPCC	Intergovernmental Panel on Climate Change
IUCN	International Union for Conservation of Nature
LL	Leaf Longevity
LPJmL	Lund-Potsdam-Jena managed Land
MaxEnt	Maximum Entropy
NDVI	Normalized Difference Vegetation Index
nMDS	Non-metric Multidimensional Scaling
NP	National Park
NPP	Netto Primary Production
OBIS	Ocean Biogeographic Information System
PA	Protected Area
PET	Potential Evapotranspiration
PFT	Plant Functional Type
RCM	Regional Climate Model
RCP	Representative Concentration Pathway
RL	Relative Likelihoods
ROC	Receiver operating curve
SAC	Species Areas of Conservation
SDM	Species distribution model
SLA	Specific Leaf Area
SPA	Special Protection Areas

SREX	Special Report on Managing the Risks of Extreme Events and Disasters to Advance Climate Change Adaptation
SST	Sea Surface Temperature
SWAT	Soil and Water Assessment Tool
T-NL	Temperate needle-leaved
WD	Wood Density

Co-funded by the European Union

1. Introduction

Europe's marine and terrestrial ecosystems are highly diverse, encompassing 11 marine and coastal, 3 freshwater as well as 48 terrestrial ecosystem types according to the latest pan-European ecosystem assessment (EEA 2015). The North-South gradient alone encompasses ecosystems from the subarctic tundra to the subtropical Mediterranean zone. Various mountain ranges add significant vertical gradients in many regions, creating a variety of micro-climates and diverse environmental conditions.

Ecosystems are currently facing a multitude of challenges. Besides the continued pressures of land management and land use/cover changes, a major risk for ecosystem persistence, its biodiversity and ecosystem services (ESS) is the change in climatic conditions. The ongoing climate change leads to lasting alterations of the natural system and is projected to continue in future decades depending on the scenarios of greenhouse gas emissions and land use change which are hypothesized (IPCC 2013). For Europe, climate change patterns will very likely involve regionally and seasonally distinct changes in precipitation and temperature distribution. Among the predicted impacts are the increase in severity and duration of heat waves and consecutive dry days, especially in the southern part of Europe (e.g. Kovats et al. 2014). General results of the 2012 IPCC SREX assessment report and subsequent studies (e.g. Ban et al., 2015, O'Gorman 2015; Fischer and Knutti 2015; Forzieri et al. 2016; Donat et al. 2016) additionally indicate further effects that likely involve an intensification of water-related climatic extremes. They include extensive droughts on the one side, leading to wildfires, an increase in water demand, stress in, among others, the agricultural sector and extreme precipitations and downpours, leading to floods and geo-hydrological risk. The different components of the hydrological cycle are strongly affected by global warming. Global temperature rise is occurring faster than during past climate changes on Earth and is accompanied by changes in precipitation (amount, intensity, distribution, besides the changes in dry and wet extremes mentioned above) and in the storage of water in the different reservoirs. Mountain glaciers, sea ice in the Arctic, and ice sheets are rapidly retreating. Snow cover is also decreasing in duration and extent. Melted ice from ice sheets and mountain glaciers contribute - together with the increase in ocean water volume in response to higher sea water temperatures - to sea level rise (Frank et al. 2015, IPCC 2012, IPCC 2013).

Numerical simulations of the future climate evolution and climate impact assessments based on ecosystem models can help to understand and anticipate possible dynamics and potentially profound changes in ecosystems. Ecosystem models are able to generate insights into possible future risks and provide practitioners and decision-makers with information on measures to better mitigate and adapt to climate introduced impacts (Bellard et al 2012). Simulations can be especially helpful to adjust knowledge-based strategies for conservation planning, particularly for protected area (PA) management decisions. By assessing future pressures and changes at PA level, additional insights can be gained in respect to distinctive responses of relatively undisturbed natural systems.

For ecosystem modelling, a wide range of different techniques is available. Empirical models, process based models (LPJmL-FIT), hybrid models and modelling chains are common options for simulating future climate change impacts on natural systems. This requires knowledge on the climatic drivers to be used as input to the ecosystem models. This input is generally provided by global or regional climate model simulations, eventually downscaled through different methods. General Circulation Models (GCMs) are the most advanced tools currently available to make projections of the future climate evolution at the global level, considering different emission and land use scenarios, and accounting for all different components of the climate systems, their interactions, and feedback mechanisms. Given their global scale and the limitation imposed by computational constraints, a scale mismatch exists between the spatial resolution which is currently achieved by GCM (even those at highest resolution, ~75 km) and the much smaller scales at which climate change impacts on hydrology and ecosystems occur. GCMs are often dynamically downscaled through Regional Climate Models (RCMs) to produce higher resolution estimates of climatic variables. RCMs are nested into GCMs, which provide the appropriate boundary conditions for the regional simulation. The latter, as a consequence, can be affected by the uncertainties coming from the large-scale simulation but, at the same time, could not exist without a "driving" global model simulation (or global reanalysis data) behind. Regional Climate Models can - if accurate - better reflect impacts of local topography or water bodies that influence

Co-funded by the European Union

convection patterns, cloud formation and pressure gradients (Gao et al. 2008). However, their spatial resolution can still be too coarse (from ~10 km to 40 km in hydrostatic models) to obtain data direct usable in hydrological or ecosystem models. A suitable meteo-climatic forcing can thus be obtained at the relevant scale by applying further statistical or stochastic downscaling to the output of RCMs (or, directly, to GCMs).

Future climate projections obtained with global or regional models are based on a set of internationally-agreed assumptions, called scenarios, on the future evolution of our society, in terms of greenhouse gas emissions, development of technologies, economic circumstances at both global and regional level, population growth, land use exploitation and changes and others, which will lead to a given atmospheric concentration of anthropogenic greenhouse gases in the atmosphere and their evolution during the 21st century and beyond. The latest set of scenarios used in the Fifth Assessment Report of the Intergovernmental Panel on Climate Change (AR5, IPCC 2013) are called “Representative Concentration Pathway” (RCP) scenarios and are grouped into four types: RCP2.6, RCP4.5, RCP6.0, RCP8.5, the number indicating the level of radiative forcing (in W/m2) reached by 2100. RCP 4.5 and RCP6.0 are the two intermediate “stabilization” pathways in which radiative forcing is stabilized at approximately 4.5 W/m2 and 6 W/m2 after 2100 (having reached a peak around mid-century); RCP2.6 is the lowest emission or “mitigation” scenario where radiative forcing peaks at approximately 3 W/m2 before 2100 and then declines; RCP8.5 is the highest emission scenario, also referred to as “business-as-usual” scenario for which radiative forcing reaches >8.5 W/m2 by 2100 and continues to rise for some amount of time.

Even with advanced simulation options, however, model-based predictions of future ecosystem states are subject to a high level of uncertainty. The uncertainty in future projections from climate models can be attributed to three main sources: 1) the internal model uncertainty, 2) the uncertainty in input data and 3) the scenario uncertainty (adapted from Hawkins & Sutton 2009). Internal model uncertainty accounts for the natural fluctuations that arise in the absence of any change in the radiative forcing of the planet and occurs on different time scales. The internal model uncertainty stems from the fact that models are always a simplification of the real world, and therefore are imperfect by construction. They are always based on a number of assumptions to describe and predict the observed processes based on empirical data. For instance, if population dynamics are found to depend strongly on fodder availability over winter, processes such as exchange with other populations of the same species to ensure genetic diversity, or the spread of disease are not reflected in the model, although we know they occur. These processes are driven, for instance, on a different time scale (genetic exchange) or by random processes. Uncertainties that can be attributed to the input data mainly relate to the potential mismatches between the modelled climate data and the locally observed or otherwise reconstructed reference data. The sensitivity towards this category of uncertainties increases especially for small scale ecosystem simulations with downscaled CMIP5-driven RCA4. The scenario uncertainty derives from the uncertainty of future demographic changes, economic development, land-use and technological changes, which, along with the environmental changes in the future climate itself, will determine future anthropogenic emissions of greenhouse gases and other pollutants. The relative importance of the scenario uncertainty grows over time within a climate simulation. The problem of exploring and quantifying uncertainty in climate model projections is partly addressed using a multi-member and/or multi-model ensemble approach complemented by the use of expert judgement to assess the plausible effect of model inadequacy (IPCC 2013). The consideration and handling of uncertainties have been further intensively described and discussed in D8.1 and D8.3. Despite great improvements in the reliability of climate models and downscaling methods over the last decades, the cascade of uncertainty for climate to eco-hydrological/impact models is still considerable and needs to be taken into account in a systematic way. Generated results of small scale assessments should thus be contextualized and further interpreted not only regarding the natural climate variabilities, the respective model limitations and the underlying scenario uncertainty but also the realities of the study area, e.g. local management practices and legislative realities. By taking into account the respective overall picture, future simulations are still able to provide meaningful insights into possible ecosystem responses and their spatial distribution. The consideration of uncertainties is also essential for an appropriate communication of study results and for their effective applicability by users.

The impacts of climate change on ecosystems are spatially distinct and exhibit different types and degrees as well as a multitude of different biological scales. From the biodiversity perspective, possible effects of climate change can operate at individual, population, species, community, ecosystem and biome scale (Bellard et al. 2012). Model approaches are therefore used to target a multitude of different ecological questions that also relate to different ecological scales.

Deliverable 8.4 aims to identify across the width of ECOPOTENTIAL modelling studies how they address uncertainties. Based on the included studies, we discuss the different types of uncertainties addressed and the general patterns that emerge from that. We further propose how the systematic integration of uncertainty analysis can be promoted in future. As the majority of the presented modelling studies follow statistical approaches commonly used in these kinds of studies, they form excellent examples and can be helpful to improve similar studies in the scientific community. The bouquet of studies includes future simulations on different temporal, spatial and ecological scales under climate change (except for Chap. 2.8 with a focus on land use change). Table 1 provides an overview of the studies including the use of climate input data and the types of uncertainties addressed (Table 1). In Chapter 2, we present studies for individual ecosystem at PA scale, including the assessment of ecosystem services and species composition. In Chapter 3, we provide large-scale perspectives of projected pan-European terrestrial and marine ecosystem change beyond the scale of ECOPOTENTIAL PAs.

Table 1: Overview of individual studies presented in Chapter 2 and Chapter 3

No.	Focus of the study	Input variables	Driving GCMs	RCM	Stochastic down-scaled by CNR	RCPs	Time period	Uncertainty types assessed
Chapter 2: PA-scale studies								
2.1	Gran Paradiso NP: Chamois population	Temperature Precipitation Snow Depth	EC-Earth, CNRM-CM5, IPSL-CM5A-MR, HadGEM2-ES, MPI-ESM-LR EM2-ES, MPI-ESM-LR	RCA4		4.5 8.5	2013-2100	Internal model Input data Scenario
2.2	Gran Paradiso NP: Topographic effects on metapopulations	Temperature DEM	*Synthetic climate input data: Temperature increased by 4 degrees in 100 years*				2016-2116	Internal model - -
2.3	Pelagos: Fin whale distribution	Chlorophyll-a Sea Surface Temp.	CCSM4, HadGEM2-ES, MIROC5	RCA4	n/a	4.5	Future: 2050 Reference period: 2000-2014	Internal model Input data Scenario
2.4	Negev: Plant composition	Temperature Precipitation	CNRM-CM5, IPSL-CM5A-MR, HadGEM2-ES, MPI-ESM-LR	RCA4	Precipitation (1 hour) Temperature (90m/ 1 day)	4.5 8.5	2000-2100	Internal model Input data Scenario
2.5	Peneda Geres: Hydrological impacts	Temperature Precipitation Solar Radiation Humidity	EC-Earth, CNRM-CM5, IPSL-CM5A-MR, MPI-ESM-LR	RCA4	Precipitation (1 km / 1 day) Temperature (1 km / 1 day)	4.5 8.5	Future: 2020-2050 Reference period: 1970-2000	- Input data Scenario
2.6	Curonian Lagoon: Physical parameters	Temperature Precipitation Wind	EC-Earth, CNRM-CM5, IPSL-CM5A-MR, HadGEM2-ES, MPI-ESM-LR	RCA4	n/a	4.5 8.5	Future: 2006-2074 Reference period: 1970-2006	- Input data Scenario
2.7	Wadden Sea: Physical parameters	Water Temperature Salinity, Sea level	HadGEM2-ES	RCA4	n/a	4.5	2010-2090	- Input data Scenario

		Radiation, Wind press, Humidity, Cloud cover Chlorophyll-a						
2.8	Sierra Nevada: Land use changes	*Focus on Land use Scenarios / climate from AR4 2020*					2040, 2070, 2090	- - -
Chapter 3: Large-scale Studies								
3.1	Climate Niches of N2000	Temperature, Precipitation	BCC-CSM1-1	n/a	n/a	6.0 8.5	2061-2080	- Input data Scenario
3.2	Adaptation of plant traits in European Woodlands	Temperature, Precipitation, Radiation	HadGEM2-ES	n/a	n/a	4.5 8.5	2006-2099	Internal model Input data Scenario
3.3	European woody plant distribution and ESS	ClimateEU - 35 bio- climatic variables https://sites.ualberta.ca/~ahamann/data/climateeu.html	CanESM2, ACCESS1.0, IPSL-CM5A-MR, MIROC5, MPI-ESM-LR, CCSM4, HadGEM2-ES, CNRM-CM5, CSIRO Mk 3.6, GFDL-CM3, INM-CM4, MRI-CGCM3, MIROC-ESM, CESM1-CAM5, GISS-E2R	n/a	n/a	4.5 8.5	1931-1990 2011-2040 2041-2070 2071-2100	Internal model Input data Scenario
3.4	Water balance and habitats of Mediterranean Wetlands	Precipitation Pot.Evapotransp.	EC-Earth, CNRM-CM5, IPSL-CM5A-MR, HadGEM2-ES, MPI-ESM-LR	SMHI - RCA4	n/a	4.5 8.5	1981-2000 2031-2050 2081-2100	- Input data Scenario

By summarizing some of the studies performed at individual PAs within ECOPOTENTIAL, Chapter 2 will address local ecological questions on population dynamics, ecosystem service provisioning and potential habitat alterations, e.g. through changes in the water table. It will also deal with transformations in the composition of vegetation communities and the climate-introduced responses of exemplary terrestrial and marine ecosystems. Within a pan-European perspective, Chapter 3 will focus on the adaptability of European plant traits, the assessment of consequent impacts on Natura2000 sites and Mediterranean wetlands as well as on impacts on ecosystem services relevant to human society.

The different studies presented in the Chapters 2 and 3 operate with distinct model approaches, e.g. empirical population models in the studies of chamois at Gran Paradiso National Park (2.1) or the process based model of LPJmL-FIT in the study on the adaptation of traits in European Woodlands (3.2) and exploit the availability of climatic forcing produced in the framework of WP8 and made available to the project partners (as described in the Deliverable D8.1, see Appendix). A joint simulation protocol had been agreed upon in Sept 2016 (see summary in Appendix and details in D8.1) to support a minimum level of comparability among the different studies focused on the various PAs. Thus, the climatic input to the various ecosystem models was extracted from an multi-member ensemble of the RCA4 regional climate model driven by five different GCMs from the Coupled Model Intercomparison Project Phase 5 (CMIP5), namely EC-Earth, CNRM-CM5, IPSL-CM5A-MR, HadGEM2-ES and MPI-ESM-LR. All regionally downscaled climate projections produced with RCA4 are part of the regional downscaling initiative EURO-CORDEX of the Rossby Centre. Most of the studies presented in the following chapter make use of these dynamically downscaled data, some also used further stochastically downscaled climate inputs when the specific application required input precipitation fields at higher spatial resolution (see all details about the downscaling strategy followed in ECOPOTENTIAL in D8.1 and Terzago et al. 2018).

References:

Ban, N., Schmidli, J., Schär, C. (2015). Heavy precipitation in a changing climate: Does short-term summer precipitation increase faster? *Geophys. Res. Lett.,* 42: 1165–1172. doi: 10.1002/2014GL062588

Bellard, C., Bertelsmeier, C., Leadley, P., Thuiller, W., Courchamp, F. (2012). Impacts of climate change on the future of biodiversity. *Ecology Letters,* 15(4): 365–377. doi: 10.1111/j.1461-0248.2011.01736.x

Fischer E. M., Knutti, R. (2015). Anthropogenic contribution to global occurrence of heavy-precipitation and high-temperature extremes, *Nature Climate Change* 5: 560–564.

Donat, M.G., Lowry, A.L., Alexander, L.V., O'Gorman, P.A., Maher N. (2016). More extreme precipitation in the world's dry and wet regions, *Nature Climate Change*, 6: 508–513.

EEA (2015): European ecosystem assessment – concept, data, and implementation. Contribution to Target 2 Action 5 Mapping and Assessment of Ecosystems and their Services (MAES) of the EU Biodiversity Strategy to 2020. EEA Technical Report 6/2015. Luxembourg. pp. 74.

Forzieri, G., Feyen, L., Russo, S. et al. (2016). Multi-hazard assessment in Europe under climate change. *Climatic Change,* 137(1-2): 105-119. doi: 10.1007/s10584-016-1661-x

Frank, D., Reichstein, M., Bahn, M., Thonicke, K., Frank, D., Mahecha, M.D., Smith, P., Van der Velde, M., Vicca, S., Babst, F., Beer, C., (2015). Effects of climate extremes on the terrestrial carbon cycle: concepts, processes and potential future impacts. *Global Change Biology,* 21(8): 2861-2880.

Gao, X., Shi, Y., Song, R., Giorgi, F., Wang, Y., Zhang, D. (2008). Reduction of future monsoon precipitation over China: Comparison between a high resolution RCM simulation and the driving GCM. *Meteorology and Atmospheric Physics*, 100(1-4): 73-86.

IPCC (2013). Climate Change 2013. The Physical Science Basis. Contribution of Working Group I to the Fifth Assessment Report of the Intergovernmental Panel on Climate Change [Stocker, T.F., D. Qin, G.-K. Plattner, M. Tignor, S.K. Allen, J. Boschung, A. Nauels, Y. Xia, V. Bex and P.M. Midgley (eds.)]. Cambridge University Press, Cambridge, United Kingdom and New York, NY, pp. 1535.

IPCC (2012). Managing the Risks of Extreme Events and Disasters to Advance Climate Change Adaptation. A Special Report of Working Groups I and II of the Intergovernmental Panel on Climate Change [Field, C.B., V. Barros, T.F. Stocker, D. Qin, D.J. Dokken, K.L. Ebi, M.D. Mastrandrea, K.J. Mach, G.-K. Plattner, S.K. Allen, M. Tignor, and P.M. Midgley (eds.)]. Cambridge University Press, Cambridge, UK, and New York, NY, USA, pp. 582.

Kovats, R.S., R. Valentini, L.M. Bouwer, E. Georgopoulou, D. Jacob, E. Martin, M. Rounsevell, and J.-F. Soussana, j.-F. (2014). In: Climate Change 2014: Impacts, Adaptation, and Vulnerability. Part B: Regional Aspects. Contribution of Working Group II to the Fifth Assessment Report of the Intergovernmental Panel on Climate Change [Barros, V.R., C.B. Field, D.J. Dokken, M.D. Mastrandrea, K.J. Mach, T.E. Bilir, M. Chatterjee, K.L. Ebi, Y.O. Estrada, R.C. Genova, B. Girma, E.S. Kissel, A.N. Levy, S. MacCracken, P.R. Mastrandrea, and L.L. White (eds.)]. Cambridge University Press, Cambridge, United Kingdom and New York, NY, USA, pp. 1267-1326.

McMahon S.M., Harrison S.P., Armbruster W.S., Bartlein P.J., Beale C.M., Edwards M.E., Kattge J., Midgley G., Morin X., Prentice I.C. (2011). Improving assessment and modelling of climate change impacts on global terrestrial biodiversity. *Trends in Ecology & Evolution,* 26: 249-259. doi: 10.1016/j.tree.2011.02.012

O'Gorman, P.A. (2015). Precipitation Extremes Under Climate Change. *Current Climate Change Reports*, 1: 49. doi: 10.1007/s40641-015-0009-3

Soranno, P. A., Cheruvelil, K. S., Bissell, E. G., Bremigan, M. T., Downing, J. A., Fergus, C. E., Filstrup, C.T., Henry, E. N., Lottig, N. R., Stanley, E. H., Stow, C. A., Tan, P.-N., Wagner, T., Webster, K. E. (2014). Cross-scale interactions: quantifying multi-scaled cause–effect relationships in macrosystems. *Frontiers in Ecology and the Environment*, 12(1): 65-73. doi: 10.1890/120366

Terzago S., Palazzi E., von Hardenberg J. (2018). Stochastic downscaling of precipitation in complex orography: a simple method to reproduce a realistic fine-scale climatology. *Nat. Hazards Earth Syst. Sci*. 18: 2825-2840. doi: 10.5194/nhess-18-2825-2018

Co-funded by the European Union

2. Future simulations for individual PAs

2.1 Gran Paradiso National Park. Population dynamics of a mountain ungulate between past and future uncertainties

By Simona Imperio, Luca Corlatti, Bruno Bassano and Antonello Provenzale

Abstract

The impact of climate change is expected to be particularly severe in mountain areas and may include changes in plant phenology, elevational range shifts of plants and animals as well as changes in wildlife demography. Understanding the potential effects of environmental changes on the dynamics of animal populations is pivotal for undertaking appropriate conservation measures. In this study, we investigated the role of density dependence and climatic forcing on the demography of a mountain ungulate, the Alpine chamois (*Rupicapra rupicapra*), over a period of 51 years in the Gran Paradiso National Park (GPNP, Italy), one of the mountain ecosystems dealt with in ECOPOTENTIAL. We estimated the response of the study population to the expected climate changes projected by state-of-the-art climate models up to 2100. The population dynamics of chamois in the GPNP was largely controlled by density dependence and snow depth in early winter and spring. A complex pattern of interaction between density dependence and snow depth through the cold season has been detected, depending likely on individual body conditions, accessibility of food resources and mating behaviour. Population projections based on unstructured population models suggested a basic stability of the chamois population in the GPNP; projections based on structured population models, however, predicted a slight decrease of the population. Our results suggest that relying on unstructured population models only, could lead to misleading results and overly optimistic predictions on the fate of chamois population in the GPNP. The results of our analysis elucidate important intrinsic and extrinsic mechanisms that regulate the population dynamics of an iconic Alpine species, thus offering the possibility to explore potential long-term demographic consequences of the impact of climate change on biotic components in extreme environments.

Methods

To estimate future population trends, we forced the best-performing models with the time series of meteorological variables (temperature, precipitation, and snow depth) generated by one Regional Climate Model, SMHI-RCA4, part of the CORDEX program (http://www.cordex.org: Giorgi et al., 2006), using future projections under the RCP4.5 and RCP8.5 scenarios for the period 2013-2100. We selected the finest resolution available to date for the European domain (EURO-CORDEX, Jacob et al. 2014), i.e. 0.11° lat-lon. We used five members of the SMHI-RCA4 regional climate models driven by five CMIP5 global climate models, (CNRM-CM5, EC-Earth, IPSL-CM5A-MR, HadGEM2-ES and MPI-ESM-LR hereafter abbreviated as CNRM, EC-Earth, IPSL, HadGEM2 and MPI, respectively). Datasets were handled with the raster package (Hijmans 2016) in R, and the daily values averaged for the whole park area (weighted with the fraction of each cell that is covered by the polygon) were extracted. To standardize the model's meteorological variables for subsequent analyses, all CORDEX time series were scaled (bias-corrected) to have the mean and variance of the observed series recorded by the Serrù station in the period 1970-2005. First, a population projection was performed using the unstructured population model. Then a projection for each demographic parameter was performed. If density dependence was present in GLMs for demographic parameters, a constant density (corresponding to the average observed density for the period 2001-2010) was considered in the simulations, to highlight the effect of a changing climate. Finally, a population projection was performed using the structured population model. Again, we performed 1000 runs for each projection to account for uncertainties in the empirical models.

Co-funded by the European Union

Results

Expected climate change effect on population dynamics

The five realizations of the RCA4 RCM predict an increase in temperature and a decrease in snow depth (but not in precipitations) in the next decades, with small differences among the 5. According to the unstructured population model, compared to the period 2001-2010 (mean ± SE: 8881 ± 49 chamois), in the RCP4.5 scenario the future chamois population will be stable or moderately increasing in the medium term, with one climate model (IPSL) predicting significantly higher numbers (mean number of chamois in 2041-2050 in the 50th percentile and t-test: 9466 ± 18, P = 0.006), and the remaining models predicting no significant difference (CNRM: 8994 ± 49, P = 0.61; EC-Earth: 9281 ± 18, P = 0.04; HadGEM2: 9010 ± 24, P = 0.45; MPI: 8542 ± 17, P = 0.07) (Fig. 1a). In the long-term (2091-2100), nearly all climate models simulated a significant increase of the population with respect to the period 2001-2010 (CNRM: 9683 ± 50, P = 0.003; EC-Earth: 9659 ± 37, P = 0.001; IPSL: 9496 ± 23, P = 0.004; HadGEM2: 9517 ± 24, P = 0.04), but one (MP1: 9207 ± 12, P = 0.07) (Fig. 1a).

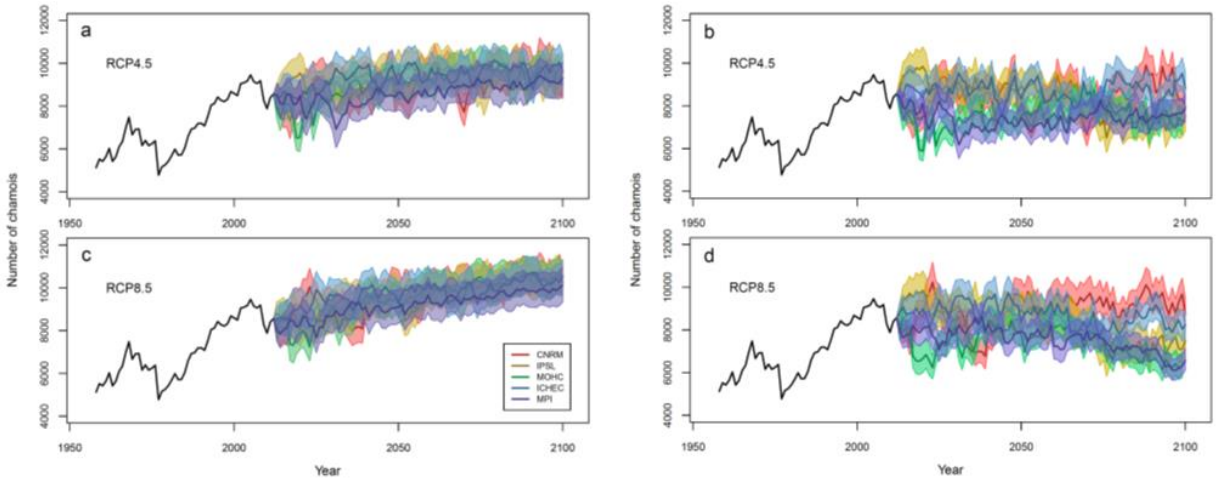

Figure 1: Population projections of chamois in GPNP for the period 2013-2100, according to the 5 CORDEX climate models for the RCP4.5 (a, b) and 8.5 (c, d) scenarios and the unstructured (a, c) or structured population model (b, d). Dark colour lines indicate 50th percentile, while shaded areas indicate 5–95th percentiles of the 1000 runs.

Under the RCP8.5 scenario, virtually all climate models predicted an increase in population size both in the medium (2041-2050; CNRM: 9690 ± 105, *P* = 0.001; EC-Earth: 9786 ± 82, *P* < 0.001; IPSL: 9527 ± 71, *P* = 0.006; HadGEM2: 9465 ± 51, *P* = 0.01; except MP1: 8973 ± 51, *P* = 0.82) and in the long term (2091-2100; CNRM: 10549 ± 70, *P* < 0.001; EC-Earth: 10355 ± 76, *P* < 0.001; IPSL: 10368 ± 54, *P* < 0.001; HadGEM2: 10426 ± 42, *P* < 0.001; MP1: 9910 ± 32, *P* < 0.001) (Fig. 1c).

Projection of single demographic parameters yielded contrasting results according to the different empirical models. Male adult survival, for a given density, is predicted to significantly increase for nearly all climate models for both the RCP4.5 (except for IPSL) and the RCP8.5 scenarios until the end of this century (Fig. 1a, c). Female survival, on the contrary, will be stable (or decreasing, for the IPSL model) under the RCP4.5 scenario and decreasing (for all climate models but CNRM) under the RCP8.5 scenario. Kid survival is predicted to increase for both scenarios except for IPSL under RCP4.5 (significantly decreasing) and MPI under RCP8.5 scenario (stable). Weaning success will decrease with nearly all climate models, except for HadGEM2 and MPI under the RCP4.5 scenario.

Results of population projections performed with the structured population model are less straightforward (Fig. 1b,d). Under the RCP4.5 scenario, chamois population in the medium term (2041-2050) will be stable (CNRM: 8406

Co-funded by the European Union

± 230, *P* = 0.10; EC-Earth: 8511 ± 188, *P* = 0.15; IPSL: 8823 ± 62, *P* = 0.73) or decreasing (HadGEM2: 7318 ± 64, *P* < 0.001; MP1: 7206 ± 76, *P* < 0.001) with respect to the period 2001-2010; in the long term (2091-2100) it will decrease according to three climate models out of five (IPSL: 7342 ± 96, *P* < 0.001; HadGEM2: 7388 ± 97, *P* < 0.001; MP1: 7598 ± 41, *P* < 0.001), while the other two predicted no significant change (CNRM: 8883 ± 199, *P* = 0.99; EC-Earth: 8660 ± 181, *P* = 0.37) (Fig. 1b). Similar results were obtained under the RCP8.5 scenario: in the medium term (2041-2050), the population is predicted to be stable with three climate models (CNRM: 8747 ± 235, *P* = 0.52; EC-Earth: 9190 ± 132, *P* = 0.23; IPSL: 8823 ± 62, *P* = 0.50) and to decrease with the other two (HadGEM2: 8073 ± 70, *P* < 0.001; MP1: 7801 ± 85, *P* < 0.001). In the long-term (2091-2100), compared to the period 2001-2010, population abundance will be marginally higher according to the CNRM climate model (9262 ± 129, *P* = 0.08) and significantly lower according to the remaining climate models (EC-Earth: 8364 ± 133, *P* = 0.02; IPSL: 7342 ± 96, *P* < 0.001; HadGEM2: 6372 ± 58, *P* < 0.001; MP1: 6452 ± 105, *P* < 0.001) (Fig. 1d).

Discussion

The results of our analysis elucidate important intrinsic and extrinsic mechanisms that regulate the population dynamics of an iconic Alpine species, thus offering the possibility to explore potential long-term demographic consequences of the impact of climate change on biotic components in extreme environments. The population dynamics of chamois in the Gran Paradiso National Park was found to be largely controlled by density-dependence, snow depth in the early winter and in spring, with significant interactions between density and snow depth in both periods. The long-term demographic projections support a positive effect of reducing snow cover on the chamois population within the protected area. On the other hand, higher spring-summer temperatures exerted a negative effect on population dynamics, and projection accounting for this effect predicted a slight reduction of population abundance.

References

Giorgi, F., Jones, C., Asrar, G. R. (2009). Addressing climate information needs at the regional level: the CORDEX framework. World Meteorological Organization (WMO) Bulletin, 58(3): 175.

Jacob, D., Petersen, J., Eggert, B., Alias, A., Christensen, O.B., Bouwer, L.M., Braun, A., Colette, A., Déqué, M., Georgievski, G. and Georgopoulou, E. (2014). EURO-CORDEX: new high-resolution climate change projections for European impact research. Regional Environmental Change, 14(2): 563-578.

Co-funded by the European Union

2.2 Gran Paradiso National Park. A metapopulation model driven by scenarios of future temperature data to assess climate change impact on the distribution of mountainous insect and bird species

By Jonathan Giezendanner and Damiano Pasetto

Introduction

The upward shift of mountainous species, which is foreseen to occur during the upcoming century due to the rapid rise in temperatures (see, e.g., Parmesan 2006, Parmesan & Yohe 2003), may lead to different species fates depending to the distribution of their habitat in these complex topographies. Several studies highlight that climate change will bring to a loss of biodiversity, especially due to the local extinction of species at high elevations, which are characterized by isolated habitats, poor colonization capacity, and adaptation to low temperatures (McCain & Colwell 2007, Elsen & Tingley 2015). At the same time, species nowadays present at lower altitudes might have access to areas at higher elevations, potentially increasing the extent of their habitat due to the complex environmental matrix of mountains (Bertuzzo et al. 2016). Because the shifts of geographic distributions may be rapid and heterogeneous (Chen et al. 2011, Tingley et al. 2012), it is of fundamental importance for conservation and management decisions to assess if mountainous species would be able to track the displacements of their habitat or, otherwise, they would go extinct (Dullinger et al. 2012, Steinbauer et al. 2018).

The monitoring of the ongoing changes in species presence and abundance along the altitudinal gradients is challenging, but required for investigating the relationships between biodiversity and abiotic/biotic parameters (Körner 2007). The analysis of the data of presence and abundance of five taxa (carabids, butterflies, spiders, staphylinids, birds) collected in 2007 in the Gran Paradiso National Park (GPNP, 720 km2, Italian Alps) highlighted a hump-shaped relationship between species richness and elevation, similar to what obtained in theoretical studies (Bertuzzo et al. 2016). For most species, elevation and temperature resulted to be the most important variables to be considered for detecting changes in richness and community composition (Viterbi et al. 2013). The collection of long-time series of these data is necessary to establish the impact of the ongoing raise in temperatures, but data collection is challenging due to the required frequent field campaigns in areas that are not easily accessible.

Ecological models support and complement these monitoring efforts by taking into account upward shifts of suitable species habitat, thus providing predictions of effects of climate change and species displacement (Dullinger et al. 2012, Rumpf et al. 2018). The goal of this study is to use a metapopulation model to investigate how the GPNP topography interplays with species traits to assess their survival as a result of given climatic changes.

Co-funded by the European Union

Methods

Species distribution in the landscape is evaluated through a spatially-explicit stochastic patch occupancy model (SPOM, Rybicki & Hanski 2013), which generalizes the metapopulation approach (Hanski 1998) by the incorporation of a fitness function describing the suitability of a species to the local elevation. The regional persistence of the focal species stems from balancing colonization, extinction and local suitability. We consider a rectangular DEM covering the GPNP having N=100x100 cells (Figure 2).

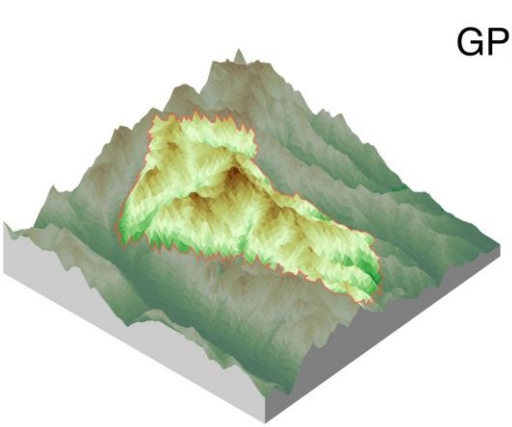

Figure 2: Sketch of the DEM of the GPNP. The red line in the DEM represents the administrative limits of the GPNP. Elevation ranges from about 400 m to about 3900 m

The model simulates the occupancy p of each cell: p_i=1 if cell i is occupied, p_i=0 otherwise. Given a distribution of occupied cells at time t, the model allows unoccupied cells to be colonized by surrounding occupied cells, and occupied cells to go extinct, with probabilities of transition modelled as exponential distributions:

$$P\left[p_{i,t+\Delta t}=1 \mid p_{i,t}=0\right] = 1-\exp(-C_{i,t}\cdot dt) \quad \text{(probability of local colonization)}$$

$$P\left[p_{i,t+\Delta t}=0 \mid p_{i,t}=1\right] = 1-\exp(-E_i\cdot dt) \quad \text{(probability of local extinction)}$$

where Δt is the simulation time step, E_i and $C_{i,t}$ are the extinction and colonization rates for cell i at time t. The colonization and extinction rates are directly related to a fitness function, f_i , which measures the suitability of the focus species to the features of the patch i:

$$E_i = e \,/\, f_i$$

$$C_{i,t} = c \sum_{j\neq i} p_{j,t} \frac{exp(-d_{i,j}\,/\,D)}{2\,\pi\, D} f_i$$

where e and c are the extinction and colonization constants, respectively, $d_{i,j}$ is the distance between cells i and j, D the dispersal distance. The species suitability to cell i is modelled as a Gaussian-shaped function of the elevation, centered around an optimal elevation z_{opt} , having niche width σ and maximum fitness f_{max} :

$$f_i = f_{max} \quad exp\left(\frac{(z_i - z_{opt})^2}{2\sigma^2}\right)$$

Thus, each species is characterized by a combination of parameters e, c, D, z_{opt}, σ, and f_{max} . Here a pool of 4000 species is selected by varying parameters D, z_{opt}, nad σ. Parameters e and c are fixed, while f_{max} is set to $f_{max}=\sigma^{-0.5}$ in order to guarantee that the selected species have the same colonization capacity (i.e., same probability of surviving) along a linear landscape. Thus, the compared species have either a narrow niche but a large fitness or a large niche but a proportionally smaller fitness.

Co-funded by the European Union

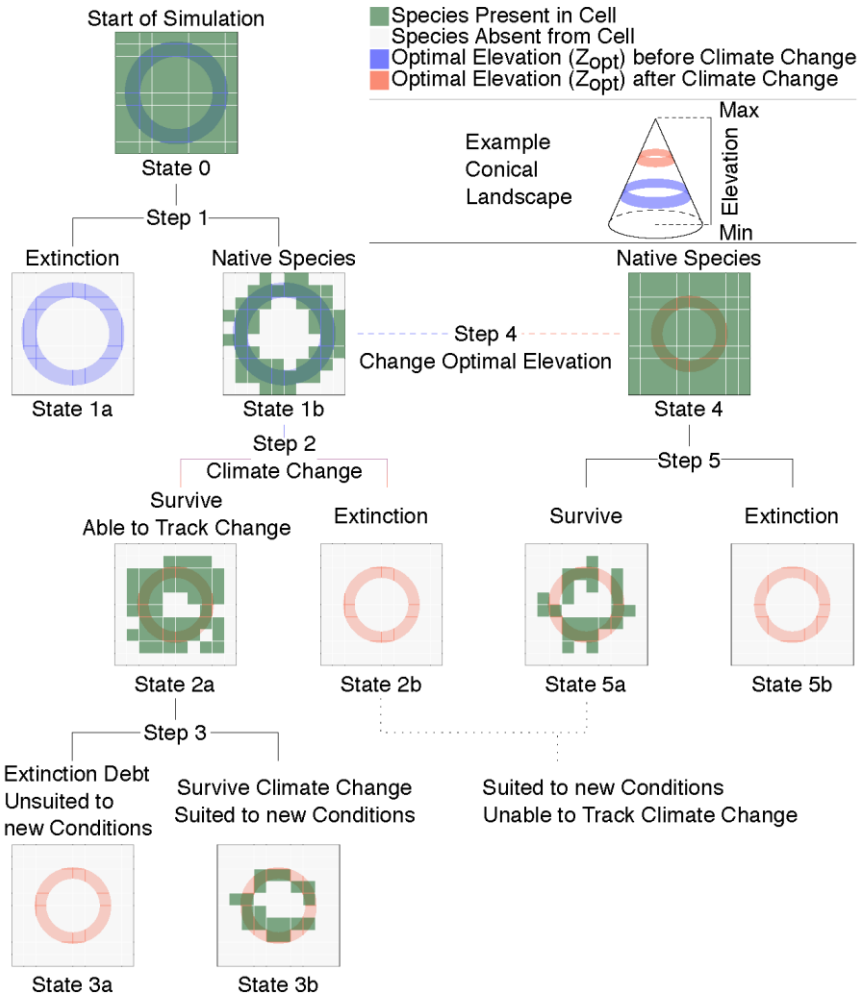

Figure 3: Overview of the different simulation steps, with the landscape displayed as a cone for simplicity.

As the considered metapopulation model is stochastic, the results are obtained by averaging 100 model runs for each of the species. Starting from a fully occupied landscape, the first simulation step selects the species traits that allow survival over the GPNP at the present conditions (Fig. 3, step 1). Species surviving with a probability larger than 50% are named 'native' species. Native species undergo the second modelling step of climatic change, which affects their fitness and, in turn, their occupancy (Fig. 3, step 2). Climate change is modelled by a gradual upward shift of the optimal elevation of each species. Considering the worst-case scenario foreseen by the IPCC reports (RCP8.5), the average increase in temperature is of ΔT = 4°C over the next century (Δt_c=100 y). We choose to uniformly change the optimal elevation of each species in time. Assuming a typical average global environmental lapse rate for air temperature of γ_w=1/150°C/m (Barry & Chorley, 2009), the optimal elevation thus changes at a speed of $\Delta z/\Delta t = \Delta T/(\gamma_w \cdot \Delta t_c) = (4 \cdot 150)/100 = 6$ m/year. Depending on the assigned metapopulation parameters and to the occupancy after step 1, some species might be unable to track climate change and go extinct during step 2, while surviving species might still undergo extinction debt. The latter is assessed by testing whether the focal species thrives in the altered habitat (step 3). The last two steps (steps 4-5) consist in understanding whether the species that went extinct during the climate change phase would be able to survive given their new optimal elevation, or if they would have gone extinct anyway.

Co-funded by the European Union

Results

For all the optimal elevations characterizing the different species, only a subset of the considered species persisted after the initial phase with constant climatic conditions (colored in Figure 4) suggesting an important effect of spatial aggregation of suitable habitat/landscape fragmentation. In the climate change phase we focus only on the fates of these surviving species, called native, without considering species that can immigrate from outside the system (e.g., from lower elevations). Among the native species, species at the highest elevations (pink color, Figure 4) are those more likely to go extinct due to unsuitability to the changed climatic conditions. Also species with a large dispersion seem to have a similar fate. This is mainly due to the fact that, to maintain the same colonization capacity among the compared species, we impose a smaller colonization pressure to species with larger dispersions. Species having an initial optimal elevation facing a rising hypsographic curve (that is, an increase of area of suitable habitat resulting from the upslope shift) experienced an increase in their occupancy (species in dark blue in Figure 4). However, note that species with small niche width are more prone to extinction due to inability to track change (red in Figure 4). Finally, part of the species surviving to climate change will not persist with the new climatic conditions (yellow). For what concern the α-diversity (Figure 5), it increases from low to mid-elevations. The peak decreases and shifts to higher elevations during climate change, and it decreases again in the final phase of the simulation. Notice a slight increase in α-diversity at steady state in the mid-elevations, that highlights a possible temporal lag between the species occupancy at the end of steady state compared to their theoretical geographical ranges which are occupied at steady state.

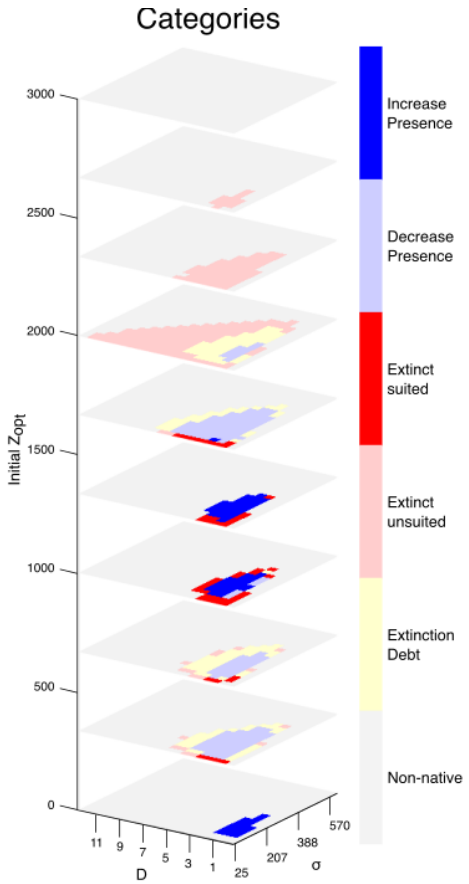

Figure 4: Fate of the species after climate change for the pool of considered parameter combinations.

Co-funded by the European Union

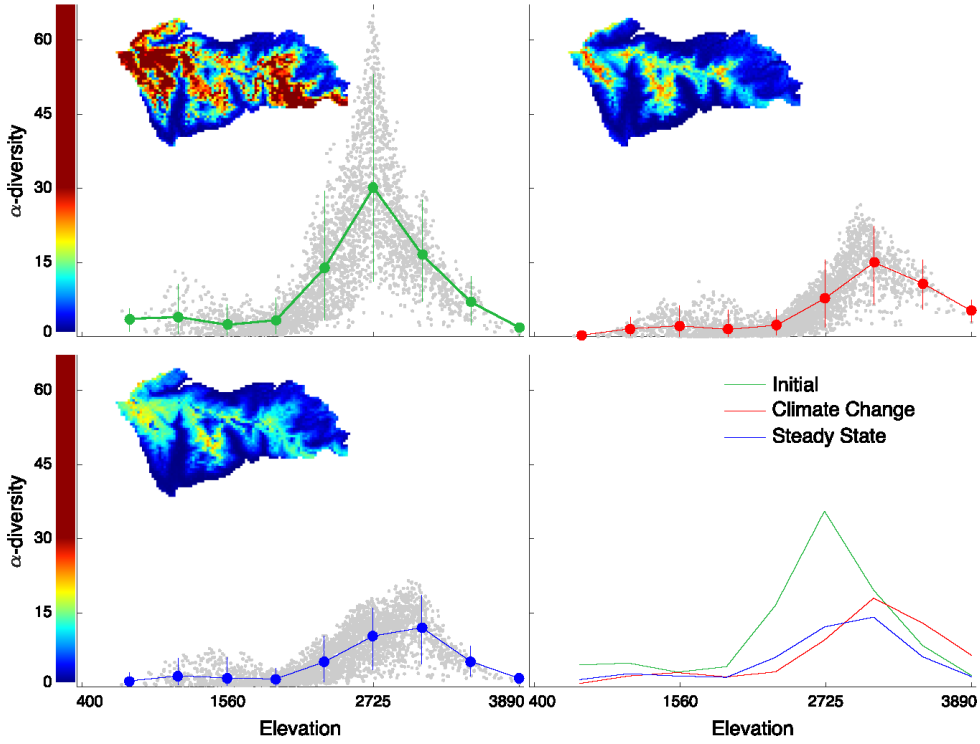

Figure 5: α-diversity as function of elevation computed from the pool of surviving species after the initial modeling step (step 1), the climate change scenario (step 2) and the final adaptation to the environmental conditions after climate change (step 3).

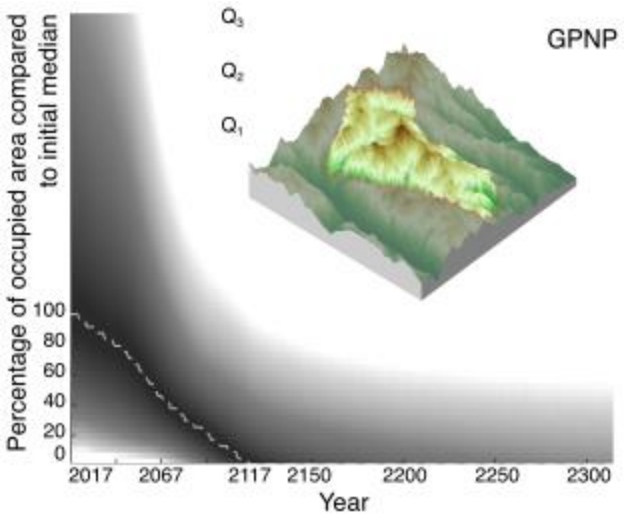

Figure 6: Species occupancy during (2017-2100) and after climate change (after 2100) relative to the initial median occupancy. The dashed line represents the median percentage of occupied area by native species that decreases during and after climate change.

The temporal changes in the percentage of occupied area by a species compared to the initial median occupation (Figure 6) show a decrease during climate change. Interestingly, a long period is required to stabilize the occupancy after the imposed change, with the median occupancy tending to zero. Owing to its geomorphological attributes, the GPNP region, which has the majority of land close to the maximum elevation, is very likely to suffer from loss in occupancy.

Conclusions

Computational studies prove essential to sort out landscape effects on the dynamics of spatial occupation of species under climate change, not simply in terms of stationary states but also describing transients and the range of possible extinction timescales, in particular showing quantitatively how extinction debts unfold. Metapopulation range dynamics proves to be a useful tool for monitoring the time evolution of the ecological effects of climate change within a given domain.

References

Barry, R., Chorley, R. (2009). *Atmosphere, weather and climate*. London: Routledge.

Bertuzzo, E., Carrara, F., Mari, L., Altermatt, F., Rodriguez-Iturbe, I., Rinaldo, A. (2016). Geomorphic controls on elevational gradients of species richness. *Proceedings of the National Academy of Sciences*, 113: 1737–1742.

Chen, I., Hill, J., Ohlemüller, R., Roy, D., Thomas, C. (2011). Rapid range shifts of species associated with high levels of climate warming. *Science*, 20: 1024–1026.

Dullinger, S., Gattringer, A., Thuiller, W., Moser, D., Zimmermann, N., Guisan, A., Willner, W., Plutzar, C., Leitner, M., Mang, T., Caccianiga, M., Dirnböck, T., Ertl, S., Fischer, A., Lenoir, J., Svenning, J.-C., Psomas, A., Schmatz, D. R., Silc, U., Vittoz, P., Hülber, K. (2012). Extinction debt of high-mountain plants under twenty-first-century climate change. *Nature Climate Change*, 2: 619–622.

Elsen, P., Tingley, M. W. (2015). Global mountain topography and the fate of montane species under climate change. *Nature Climate Change*, 5, 5–10.

Hanski, I. (1998). Metapopulation dynamics. *Nature*, 396: 41–49.

Körner, C. (2007). The use of 'altitude' in ecological research. *Trends in Ecology & Evolution*, 22: 569–574.

McCain, C., Colwell, R. (2007). Assessing montane biodiversity from discordant shifts in temperature and precipitation in a changing climate. *Ecology Letters*, 14: 1236–1245.

Parmesan, C. (2006). Ecological and evolutionary responses to recent climate change. *Annual Review of Ecology, Evolution, and Systematics*, 15.

Parmesan, C., Yohe, G. (2003). Rapid range shifts of species associated with high levels of climate warming. *Nature*, 421: 37–42.

Rumpf, S., Hülber, K., Klonner, G., Moser, D., Schütz, M., Wessely, J., Willner, W., Zimmermann, N. E., Dullinger, S. (2018). Range dynamics of mountain plants decrease with elevation. *Proceedings of the National Academy of Sciences*, 115: 1–6.

Rybicki, J., Hanski, I. (2013). Species-area relationships and extinctions caused by habitat loss and fragmentation. *Ecology Letters*, 16: 27–38.

Steinbauer, M., Grytnes, J. A., Jurasinski, G., Kulonen, A., Lenoir, J., Pauli, H., Rixen, C, Winkler, M., Bardy-Durchhalter, M., Barni, E., Bjorkman, A.D., Breiner, F.T., Burg, S., Dawes, M.A., Delimat, A., Dullinger, S., Erschbamer, B., Felde, V.A., Fernández-Arberas, O., Fossheim, K.F., Gómez-García, D., Georges, D., Grindrud, E.T., Haider, S., Haugum, S.V., Henriksen, H., Herreros, M.J., Jaroszewicz, B., Jaroszynska, F., Kanka, R., Kapfer, J., Klanderud, K., Kühn, I., Lamprecht, A., Matteodo, M., di Cella, U.M., Normand, S., Odland, A., Olsen, S.L., Palacio, S., Petey, M., Piscová, V., Sedlakova, B., Steinbauer, K., Stöckli, V., Svenning, J.C., Teppa, G., Theurillat, P.J., Vittoz, P., Woodin, S.J., Zimmermann, N.E., Wipf, S. (2018). Accelerated increase in plant species richness on mountain summits is linked to warming. *Nature*, 556(7700):231-234. doi: 10.1038/s41586-018-0005-6.

Tingley, M. W., Koo, M. S., Moritz, C., Rush, A. C., & Beissinger, S. R. (2012). The push and pull of climate change causes heterogeneous shifts in avian elevational ranges. *Global Change Biology*, 18: 3279–3290.

Co-funded by the European Union

2.3 Pelagos: Modelling the impact of climate change on the distribution of fin whales using species distribution models

By Samuel Bosch, Bénédicte Madon and Ward Appeltans

Introduction

In the Mediterranean Sea, large numbers of whales and dolphins are present in the waters between mainland France, Italy and the island of Corsica. Since 1999, this area has been established as an international marine protected area, known as the Pelagos Sanctuary for Mediterranean Marine Mammals that spans over 87,000 square kilometers. Fin whales (*Balaenoptera physalus*) have a large influence on the ecosystem of the Pelagos Sanctuary for Mediterranean Marine Mammals by controlling the biomass at lower trophic levels, shuttling nutrients throughout the water, and contributing to the carbon storage. Within the Sanctuary, whales and dolphins also generate significant benefits for human society, having emblematic and cultural significance, while supporting recreational and tourist activities. At the same time, these species have to share their habitat with very high and increasing levels of human activity, including some of the busiest marine traffic in the world, and the effects of many industries and large urban centres located along the coast.Besides these diffuse direct human interferences, climate change is an important potential threat for fin whales in the Pelagos Sanctuary.

The ecological importance of fin whales highlights the need for predicting their future distribution. Species distribution modelling (SDM) links species occurrences with the environmental characteristics, and has the potential to predict distributions in a geographically explicit framework, including extrapolation in space and time. In this study we aim to predict the long term distribution of fin whales in the Pelagos Sanctuary. To this end we build species distribution models using climatological data and project these into the future using future climate data.

Methods

Study area and species records

The study area for modelling the distribution was defined as a bounding box, fully encompassing the Pelagos ranging from 0.0 to 20.0 degrees longitude and from 30.25 to 45.5 degrees latitude. We extracted all distribution records for fin whales from the Ocean Biogeographic Information System (OBIS)from 1950 onwards. Records where filtered by rounding to the nearest one thousandth of a degree which is approximately equivalent to filtering on a hundred by hundred meter grid. Records from every fourth year were set aside for the validation data set. The training and test sets for the 5-fold cross-validation were created using the disc based approach implemented in the *marinespeed* R package (Bosch et al. 2018). This approach randomly samples a starting point and selects the nearest one-fifth of all distribution records to get the first fold. Then, the distribution record farthest away from the starting point is used as a new starting point and the nearest one-fifth of the distribution records are included to create the second fold. This process is repeated five times until all records are assigned to a fold.

Environmental data

The Bio-ORACLE 2 dataset was used as a source for environmental predictor variables. It consists of global rasters with a spatial resolution of 5 arcmin (Tyberghein et al. 2012, Assis et al. 2018). The environmental layers were retrieved using the *sdmpredictors* R package (Bosch et al. 2016). Predictor selection is a major concern when building transferable SDMs. In this study, the selection of variables was made a priori based on previous studies of modelling the distribution of fin whales (Druon et al. 2012). Three variables were selected a priori as potentially influencing the distribution of fin whales in the Pelagos Sanctuary: sea surface temperature (SST), chlorophyll *a* fronts and bathymetry. The chlorophyll *a* fronts were calculated using the Belkin & O'Reilly (2009) front detection

algorithm. This algorithm follows 3 steps: (1) apply a contextual median filter, (2) horizontally and vertically apply convolutions with sobel kernels and (3) extract gradients.

Modelling methods

The distribution of fin whales was modelled using two different algorithms: generalized linear models (GLM) and maximum entropy (MaxEnt, Phillips et al. 2004) in R. Presence-only methods use species occurrence records and background points, which are selected randomly in the study area. As suggested by Phillips & Dudík (2008) we used 10.000 background points in our study, which is adequate to cover the whole area. Models were evaluated using the area under the receiver operating curve (AUC). Although AUC values have been criticized in the context of species distribution modelling (Lobo et al. 2008), its use was motivated because it is objective, threshold independent and insensitive to imbalanced datasets (Hand 2009).

Future models

Based on the different models a future climate model was created using the RCP 4.5 projections for the year 2050. Modelling was done by creating an ensemble model of all 5-folds and the two algorithms. In addition to this, a map with the standard deviations was created in order to get insights on areas with high disagreements between the models. The future climate environmental data was sourced from Bio-ORACLE 2 and consists of layers created by averaging data from distinct atmosphere–ocean general circulation models provided by the CMIP 5.

Results

Species data

After filtering based on the study area and retaining only records from after 1950 we collected a total of 581 records from OBIS with 391 records in the training and test sets (Fig. 7) and 190 records in the validation set (Fig. 8).

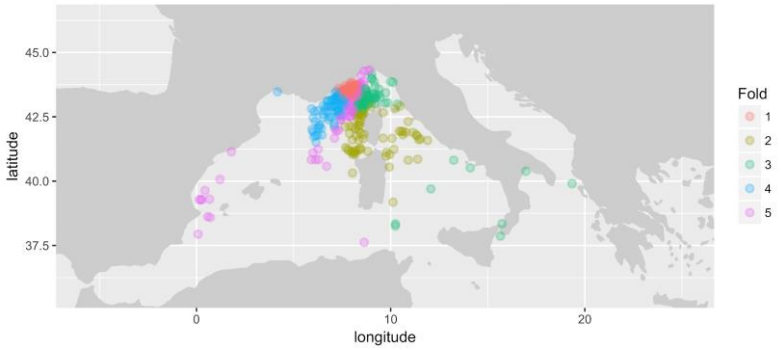

Figure 7: Map of the fin whales occurrences used for modelling with an overview of the different folds for the 5-fold cross-validation that the records are a part of.

Co-funded by the European Union

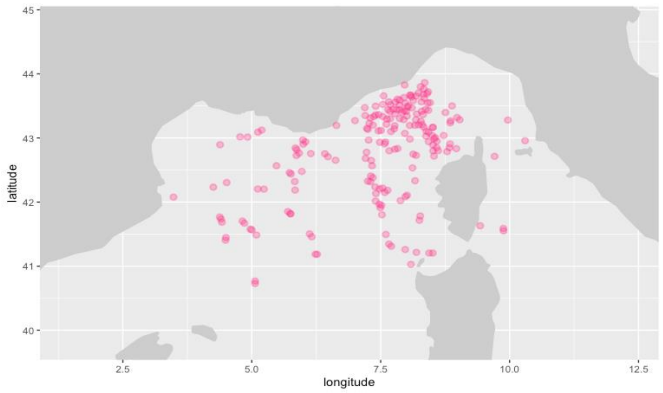

Figure 8: Map of the validation data used for evaluating the fin whales, selected by taking records from every fourth year.

Current climate models

Modelling for the current climate resulted in models with AUC values ranging from 0.77 to more than 0.9 for the different folds and algorithms (Fig. 9). Note that MaxEnt has similar or better performance than GLM except for the fifth fold.

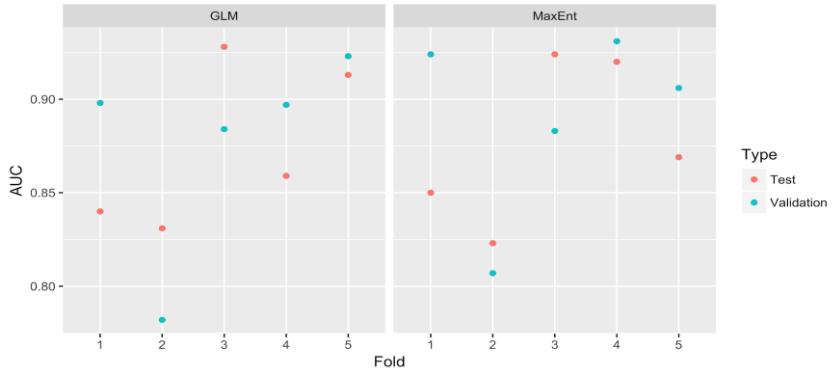

Figure 9: Model evaluation values as measured by AUC for the test set from the different folds and for the validation set for the two species distribution modelling methods: GLM and MaxEnt.

In Figure 10A we see that SST is the most important variable across the different folds and algorithms, while chlorophyll and bathymetry show a high variability but with the former being generally more important than the latter. Figure 10B to D depict the response curves for the models build with the different folds and algorithms.

Co-funded by the European Union

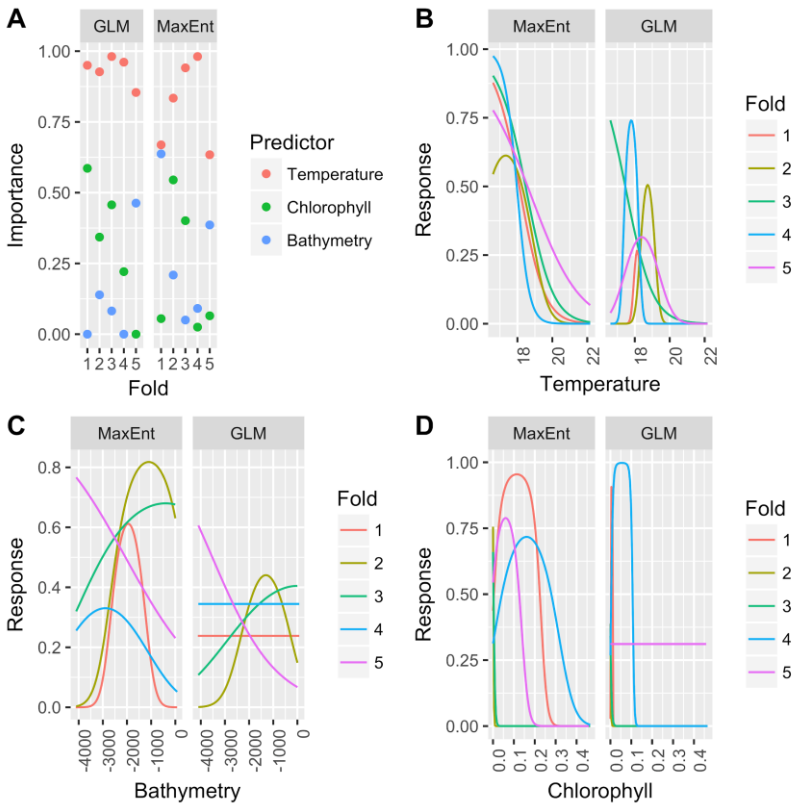

Figure 10: Overview of the variable importance and response plots for the different algorithms and folds of the 5-fold cross-validation.

The ensemble model for the current climate, created by averaging out the models with from different folds and algorithms, predicts a high suitability in the western part of the Pelagos Sanctuary and to the west of it along the French and northern Spanish coast. The standard deviation is particularly high compared to the predicted suitability in the Golfe Du Lion in France, between Corsica and Italy and in the Adriatic Sea.

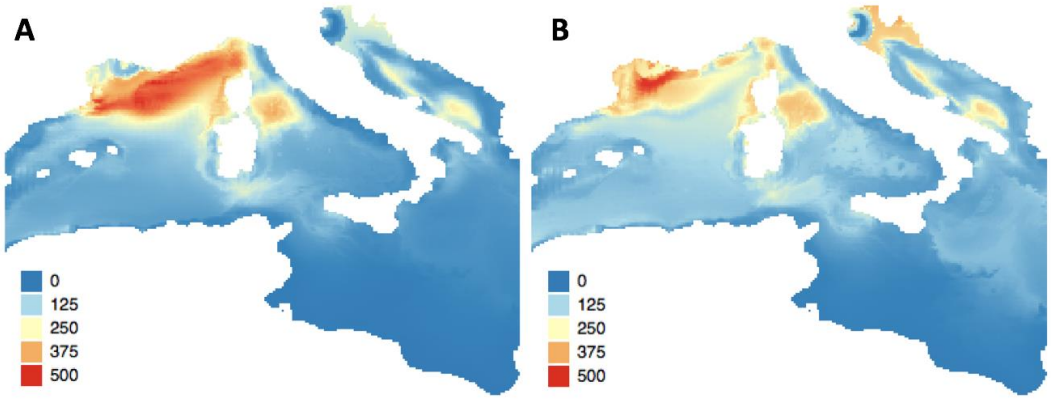

Figure 11: Ensemble of the habitat suitabilities for the different folds and algorithms for the current climate (A) and the standard deviation of the ensemble (B).

Co-funded by the European Union

Future climate projections

The ensemble model of the future climate projections for the year 2050 of the RCP model predicts a north-eastward shift and a strong decrease in suitability of the study area (Fig. 12A) compared to the current climate (Fig. 11A). The standard deviation for the resulting ensemble is very high in the areas with a high predicted suitability (Fig. 12B).

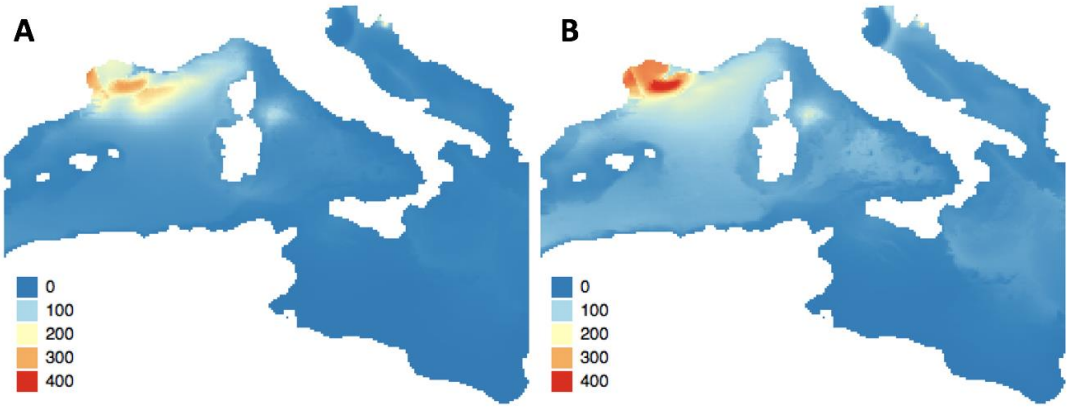

Figure 12: Ensemble of the habitat suitabilities for the different folds and algorithms for the year 2050 for the RCP 4.5 scenario (A) and the standard deviation of the ensemble (B).

Discussion

Based on the data in OBIS we were able to create current and future climate distribution models for fin whales in and around the Pelagos Sanctuary for the Conservation of Mediterranean Marine Mammals. The AUC values, indicating the quality of the obtained models for the current climate were generally high across the different folds and algorithms. But, the high variation in response curves between the different folds and algorithms and the high standard deviation in both the current and future climate model ensembles indicate that more research is needed in order to get reliable future climate models of fin whales in the study area. Furthermore the results indicate the importance of further research as according to the models obtained, the predicted suitable area strongly decreases by 2050.

References

Assis, J., Tyberghein, L., Bosch, S., Verbruggen, H., Serrão, E. A., De Clerck, O. (2018). Bio-ORACLE v2. 0: Extending marine data layers for bioclimatic modelling. *Global Ecology and Biogeography*, *27*(3): 277-284.

Austin M.P. (2002). Spatial prediction of species distribution: an interface between ecological theory and statistical modelling. *Ecological Modelling*, 157: 101–118.

Belkin I. M., O'Reilly J. E. (2009). An algorithm for oceanic front detection in chlorophyll and SST satellite imagery. *Journal of Marine Systems*, 78: 319-326.

Bosch S. et al. (2016) sdmpredictors: Species Distribution Modelling Predictor Datasets. R package version 0.9. Available at: https://github.com/lifewatch /sdmpredictors.

Bosch, S., Tyberghein, L., Deneudt, K., Hernandez, F., De Clerck, O. (2018). In search of relevant predictors for marine species distribution modelling using the MarineSPEED benchmark dataset. *Diversity and Distributions*, *24*(2): 144-157.

Druon, J. N., Panigada, S., David, L., Gannier, A., Mayol, P., Arcangeli, A., Cañadas, A., Laran, S., Di Méglio, N., Gauffier, P. (2012). Potential feeding habitat of fin whales in the western Mediterranean Sea: an environmental niche model. *Marine Ecology Progress Series*, *464*: 289-306.

Hand D.J. (2009). Measuring classifier performance: A coherent alternative to the area under the ROC curve. *Machine Learning*, 77: 103–123.

Lobo J.M., Jiménez-Valverde A., Real R. (2008). AUC: a misleading measure of the performance of predictive distribution models. *Global Ecology and Biogeography,* 17: 145–151.

Phillips S.J., Dudík M., Schapire R.E. (2004). A maximum entropy approach to species distribution modeling. Twenty-first international conference on Machine learning - ICML '04: 655–662.

Phillips S.J., Dudík M. (2008). Modeling of species distributions with Maxent: new extensions and a comprehensive evaluation. *Ecography*, 31: 161–175.

Tyberghein, L., Verbruggen, H., Pauly, K., Troupin, C., Mineur, F., De Clerck, O. (2012). Bio-ORACLE: a global environmental dataset for marine species distribution modelling. *Global Ecology and Biogeography*, 21(2): 272-281.

Co-funded by the European Union

2.4 Negev: Vulnerability of vegetation cover in the transition zone towards the Negev desert

By Kristina Steinmar, Britta Tietjen, Jennifer Schulz, Sebastian Fiedler, Arnon Karnieli and Ariane Walz

Introduction

The drylands of Israel's northern Negev desert are located in a transition zone between Mediterranean and semi-arid climates which is known to be vulnerable to climate change. It provides a high diversity and richness in species, genes and ecosystems, and maintains essential ecosystem services for society (Pe'er & Safriel 2000, Orenstein et al. 2012). Main features of the northern Negev are rocky and loessial watersheds with patches of dwarf-shrubs, perennial herbs and annual grasses, as well as a biological soil crust during the rainy season (Waide et al. 1998). The ecosystem functioning of this landscape has been intensively studied including the structure and dynamics of the composition of dryland vegetation communities. Climate models predict a significant temperature rise alongside with a reduction in precipitation until 2050, while the inter-annual and seasonal variability of rainfall distribution increases (Golan-Angelko & Bar-Or 2008). Since water is the main limiting resource of these semi-arid ecosystems, changes in the precipitation regime can affect the establishment and growth of the highly adapted vegetation, with serious consequences such as degradation, soil loss and altered ecosystem functions (Miranda et al. 2011, Golodets et al. 2015). In this study, we therefore assess the changes in functional composition of the vegetation we need to expect from climate change in the transitional zone between Mediterranean and desert biomes until the end of this century.

Methods

EcoHyD is an eco-hydrological vegetation model developed specifically for drylands, with strong a representation of small-scale hydrological processes and vegetation responses for different plant functional types (PFTs), namely annual grasses, perennial grasses and shrubs. EcoHyD runs on a spatial resolution of 5 m and outputs weekly and annual changes in the vegetation cover. The model was used to estimate the impact of the changes in climate conditions on the northern Negev vegetation structure. The EcoHyD model was therefore adapted to the local soil and topographic conditions and validated using time series based on Rapid Eye remote sensing data, where the calculated vegetation cover was compared to the fractional vegetation cover (FVC) calculated with the Normalized Difference Vegetation Index (NDVI).

Climatic forcing input (temperature and precipitation) was derived from the RCA4 CORDEX simulations, bias-corrected and downscaled for four global GCMs (CNRM, ICHEC, IPSL, MPI). In particular, the downscaled fields consisted of temperature at 90 m spatial resolution downscaled using an orographic lapse-rate correction and precipitation data at 750 m spatial resolution using the RainFARM stochastic method (D'Onofrio et al. 2014), providing five different stochastic realizations for each RCA4 member. The downscaled temperature and precipitation data covered the period 1970-2100 at 3h temporal resolution. EcoHyD was then run by each CMIP5-driven RCA4 of the RCP4.5 and RCP8.5 scenarios, with five realizations of each downscaled data set. The climate data were used as an input while all further parameters were kept fixed. Subsequently, the mean annual vegetation cover across plant functional types was calculated for each realization for the scenarios RCP4.5 and RCP8.5.

Within Shaked Park, the model was applied to a 300 m x 350 m plot, which has been selected for its hilly topography and mostly natural conditions. Vegetation on the study site consists of a shrub-steppe with small patches of dwarf shrubs.

Simulated inputs data was compared with observed precipitation data from the site to check consistency. After a

Co-funded by the European Union

validation based on high resolution remote sensing data (see D8.2), current vegetation dynamics were also simulated with the EcoHyD model based on measured weather records, soil parameters, estimated vegetation parameters and topography information for a 17 year period in the past (July 1999 – June 2016). Therefore, changes in vegetation cover of shrubs, perennial plants, annual plants and the sum of these three PFTs were simulated with ten repetitions and then compared to remote sensing based FVC.

Results

Consistency Check

Annual precipitation of five realisations of the four downscaled CMIP5-driven RCA4 of the scenarios RCP4.5 and RCP8.5, and the locally observed precipitation (mm) between 2000-2016 have been checked for consistency between modelled inputs climate and observed precipitation (Fig. 13A). The simulated precipitation does not perfectly match the observed of the annual precipitation (Fig. 13A). MPI-4.5 performs best with similar mean precipitation and similar variability between years over the 17 year period. ICHEC covers a similar spread between years as the observed data, but shows lower mean annual precipitation the entire period, whereas IPSL is closer in mean precipitation but shows less variability between years. In general, the overall deviation from the observed mean precipitation, however, is low.

Model validation

To validate simulated vegetation cover, simulation results were compared with high resolution remote sensing data from the site. Here, the simulated results from the downscaled GCMs generally underestimate the vegetation cover compared to the simulated vegetation cover based on measured meteorological data (Fig. 13B). The simulation driven by the observed meteorological data results in a vegetation cover of around 38 %, whereas the results by the best GCM reaches only a vegetation of 32-36 % (IPSL). Although mean and variability of annual precipitation over the validation period is best reflected by MPI-4.5, vegetation cover is strongly underestimated for these input data, with around 22%. Figure 13B nicely reflects how differences between climate models are consistently higher than between RCPs for this past period. Furthermore, it reflects systematic differences in the distribution of precipitation over the year which lead to diverting responses in the ecological model.

Co-funded by the European Union

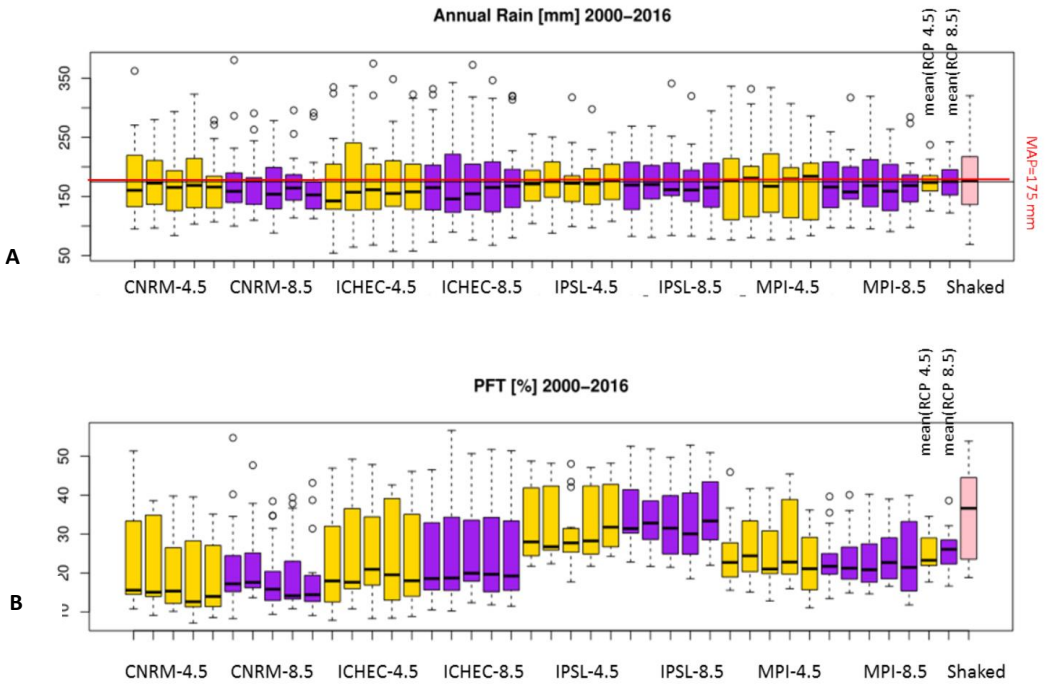

Figure 13: Consistency check of input data and model validation for annual rain in mm (A) and PFTs in % soil cover (B).

Estimated future impacts

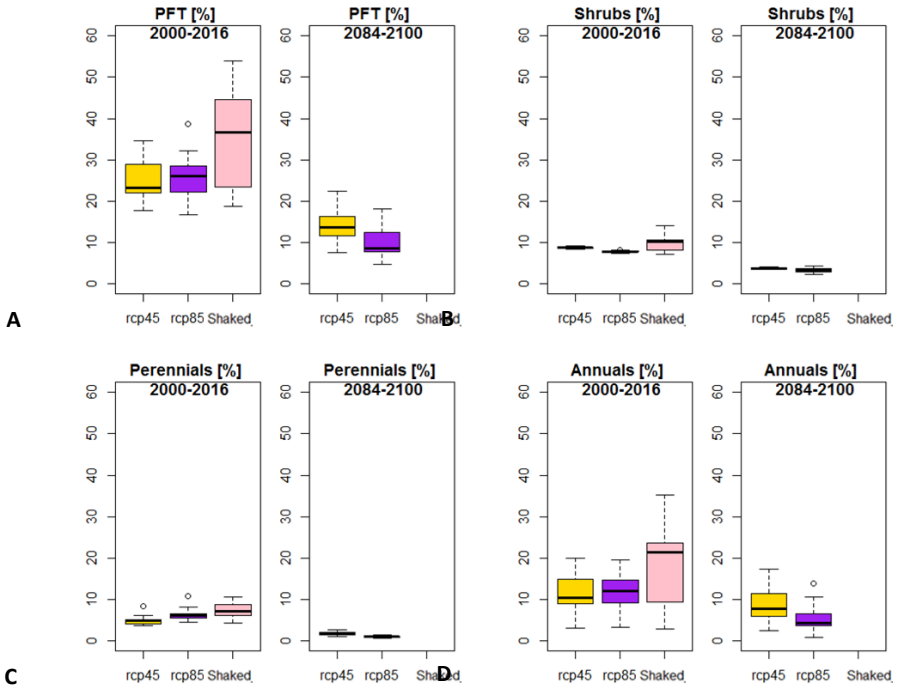

Figure 14: Estimated plant cover in % across all PFTs (A), for shrubs (B), perennials (C), annuals (D) as a mean from simulations driven by climate inputs from CNRM, ICHEC, IPSL and MPI for the reference period 2000-16 and the projected period 2084-2100.

The results for the period 2084-2100 show a decline of vegetation cover across all PFTs by 50 % and 60 % for RCP4.5 and RCP8.5, respectively (Fig. 14A). These distinctions reflect the difference in mean annual precipitation for the two RPCs across all GCMs by the end of the 21st century, with around 150 mm and 110 mm respectively. Shrubs (Fig. 14B), perennials (Fig. 14C) and annuals (Fig. 14D) show a consistently a higher loss of vegetation cover under RCP8.5, although the vegetation cover of perennials and shrubs is nearly zero already under RCP4.5. For RCP4.5,

Co-funded by the European Union

the overall simulated vegetation is predicted to cover around 12 % of the soil towards 2100, with a strong dominance of annual grasses and decline in shrubs and perennials. Similarly, also scenario RCP8.5 leads to a shift in towards annual grassland vegetation resulting in an overall vegetation cover of 8% at the end of this century.

Discussion and Conclusion

The results indicate a considerable uncertainty in the climate input data, as well as their implication for vegetation modelling. The consistency assessment reveals deviance in mean and variability between the modelled precipitation inputs and observed data. It furthermore indicates that neither mean nor variability between years are good predictors of the vegetation cover, but differences in the distribution of precipitation at a smaller temporal scales control the modelled overall vegetation cover.

Despite these uncertainties, a strong climate change impact is expected in the vegetation composition of the semi-arid transition zone in the northern Negev, with a heavy decline in shrubs and perennials, and a reduction in overall vegetation cover and biomass. These results are consistent with other studies of the Negev desert that predict increased degradation, recomposition of the vegetation structure with a reduction of primary production, and further implications also for wildlife and livestock, possibly even desertification along with the expected increase in aridity and evapotranspiration (Shachak 2005, Orenstein et al. 2012, Zaady & Moshe 2001, Kafle & Bruins 2009, Ziv et al. 2014).

References

D'Onofrio, D., Palazzi, E., von Hardenberg, J., Provenzale, A., Calmanti, S. (2014). Stochastic rainfall downscaling of climate models. *Journal of Hydrometeorology*, *15*(2), 830-843.

Golan-Angelko, A., Bar-Or, Y. (2008). Israeli preparation for global climate change. Ministry for Environmental Protection, Office of the Chief Scientist [Hebrew], Jerusalem.

Golodets, C., Sternberg, M., Kigel, J., Boeken, B., Henkin, Z., No'am G, S., & Ungar, E. D. (2015). Climate change scenarios of herbaceous production along an aridity gradient: vulnerability increases with aridity. *Oecologia*, *177*(4), 971-979.

Kafle, H. K. and Bruins, H. J. (2009). Climatic trends in Israel 1970–2002: warmer and increasing aridity inland. *Climatic Change*, *96*(1-2), 63-77.

Lavee, H., Imeson, A. C., Sarah, P. (1998). The impact of climate change on geomorphology and desertification along a Mediterranean-arid transect. *Land degradation & development*, *9*(5), 407-422.

Miranda, J. D. D., Armas, C., Padilla, F. M., Pugnaire, F. I. (2011). Climatic change and rainfall patterns: effects on semi-arid plant communities of the Iberian Southeast. *Journal of Arid Environments*, *75*(12), 1302-1309.

Orenstein, D., Groner, E., Argaman, E., Boeken, B., Preisler, Y., Shachak, M., Ungar, E.D., Zaady, E. (2012). An Ecosystem Services Inventory: Lessons from the Northern Negev Long-Term Social Ecological Research (LTSER) Platform. Geography Research Forum. 32. 96-118.

Pe'er, G. and U. N. Safriel (2000). Impact, Vulnerability and Adaptation to Climate Change in Israel. In: Israel's National Report on Climate Change under the United Nations Framework Convention on Climate Change. Sde Boqer Campus of Ben-Gurion University of the Negev, Sde Boqer. (available online: http://www.bgu.ac.il/BIDR/rio/Global91-editedfinal.html)

Waide, R., French, C., Spratt, P., Williams, L (1998). The long-term Ecological Research Network. USLTER Network Publication. Albuquerque: University of New Mexico.

Zaady, E., Shachak, M., Moshe, Y. (2001). Ecological approach for afforestation in arid regions of the northern Negev Desert, Israel. *Deforestation, Environment and Sustainable Development, A Comparative Analysis, edited by: Vajpeyi, D*, 219-238.

Ziv, B., Saaroni, H., Pargament, R., Harpaz, T., Alpert, P. (2014). Trends in rainfall regime over Israel, 1975–2010, and their relationship to large-scale variability. *Regional environmental change*, *14*(5), 1751-1764.

Co-funded by the European Union

2.5 Peneda-Gerês: Hydrological impacts under scenarios of climate change in the Vez watershed

By Claudia Carvalho-Santos, Bruno Marcos, Adrián Regos, António T. Monteiro, Elisa Palazzi, Silvia Terzago, João Pedro Nunes and João Pradinho Honrado

Introduction

The provision of freshwater ecosystem services is very important for the human well-being, but fires and climate change are strongly influencing their provision. Climate change may potentially have a significant impact on surface runoff, soil erosion and water quality. The aim of this study is to simulate climate change impacts with the SWAT (Soil and Water Assessment Tool) hydrological model to a medium watershed of Portugal, Vez watershed (Carvalho-Santos et al., 2016).

Methods

The Vez is a subsidiary of river Lima, and drains a medium watershed (260 km2) in northwest Portugal (Figure 15). This mountainous watershed, mainly constituted by granite rock, has a complex topography with altitudes ranging from 30 m up to 1400 m and slopes higher than 25% in half of the watershed. It receives high levels of precipitation all over the year with exception of two dry months in summer (June and July). Annual precipitation is about 2000 mm and average temperature is 13ºC. The main land cover in the watershed is shrubland (tall and dwarf), followed by forests (European oak, Pines and Eucalypts) and agriculture in the valleys rotating grass in the winter and corn in summer.

In a parametrized SWAT model for Vez watershed (Carvalho-Santos et al., 2016), climate change scenarios RCP 4.5 and 8.5 for 2020-2050, developed by CNR team, were simulated using four climate models for each scenario (CNRM-CM5, EC-EARTH, IPSL-CM5A-MR, MPI-ESM-LR) and compared to the respective historical period of 1970-2000. The following variables were available at daily scale: precipitation, maximum and minimum temperature, relative humidity and solar radiation.

Co-funded by the European Union

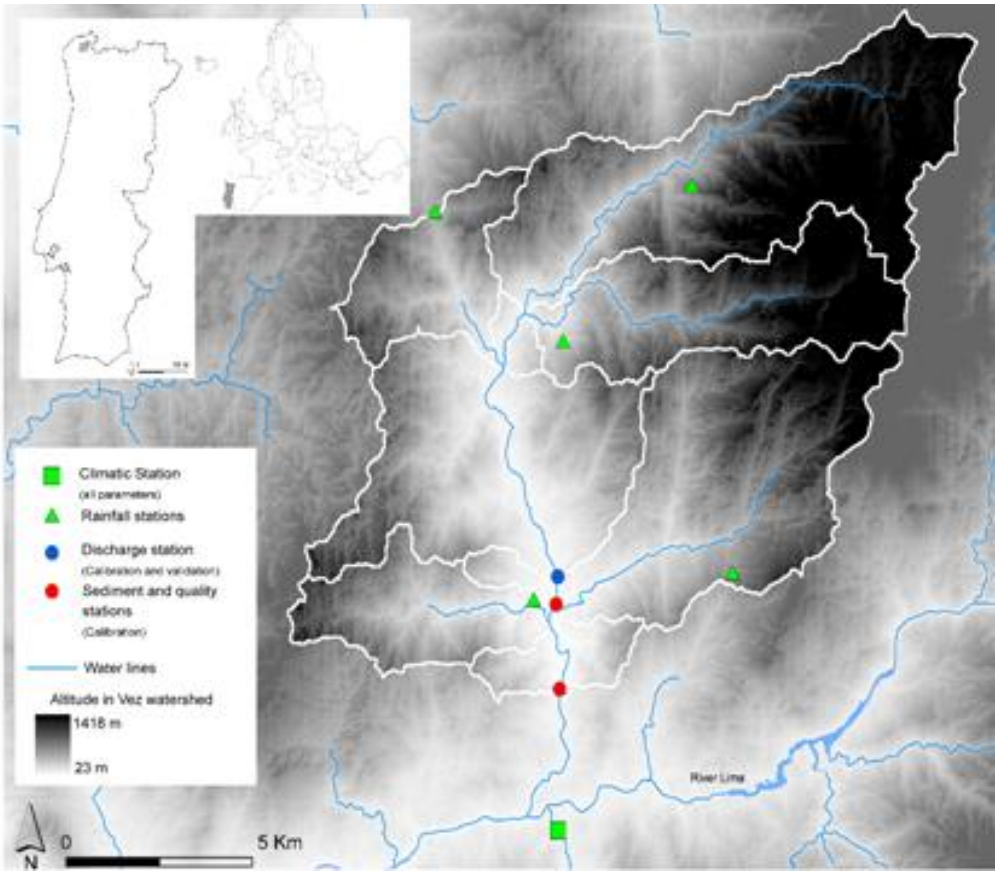

Figure 15: Vez watershed

Results

Climate projections forecast an increase in temperatures (between 1ºC to 1.5ºC) by 2050 in the Vez watershed (Fig. 15), whereas precipitation is predicted to slightly decrease (up to 15mm less annually), or even increase in model EC-Earth. This irrelevant decrease is a result of a net loss in summer being outweighed by a gain in winter, emphasizing the dry and wet periods. These expected changes in climate conditions have been investigated in previous studies for the Vez watershed in the transition climatic zone Atlantic/Mediterranean (Carvalho-Santos et al., 2016; Carvalho-Santos et al., 2017). Overall, future climate tends to be warmer all over the year, wetter in winter and dryer in summer.

Co-funded by the European Union

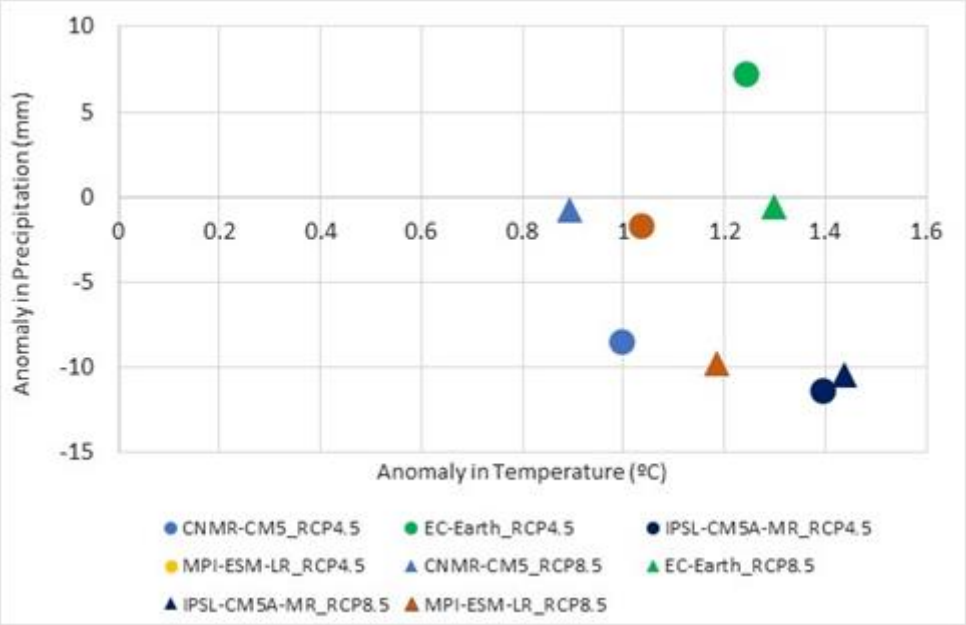

Figure 16: Anomaly in Temperature (average ºC) and Precipitation (mm) for the 4 models used in the study, and respective scenarios (RCP 4.5 and 8.5), for 2020-2050 compared to 1970-2000.

Regarding the impact of future climate on water resources, and as it was expected from the precipitation pattern, there is a tendency for increasing seasonal discrepancies, namely more river discharge in Winter months and less in Spring, Summer and Autumn (Fig. 17). This is in line of what was observed in the previous study, although using different climate projections and different methods for downscaling projections (C. Carvalho-Santos et al. 2016). In terms of scenarios, RCP4.5 presents more water in the river during winter months, which can increase the probabilities of flooding events in years of extremes in precipitation. When observing the total annual water yield in the watershed (Fig. 18), there is a tendency for decrease water in all models when compared to 1970-2000, except for EC-Earth model, which gives more water in the watershed, especially under scenario RCP4.5.

By 2050, average soil erosion in the Vez watershed will increase, more for the simulations with models EC-Earth and IPSL-CM5A-MR, and in general more for scenario RCP8.5 (Fig. 19). More precipitation in winter months, associated probably to more extreme precipitation episodes, may lead to more soil erosion.

Co-funded by the European Union

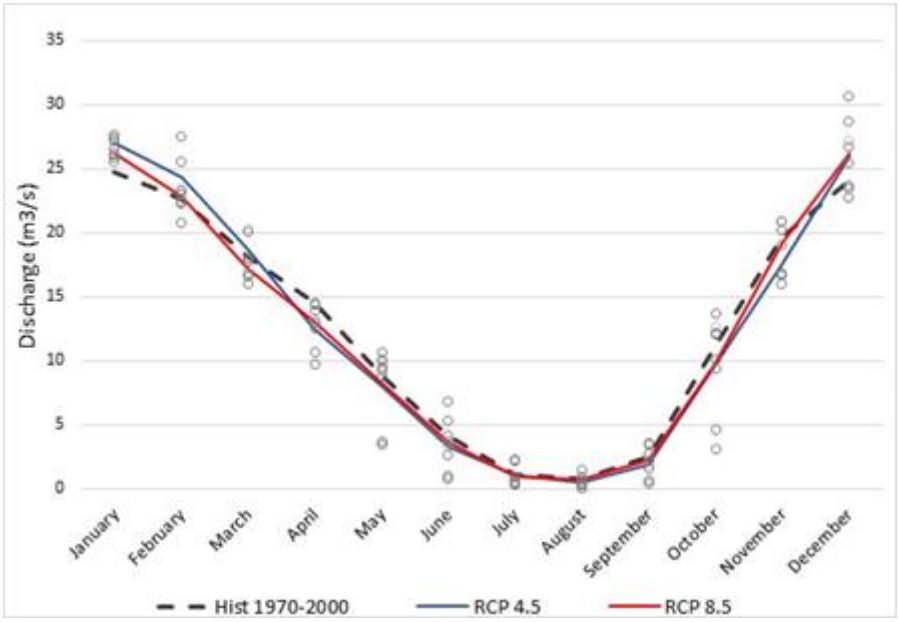

Figure 17: Discharge (m3/s) at the outlet of River Vez watershed, by month, average for the historic period 1970-2000 compared with 2020-2050, scenarios RCP 4.5 and 8.5. Grey dots represent the variation from the simulation by different climate models (CNRM-CM 5, EC-EARTH, IPSL-CM5A-MR, MPI-ESM-LR).

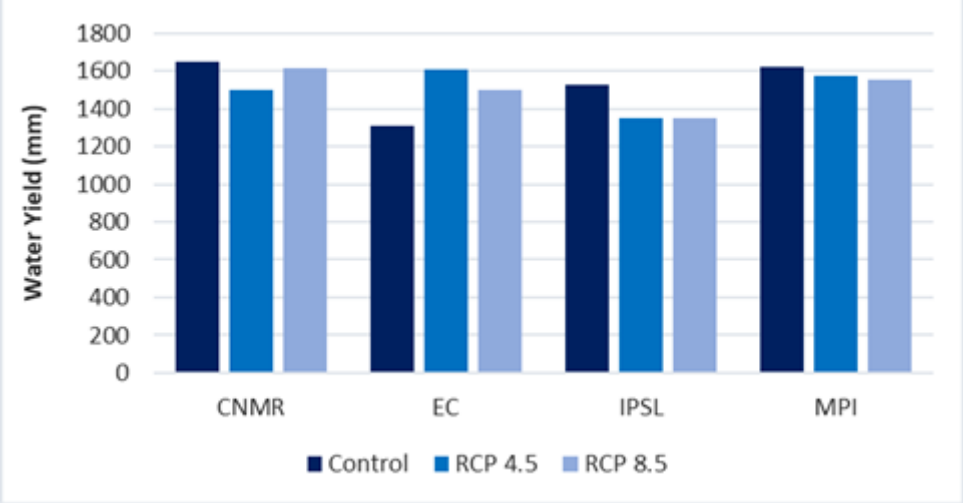

Figure 18: Water yield (mm) by climate model in Vez watershed, for 2020-2050 compared to control period 1970-2000.

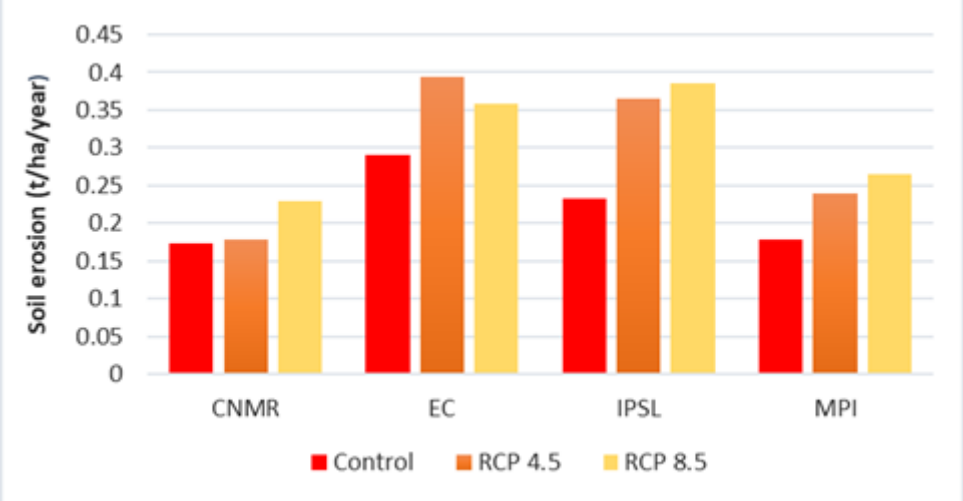

Figure 19: Average soil erosion (t/ha/year) by 2020-2050 compared to control period 1970-2000.

Co-funded by the European Union

Conclusion

Seasonal climate patterns will be more defined in the future, with consequences on the quantity of water available in the Vez watershed. On one hand, there will be more water during winter with possible risk for floods. On the other hand, less water in spring, summer in autumn will bring concerns around lack of water in the river and in general in the watershed, with consequences for water supply and quality, irrigation and on the adaptation of freshwater organisms. The understanding of climate change impacts on hydrological services provision can help decision makers to choose better options regarding landscape adaptation measures.

References

Carvalho-Santos, C., Monteiro, A.T., Azevedo, J.C., Honrado, J.P., Nunes, J.P. (2017). Climate Change Impacts on Water Resources and Reservoir Management: Uncertainty and Adaptation for a Mountain Catchment in Northeast Portugal. *Water Resour. Manag*. 31. https://doi.org/10.1007/s11269-017-1672-z.

Carvalho-Santos, C., Nunes, J.P., Monteiro, A.T., Hein, L., Honrado, J.P. (2016). Assessing the effects of land cover and future climate conditions on the provision of hydrological services in a medium-sized watershed of Portugal. *Hydrol. Process.* 30. https://doi.org/10.1002/hyp.10621.

Co-funded by the European Union

2.6 Curonian Lagoon: How will the climatic changes alter the physical functioning of the Curonian Lagoon?

Georg Umgiesser, Arturas Razinkovas-Baziukas, Dalia Baziuke, Natalja Čerkasova, Petras Zemlys and Jovita Mezine

Abstract

The ecosystem of Curonian lagoon is known to be highly eutrophic and experiencing heavy cyanobacteria blooms. However, the development of the cyanobacteria is largely controlled by the ambient physical factors such as riverine discharges, wind induced intrusions of marine water and the ambient temperature itself. The SHYFEM model was run to reproduce the hydraulic circulation of the Curonian lagoon including the spatial structure of the renewal time for years 2004-2016 to produce statistical evidence of the relationship between the hydrological and climatic characteristics as riverine loads on ambient temperature, salinity, renewal time and water fluxes during the same period.

Using the climate scenarios RCP4.5 and RCP8.5 data downscaled to the Lithuanian coast the SHYFEM model was run to represent the hydraulic circulation of the lagoon in the years 2015-2075 and derive the parameters that could be used to predict temperature and salinity levels as well as renewal time in the Curonian Lagoon.

Introduction

The Curonian lagoon is a shallow and large estuarine lagoon with complex interactions between biotic and abiotic components that strongly depend on the riverine water discharged by the Nemunas River into the lagoon as well as saline water intrusions from the Baltic Sea (especially the northern part) and the exchange capabilities of the basin. The Curonian lagoon is a hypereutrophic water body experiencing cyanobacteria blooms quite regularly, which in turn can strongly alter the functioning of the ecosystem. Long dynamics of commercial fishing show clear negative trends as well as changes in the structure of the landings. Therefore, there is an ongoing discussion on whether the fishery policy or the general trend in the ecosystem development (including climatic changes) is the main driver of these changes.

The Curonian lagoon is a mainly freshwater dominated waterbody that is connected to the south-eastern part of the Baltic Sea by a narrow (~300m) strait. Its area is 1584 km^2, which makes it the biggest lagoon in Europe (Fig. 20). Its mean depth is 3.8 meters, and its maximum depth can be found in the Klaipeda strait with 14 meters. Salinity is controlled by the Nemunas River, which brings 98% of the total freshwater runoff (annual discharge 23 km^3) and enters the lagoon in its central area and by water intrusions from the Baltic Sea. It fluctuates in the range 0-7 ‰ with higher salinities in the northern part and fresh water in the southern part.

Co-funded by the European Union

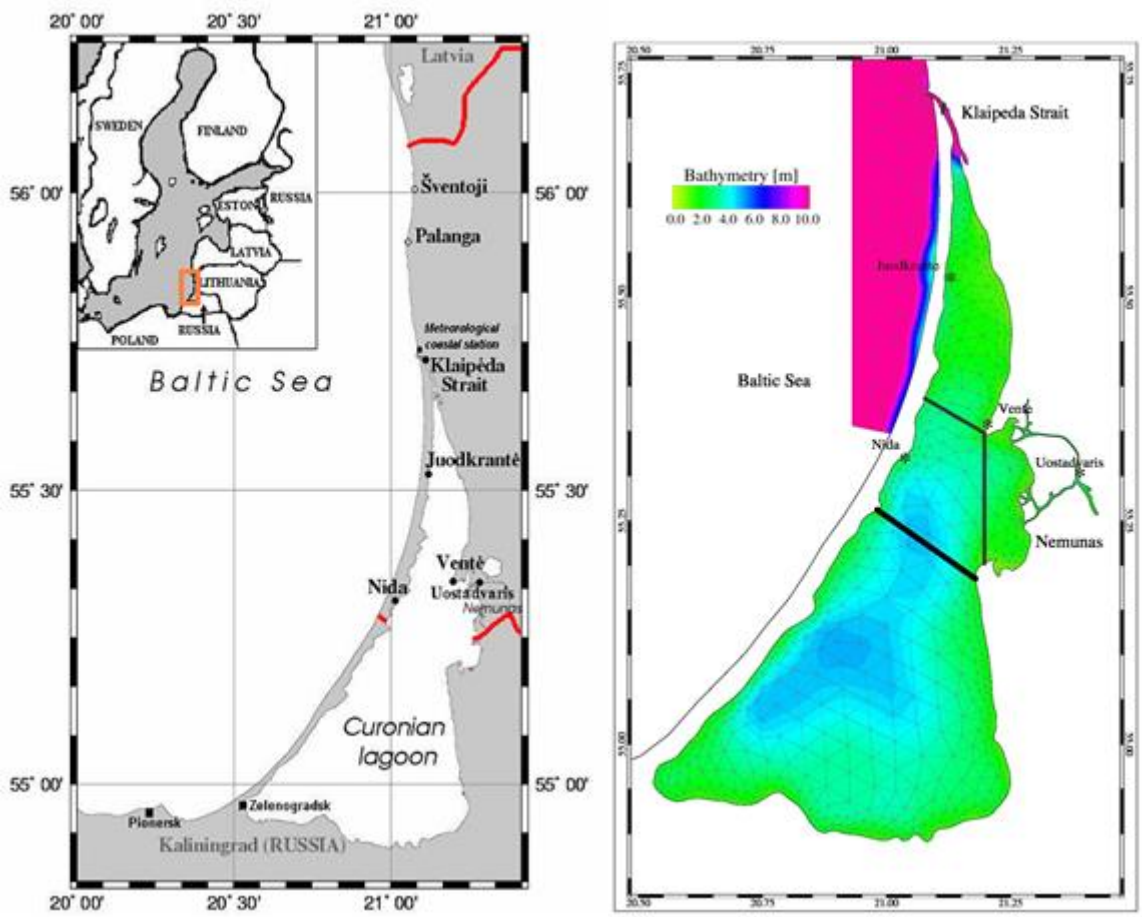

Figure 20: The Curonian Lagoon and its representation in the numerical model.

Methods

A hydrodynamic model (SHYFEM) that was already calibrated and validated in previous works (Umgiesser at al. 2016, Zemlys et al. 2013) was used to evaluate the changes in physical parameters occurring in the Curonian Lagoon under climate change. The horizontal discretization was done on an unstructured grid with 1309 nodes and 2027 elements that simulate the inner lagoon and part of the shelf in front of the lagoon. The vertical discretization used 12 sigma layers.

For the analysis run, data from HIRLAM for meteo data, Lithuania hydro-meteorological service for river discharges and HIROMB (SMHI) forecasts for sea boundary data were used to force the hydrodynamic model. These simulations served as best available data to be compared with the control runs using the climatological data sets.

For the control run and the future scenarios the following climate models were available: CORDEX Rossby Centre regional climate model (RCA4), consisting in 5 sets of simulations (downscaling) driven by the following five GCMs: EC-Earth (ICHEC), CNRM-CM5 (CNRM), IPSL-CM5A-MR (IPSL), HadGEM2-ES (MOHC), MPI-ESM-LR (MPI). Both the sea data and the Nemunas discharge were taken from the RCO-SCOBI model of SMHI. The simulation periods for the analysis run are 2004 – 2015, for the control run 1970 – 2006, and for the future scenario runs 2006 – 2074.

Comparing the coincident years of the analysis data with the one of the control run, a scaled RMS error was computed that shows the percentage error of all meteorological parameters used. The results can be seen in Table 2, and an example of the performance of the model for precipitation can be found in Figure 21. As can be seen, some variables (e.g. rain) show a strong bias with respect to the analysis data. Based on these results and the fact

Co-funded by the European Union

that the data from ICHEC has the lowest errors in the most important parameters (rain, wind), the EC-Earth (ICHEC) meteo data has been chosen for the future simulations.

Table 2: The Curonian Lagoon and its representation in the numerical model.

CNRM:	14.12
ICHEC:	13.38
IPSL:	17.85
MOHC:	12.67
MPI:	13.31

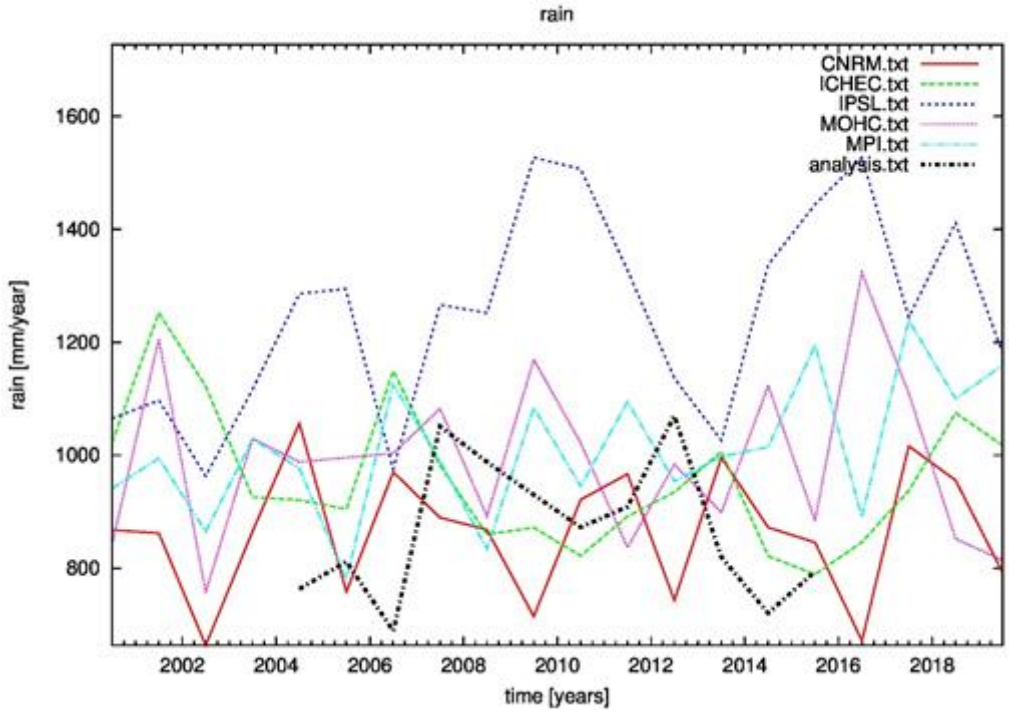

Figure 21: Comparison between climate inputs by several GCMs and observed data (analysis.txt) for precipitation.

Co-funded by the European Union

Results

For water temperature a clear trend towards higher temperatures can be identified. There is no statistical difference between RCP 4.5 and 8.5, however both trends are significant with respect to the present situation. The control run reproduces the analysis data well.

A clear trend in salinity can be identified at Klaipeda Strait. This trend is due to the decreasing salinity of the Baltic Sea. However, data from the climatological control runs is lower than from the analysis run. The analysis data is too short to see if the trend in the control run is coinciding with the trend in the analysis simulations. A salinity trend can also be identified at Juodkrante, inside the lagoon, whereas at Nida salinity is stable (Fig. 22).

Volume fluxes of water exchange at Klaipeda Strait seem to be stable. However, climatological models underestimate these fluxes with respect to the analysis runs. There is no statistical difference between RCP 4.5 and 8.5

In addition, salinity fluxes at Klaipeda Strait are decreasing. This is due to a combined lowering of salinity and water fluxes in the Curonian Lagoon. However, please note that due to the underestimation of salinity and fluxes, the salinity fluxes at Klaipeda Strait are much too low when compared with the analysis run. Salinity intrusion events are slightly decreasing. This fact will be important for the distribution of benthic species that are sensitive to salinity variations. There is no statistical difference between RCP 4.5 and 8.5.

Results concerning water renewal time show a stable trend until the end of the century. There is no statistical difference between RCP 4.5 and 8.5. Even if the northern and southern basin is analysed separately, the picture does not change, and water renewal times are not changing over the analysed century (Fig. 23 and 24).

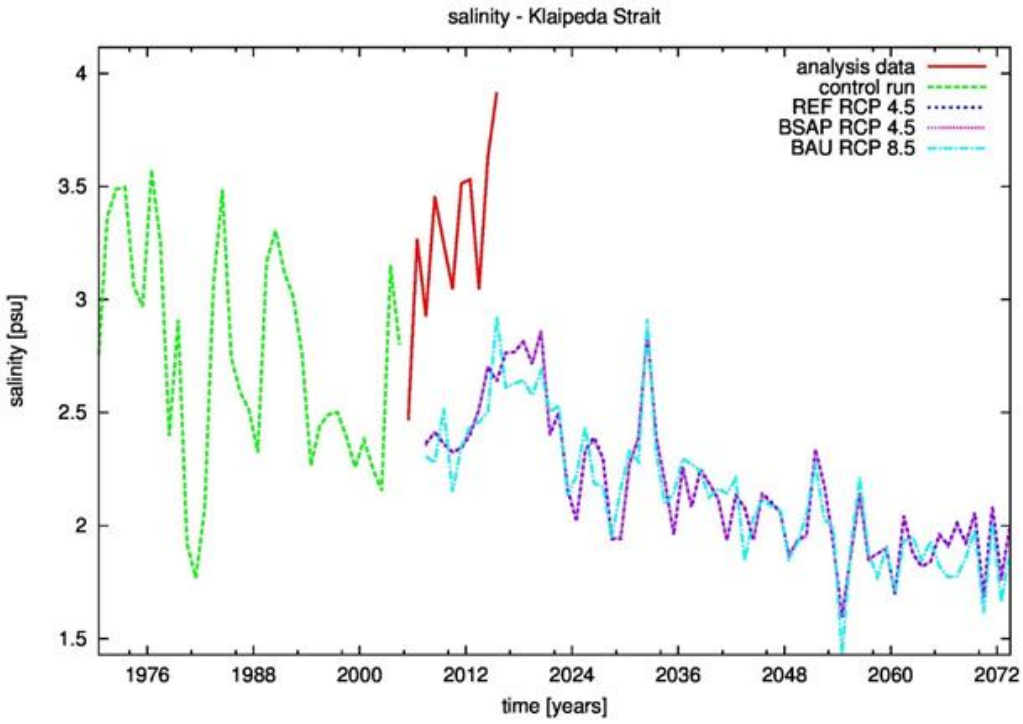

Figure 22: Salinity values: analysis, control run and future projections.

Co-funded by the European Union

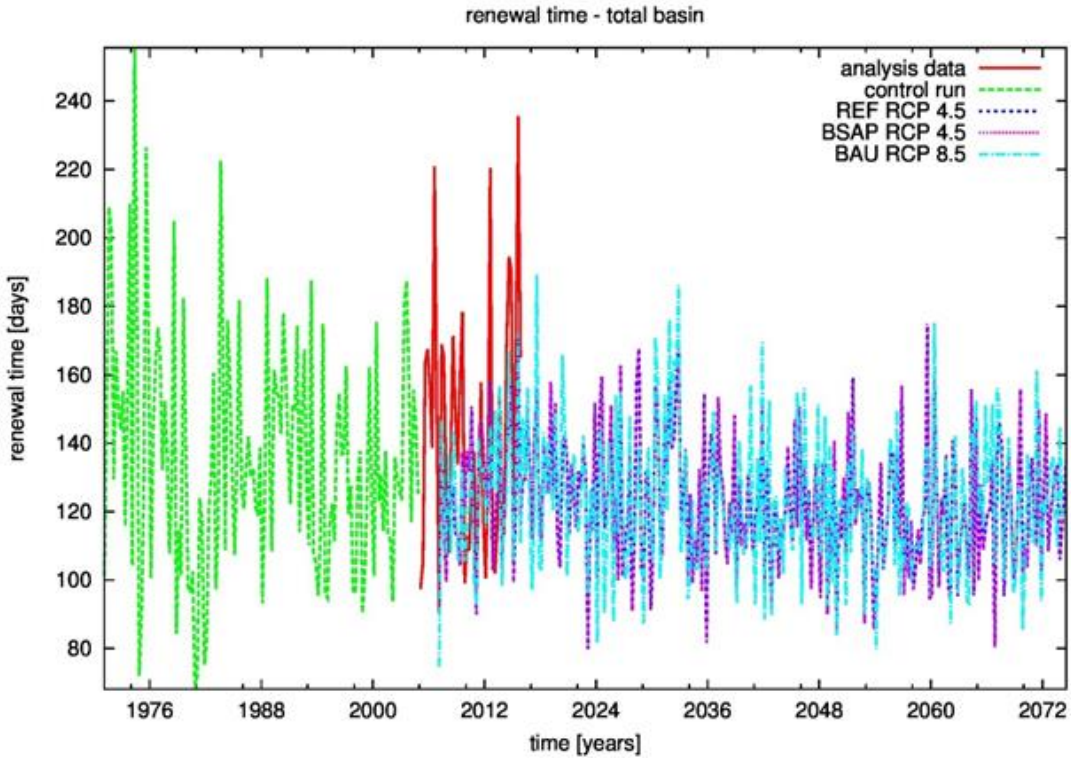

Figure 23: Renewal times: analysis, control run and future projections.

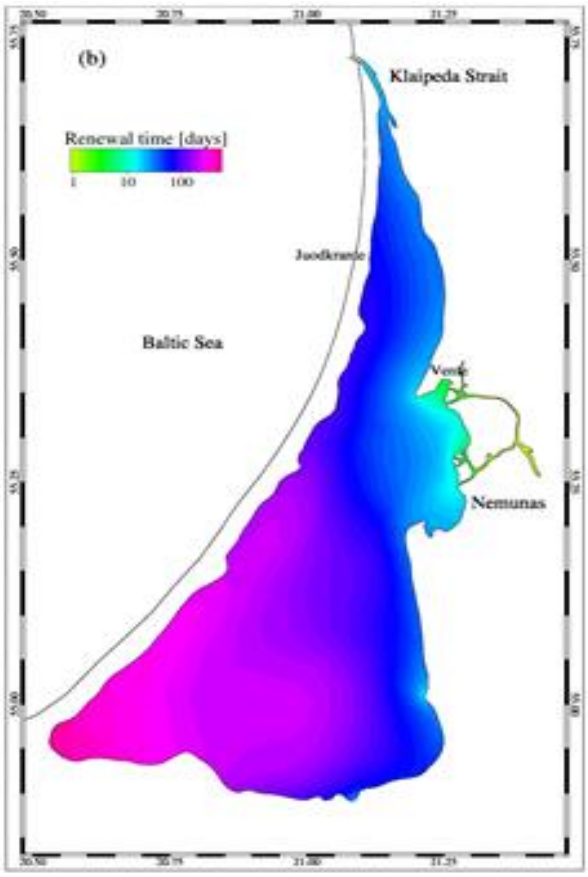

Figure 24: Pattern of water renewal times for the RCP4.5 situation versus the end of the century.

Co-funded by the European Union

Conclusions

Future simulations based on inputs from 5 downscaled GCMs suggest increasing water temperature for the Curonian lagoon.

They also indicate decreasing salinity and stable water fluxes between the lagoon and the Baltic Sea. However, since forcing with climate models do severely underestimate these salinity levels and fluxes, the absolute values of the salinity fluxes will have to be treated with some care.

Salinity intrusions are projected to be less frequent, indicating that salinity variations in the northern part will be less important. This should give rise to a stable benthic community that will not be bothered too much with varying salinity levels.

Finally, water renewal times seem to be stable, and are predicted to not change in the future. This also indicates that the ecological conditions for plants and fish should basically be similar to the present ones.

References

Umgiesser, G., Zemlys, P., Erturk, A., Razinkova-Baziukas, A., Mėžinė, J., Ferrarin, C. (2016). Seasonal renewal time variability in the Curonian Lagoon caused by atmospheric and hydrographical forcing. *Ocean Science, 12(2).*

Zemlys, P., Ferrarin, C., Umgiesser, G., Gulbinskas, S., Bellafiore, D. (2013). Investigation of saline water intrusions into the Curonian Lagoon (Lithuania) and two-layer flow in the Klaipėda Strait using finite element hydrodynamic model. *Ocean Science*, *9*(3): 573-584.

Co-funded by the European Union

2.7 Wadden Sea: Model experiment for the Wadden Sea to assess Climate Change impacts on the ecosystem

By Alex Ziemba, Sonja Wanke and Ghada El Serafy

Introduction

Climate change as an inevitable process, leads to science's engagement to monitor its effects and understand the earth's ecosystem processes. An ecosystem-based approach on the impact of climate change in the Wadden Sea was conducted. Thereby, downscaled global meteorological projection data and predictions changing salinity (SAL) and water temperature (T_w), were utilized to assess ecological and hydrological changes triggered by varying hydro-climatological parameters in the Dutch Wadden Sea. Ecological changes were indicated and assessed with phytoplankton, which served as a bioindicator for ecosystem sanity and functioning.

Methods

Study Area: The Wadden Sea

Denoted as world heritage site by UNESCO in 2009, the Wadden Sea is a precious ecosystem which finds itself exposed to the effects of climate change (UNESCO 2018). The Wadden Sea forms an unique ecosystem, inheriting the greatest chain of intertidal flats in the world and thereby providing a habitat for a wide range of flora and fauna. This includes millions of migratory birds annually and mussel beds as well as thousands of seals. The vulnerable area finds itself exposed to not only direct anthropogenic impacts, such as gas drilling, however, is subject to climatic change, which is triggered by global economic growth and a fast growing populations, requiring an increasing supply of resources and goods. Hence, as much as humans profit from nature's ecosystem services, the constant pressures exerted on the environment is harmful for the ecosystems and the species it inhabits (Figure 1). Once altered by climate change, the Wadden Sea will no longer be the fruitful ecosystem we know and oystercatchers, and other animals will lose their havens (Nelsen 2017).

Phytoplankton as Bioindicator

Monitoring the complex environmental conditions in the study site may be facilitated by the use of phytoplankton as a bioindicator for the intactness of the ecosystem. According to Falkowski et al. (2004) phytoplankton is the major primary producer in the world's oceans, contributing to 50% of the global oxygen (~ 50 Gt C/year) and enhancing carbon sequestration. On a species basis they are single-celled, microscopically sized plants, which form the lowest level of the marine food chain, thus, determining the wellbeing and functioning of the entire species web (Richardson and Schoemann 2004). Phytoplankton is majorly consumed by zooplankton, which is then consumed by small fish and species of higher trophic levels, which are then again consumed by predators, e.g. marine birds as well as humans (Valiela 2015). Besides forming the base of the food network, phytoplankton exports carbon from the euphotic zone to the deeper layers of the ocean, shapes biochemical cycles and influences energy fluxes through the food network. In open oceans phytoplankton are the only primary producers, thereby supporting pelagic food webs. In coastal areas halophytes, macroalgae and microphytobenthos also fixate carbon (Guinder and Molinero 2013). In agreement with Langlois and Smith (2000), phytoplankton may be typically found within the upper 50 meters of the water column in nearshore areas. Chl-a concentrations have been widely used for measuring quantities and abundance of phytoplankton.

Meteorological Data Retrieved from Euro-CORDEX

The climate change ensemble that was used for the simulation was established by the European Coordinated Regional Downscaling Experiment (EURO-CORDEX) initiative. The data provided for the region of the Wadden Sea was developed by EURO-CORDEX through a dynamical downscaling process of global climate models and offers

climate change projections of meteorological variables for the representative concentration scenarios RCP4.5 and RCP8.5. These RCPs describe two scenarios which are determined by the assumptions of increasing radiative forcing up to 4.5 and 8.5 W/m², respectively, until 2100 in respect to pre-industrial conditions.
The projection data presents the values of various hydroclimatological variables until 2100. Specifically, the Wadden Sea climate projection data sets were downscaled with the help of the regional climate model SMHI-RCA4 driven by the following GCMs: EC-Earth, CNRM-CM5, IPSL-CM5A-MR, HadGEM2-ES and MPI-ESM-LR. Given that there are five different GCMs which provided the lateral conditions for the regional climate projections for the study region, there are five input sets, for each RCP4.5 and RCP8.5.

Based on the trends of the data and the statistical analysis, it was decided to use the dataset HadGEM2–Es, provided by the Met Office Hadley Centre, England. This does not go without mentioning that neither of the GCMs are better or worse than another and that all are equally likely or unlikely to occur.

Parameter	Abbreviation	Unit	Frequency [h]
Near Surface Air Temperature	tas	°C	3
Precipitation	pr	mm/day	3
Surface Downwelling Shortave Radiation	rsds	w m-2	3
Eastward Near Surface Wind	uas	m s-1	6
Northward Near-Surface Wind	vas	m s-1	6
Surface Pressure	ps	pa	24
Near-Surface Relative Humidity	hurs	%	24
Total Cloud Cover	clt	%	24

General Modelling Approach
Based on climate change projections of meteorological data derived from GCMs, estimations on the decrease of salinity content and increase of water temperature in the North Sea, climate change impacts are modelled for the Dutch Wadden Sea with the model Delft3D. Thereby, the meteorological data includes radiation, wind, pressure, air temperature, humidity and cloud cover. For the meteorological input, as well as the sea level time series, it was chosen to utilize projections made under the CC scenario RCP4.5. The scenario RCP4.5 describes a moderate, less extreme development of climate, compared to the scenario RCP 8.5, which was also available. Nevertheless, it has to be stated that the RCP scenarios are not assigned with probabilities of occurrence and are thus equally likely to occur (compare IPCC, 2018). For the meteorological data the CORDEX dataset was adopted. The dataset provides projections which reach from 2006 until November 2099. Additionally, it assumes that one year consists of 360 days, where each month has 30 days.

Throughout the simulation process, changes of hydrodynamic components are analysed with the component D-Flow. Moreover, outputs generated by this Delft3D module are utilized to simulate water quality statuses with

D-WAQ. The outputs observed from the D-Flow simulation include changes of water temperature (T_w) and salinity (SAL). The outputs computed by D-WAQ include chl-a content, which in this case serves as proxy to make conclusions about phytoplankton biomass and net primary production.

Results

Three different stations, namely Dantziggat, Marsdiep and Harlingen, in the Dutch Wadden Sea were selected to show the effects of projected Climate Change looking at salinity, water temperature and chlorophyll-a concentration.

It was shown that T_w behaves as expected (Fig. 25-27): with proceeding time the temperature of the sea water was shown to rise as a direct effect of global warming. The increase of T_w peaks at approximately 2 °C in Harlingen, while Dantziggat and Marsdiep follow with 1.81 °C and 1.76 °C, respectively, until 2090 compared to 2010. Additionally, an elongation of the warm period can be observed. A trend towards increasing ranges of magnitude of water temperatures was assessed with increasing differences between max and min values in all stations (Tab. 3).

Results for Salinity and Water Temperature

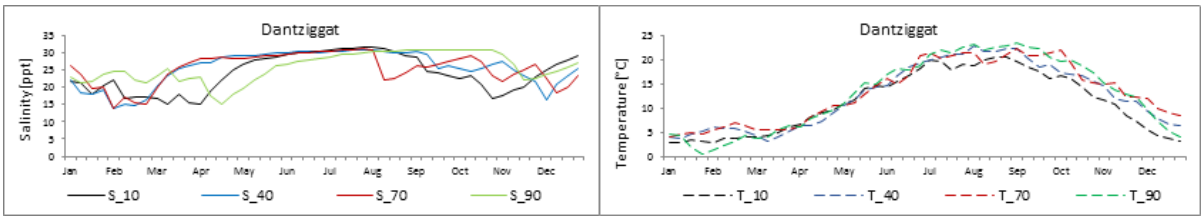

Figure 25: SAL (left) and Tw (right) predictions in Dantziggat derived under the pressures of climate change for 2010, 2040, 2070 and 2090 for the top vertical layer σ=1.

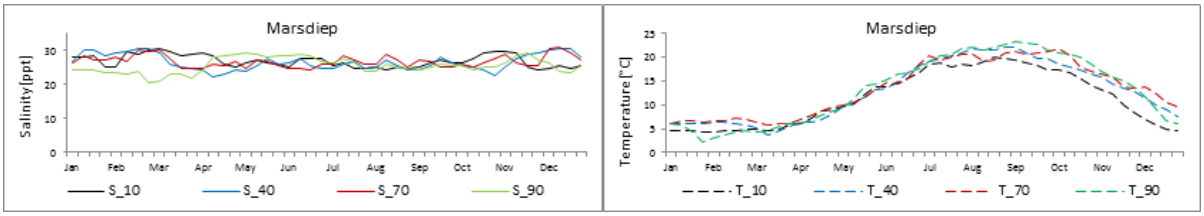

Figure 26: SAL (left) and Tw (right) predictions in Marsdiep derived under the pressures of climate change for 2010, 2040, 2070 and 2090 for the top vertical layer σ=1.

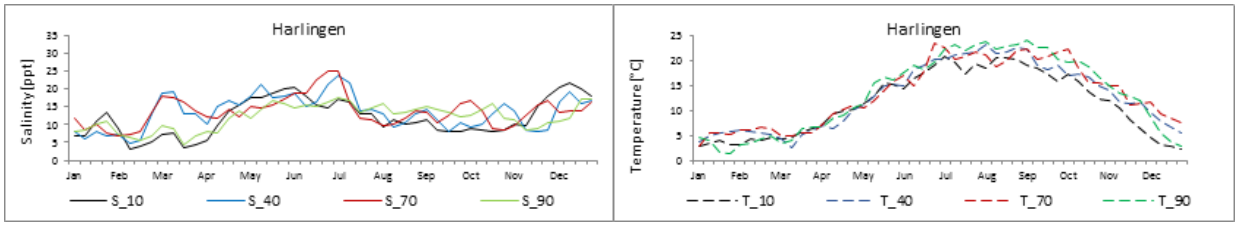

Figure 27: SAL (left) and Tw (right) predictions in Harlingen derived under the pressures of climate change for 2010, 2040, 2070 and 2090 for the top vertical layer σ=1

Table 3: Key Values of Weekly Tw [°C] for σ = 1 (top layer) under the Impacts of Climate Change

	Dantziggat				**Marsdiep**				**Harlingen**			
	Max	Min	Mean	Change to baseline	Max	Min	Mean	Change to baseline	Max	Min	Mean	Change to baseline
2010	19.91	4.24	11.45	0.00	20.53	2.90	11.18	0.00	20.70	2.10	11.34	0.00

Co-funded by the European Union

2040	22.05	3.69	12.89	1.44	22.86	3.12	12.54	1.36	23.15	2.49	12.75	1.40
2070	21.72	5.86	13.49	2.04	22.09	3.97	13.19	2.01	23.36	2.95	13.35	2.01
2090	23.42	2.27	13.25	1.81	23.49	0.36	12.49	1.76	24.04	1.25	13.23	1.89

SAL values did not behave as uniformly among the stations as T_w: while Dantziggat and Harlingen experienced an increase of mean SAL values during the projected years, only Marsdiep displayed the expected decrease of SAL (see Fig. 26). While the change of SAL in Harlingen was rather minor with solely an increase of 0.19 ppt in 2090 compared to 2010, SAL in Dantziggat rose by nearly 2 ppt. Marsdiep, on the other hand, simulated a decrease of SAL of approximately 1.30 ppt for 2090 (Tab. 4). As mentioned Harlingen and Dantziggat are much shallower than Marsdiep (approximately half the depth), suggesting greater impacts of the increasing SAL triggered by increasing SLR at the boundaries of the model, as well as greater impacts of meteorological processes. Very interesting is to see that even though the trend of the annual mean did not degrade for all stations, the max values of SAL at all three stations uniformly decreased (Tab. 4). Trending differences were found in the min values, which decreased as well in Marsdiep, however, increased in Dantziggat and Harlingen, suggesting a redistribution of this variable and a densification of higher values in the range of magnitude.

Table 4: Key Values of Weekly SAL [ppt] for σ = 1 (top layer) under the Impacts of Climate Change.

	Dantziggat				**Marsdiep**				**Harlingen**			
	Max	Min	Mean	Change to baseline	Max	Min	Mean	Change to baseline	Max	Min	Mean	Change to baseline
2010	31.41	14.94	23.93	0.00	30.36	24.35	26.91	0.00	21.49	3.06	11.91	0.00
2040	30.83	13.94	25.45	1.51	30.71	22.36	26.66	-0.25	23.61	4.73	13.44	1.54
2070	30.97	14.03	25.45	1.31	30.96	24.12	26.79	-.012	25.08	6.98	13.75	1.84
2090	30.87	15.28	25.77	1.84	29.22	20.76	25.58	-1.33	17.66	4.38	12.10	0.19

Projected chl-a concentrations for all monitoring stations for the top vertical layer σ=1 are presented in Figure 28-30. Seasonal trends which were determined prior in the baseline assessment do not seem to be affected by climate change processes on the first glance. However, viewing each monitoring station separately, some changes in peaks and magnitudes may be encountered. In Dantziggat, a decrease of chl-a in spring occurred compared to the baseline, while a slight increase took place in the winter months. In Marsdiep on the other hand an increase of chl-a took place in spring, as well in the months up to October, where the projections cross the baseline simulation trend, leading to lower predictions of chl-a in winter. Additionally, the spring and autumn peaks were shifted left, occurring earlier than in the baseline for the years 2070 and 2090. In Harlingen, a shift of the blooming periods to the left occurred likewise, leading to higher chl-a concentrations in February and March and to lower concentration in the following spring months. Once again, an increase of chl-a occurred in summer while a decrease took place in winter. In order to see the development of total annual concentrations the cumulative values were presented in the right column of Figure 28-30. In Dantziggat a decrease of chl-a concentrations occurred in the projected years, while in Marsdiep there was a clear trend to increasing chl-a concentrations. For Harlingen high chl-a concentration were computed for 2040, while low concentrations were computed for 2070 and 2090 in respect to the baseline. For further analytical assessment the key values were summarized in Table 5.

Table 5: Key Values chl-a Concentration [mg/m3] for σ = 1 (top vertical layer) under the Impacts of Climate Change.

	Dantziggat				Marsdiep				Harlingen			
	Max	Min	Mean	Change to baseline	Max	Min	Mean	Change to baseline	Max	Min	Mean	Change to baseline
2010	14.97	0.12	4.05	0.00	12.31	0.11	3.65	0.00	9.34	0.00	2.85	0.00
2040	12.98	0.37	4.01	-0.04	13.14	0.04	3.73	0.08	9.64	0.00	2.96	0.11
2070	11.70	0.10	3.57	-0.48	12.76	0.04	3.55	-0.10	9.63	0.00	2.51	-0.33
2090	12.31	0.11	3.65	-0.40	12.95	0.03	3.55	-0.10	10.15	0.00	2.53	-0.31

Results for Chlorophyll-a Concentrations

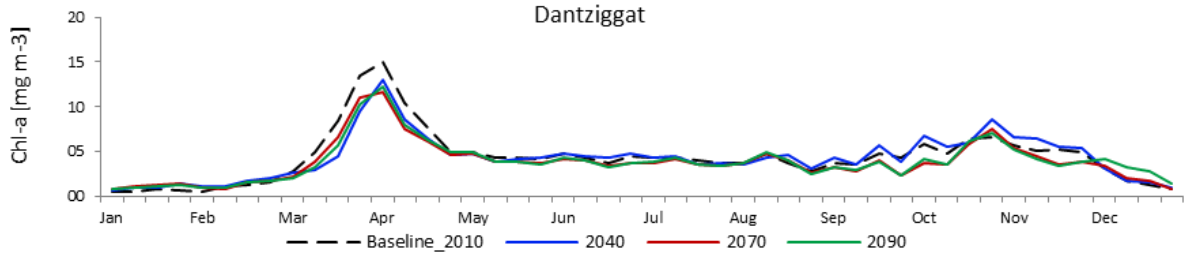

Figure 28: Time series of total chl-a concentration for each the baseline year (black, dotted line), as well as for the projected years 2040 (blue line), 2070 (red line) and 2090 (green line) for the Dantziggat monitoring.

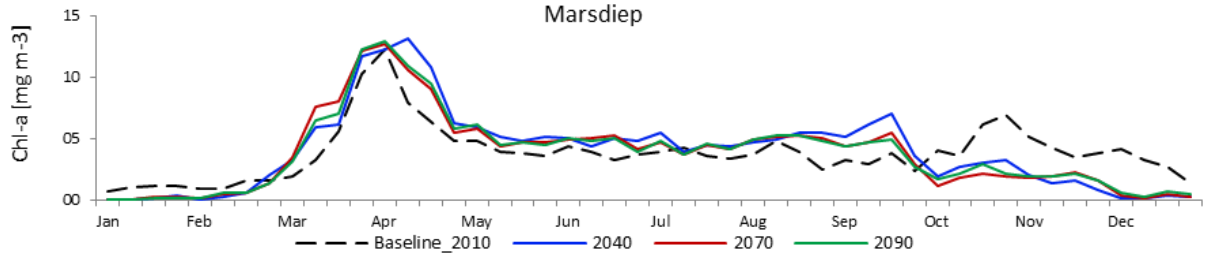

Figure 29: Time series of total chl-a concentration for each the baseline year (black, dotted line), as well as for the projected years 2040 (blue line), 2070 (red line) and 2090 (green line) for the Marsdiep monitoring.

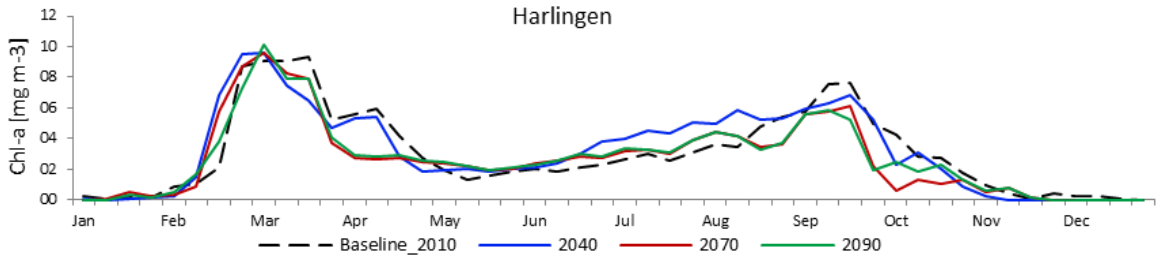

Figure 30: Time series of total chl-a concentration for each the baseline year (black, dotted line), as well as for the projected years 2040 (blue line), 2070 (red line) and 2090 (green line) for the Harlingen monitoring.

Co-funded by the European Union

Conclusion

Modelling was applied with the objective to better understand the effects of climate change on the hydrodynamic and ecological realms. The results suggest that predictions of the hydrodynamic parameters, ocean salinity and water temperature, strongly impact the development of biotic variables. Ecological change was monitored with the bioindicator phytoplankton, simulated using chlorophyll-a as a proxy. It was found that phytoplankton abundance decreased until 2090. In addition, shifts in species compositions were predicted. These findings imply a reduction of photosynthetic biomass in the Wadden Sea system, as well bottom-up cascading effects impacting higher trophic levels. The shifts of species compositions were shown to bear threats by provoking harmful algae blooms.

References

Guinder, V. A., Molinero, J. C. (2013). Climate Change Effects on Marine Phytoplankton. In *Marine Ecology in a Changing World* (pp. 10.1201/b16334-4).

Langlois, G. W., Smith, P. (2000). Biology and Ecological Niches in the Gulf of the Farallones: Phytoplankton. *Beyond the Golden Gate - Oceanography, Geology, Biology, and Environmental Issues in the Gulf of the Farallones* , 32-35.

Nelsen, A. (2017, Jun 16). Gas Grab and Global Warming Could Wipe out Wadden Sea Heritage Site. *The Guardian*.

Richardson, A. J., & Schoeman, D. S. (2004, September 10). Climate Impact on Plankton Ecosystems in the Northeast Atlantic. *Science Vol. 305, Issue 5690*, pp. 1609-1612.

UNESCO (World Heritage Centre). (2018, March 16). *Wadden Sea*. Retrieved from http://whc.unesco.org/en/list/1314.

Valiela, I. (2016). *Marine Ecological Processes - Third Edition.* Springer.

Co-funded by the European Union

2.8 Sierra Nevada: Climate and land use changes effects on ecosystem services status

By Ricardo Moreno, Domingo Alcaraz-Segura, Javier Herrero Lantarón, Francisco Javier Bonet García and Agustín Millares Valenzuela

Abstract

Climate and land use changes are the main drivers that can affect the ecosystem services provision in Sierra Nevada. It is necessary to develop methods to help decision makers in maintaining or improving ecosystem services in protected areas in the future. We are developing a Bayesian Belief Network (BBN) model to assess land use future scenarios. Once future land uses have been developed, we will assess ecosystem services using several models like WiMMed. Future climate scenarios are very useful as an input in both processes. Finally, we will evaluate the effects of several climate and land use scenarios on the ecosystem services status. All this information could help decision makers to understand how the key factors will affect ecosystem services and how to prevent its deterioration.

Introduction

Land-use change (deforestation for crops and pastures, reforestation, firewood removal, etc.) constitutes one of the primary drivers of global change, since human activity is to a greater or lesser degree altering the vegetation cover of the planet. The combined effects of climate change and shifts in land use determine the distribution and structure of the vegetation of the Sierra Nevada, and the associated ecosystem services. The surface cover of tree formations in Sierra Nevada has expanded from 15% to 51.23% over the last 60 years. Similarly, a densification of the scattered tree cover and the natural forests and a decline in the surface area occupied by cultivated fields (from 17.8% to 4.72%) has occurred in the last six decades (Marcellus-Zamora et al. 2016). Therefore, it is important to ascertain future land use change and its effects on the ecosystem services provided.

The main purpose of this study is to facilitate the land-use management of Protected Areas (PAs) based on ecosystem services evolution under different land use and climate scenarios.

Methods

Study area

Sierra Nevada (Andalusia, SE Spain), is a mountainous region covering more than 2000 km^2 with an altitudinal range of between 860 m and 3.482 m a.s.l. (Fig. 31). The climate is Mediterranean, characterized by cold winters and hot summers, with pronounced summer drought (July-August). The annual average temperature decreases in altitude from 12–16°C below 1.500 m to 0°C above 3.000 m a.s.l., and the annual average precipitation is about 600 mm.

Co-funded by the European Union

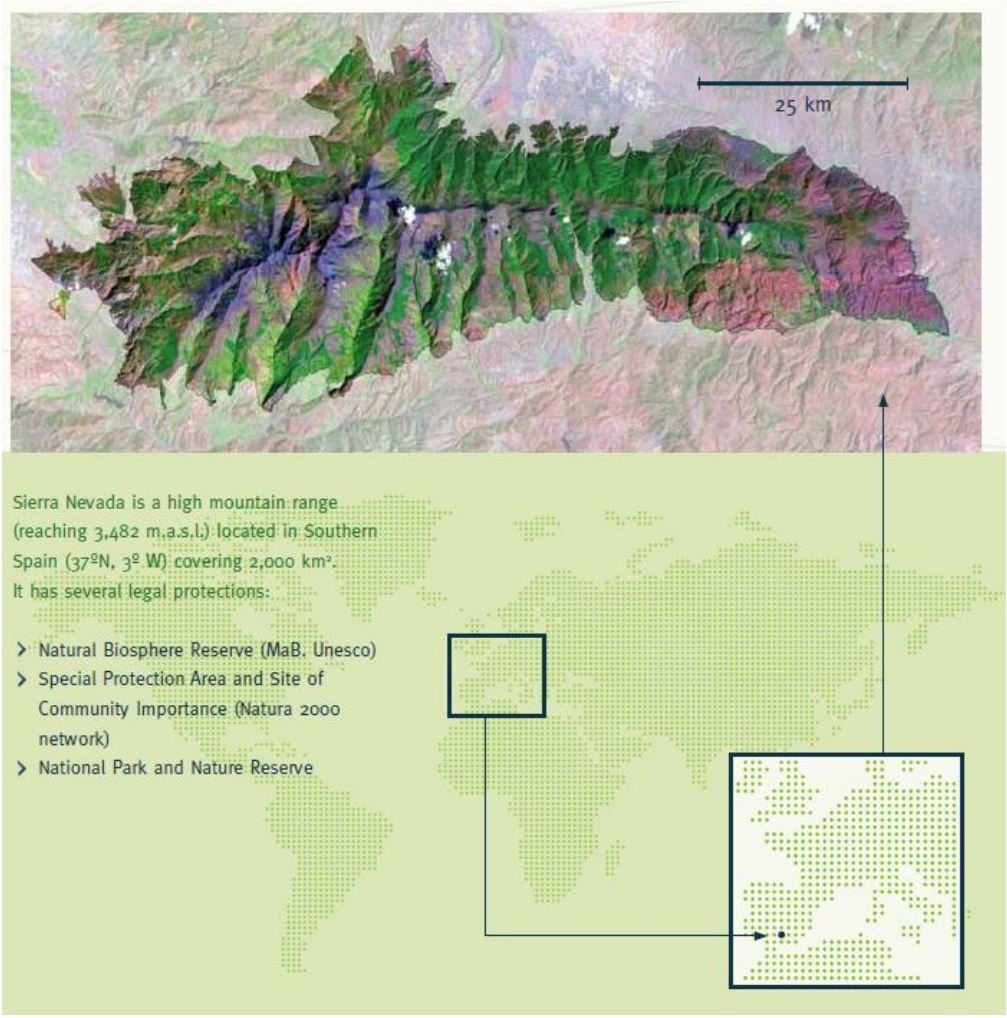

Figure 31: Location of Sierra Nevada

Global process

The first step is to develop future land use scenarios for Sierra Nevada. For this purpose we are developing a BBN. Afterwards, the land use scenarios generated will be the main input to assess derived ESS using models as WiMMed (Fig. 32).

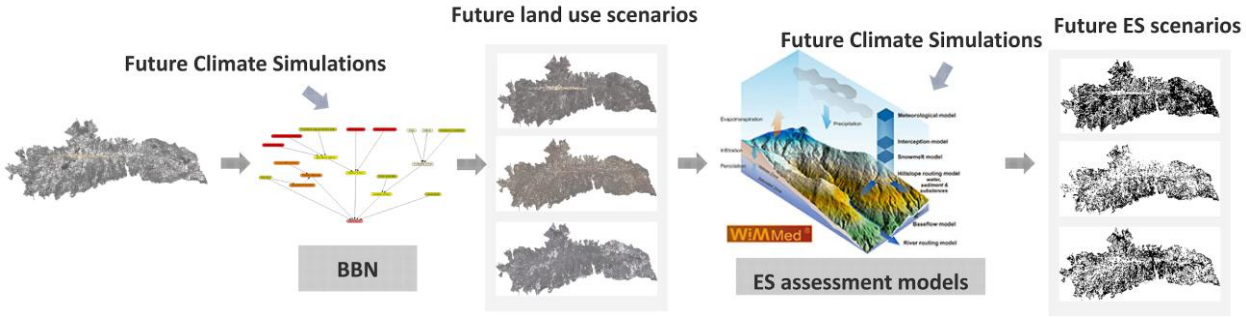

Figure 32: Global process of future ESS scenarios assessment. Future climate scenarios act as an input to develop land uses scenarios BBN and in the following ESS assessment.

Co-funded by the European Union

BBN to develop future land-use scenarios

A BBN is being designed to develop future land-use scenarios for the Sierra Nevada under different environmental (climate among others) and management conditions. Afterwards, these land use scenarios will be implemented in other ESS assessment models, such as WiMMed. The analysis of ESS trade-offs in several scenarios will help managers to predict the state of ESS and their relations in the future.

The development of Sierra Nevada BBN started with an extensive review of literature in order to find the main variables that influence land-use changes in mountain regions. The selection of variables was validated with interviews and workshops with experts in the area of Sierra Nevada. Likewise, the states of the variables and the preliminary structure of the network were established. The initial BBN was discussed with stakeholders that influence the land-use change in Sierra Nevada: farmers, cattle ranchers, entrepreneurs, local managers and local development actors. In the next step, stakeholder and expert knowledge will be elicited to fill the CPTs of the network (Bromley 2005, Cain 2001). To assess land use changes in the future, the BBN needs some climate data inputs. So, the different climate scenarios of AR4 will be an input to determine their effects in the evolution on land use in the future.

ESS assessment

Provisioning services have been quantified by the production of agricultural products and livestock in the last decades by the rural economy.

Regulation services are being assessed with WiMMed model (Watershed Integrated Model in Mediterranean Environments), that is a physically-based, fully distributed hydrological model. It uses hourly and daily meteorological data, along with certain physical properties of the soil and subsoil to perform the spatial interpolation and temporal distribution of meteorological variables, rainfall interception, snowmelt, infiltration, runoff, surface slope circulation, calculation of the water in aquifers, and basin flow circulation. It thus provides instantaneous value or evolution of the principal flows and state variables, such as water flow volumes, amount of stored water, flooded surfaces, etc. A detailed description of this model is given by Herrero et al. (2009), and examples of the application of this model to the Guadalfeo River basin can be found in Herrero (2007), Millares (2009) and Aguilar (2008). WiMMed deals with climate and meteorological particularities with special consideration to Mediterranean environments (Herrero et al. 2014). Processes as spring and autumn torrential rain storms, high risk of persistent droughts, or high rates of sediment generation and soil loss can be correctly reproduced by the model. Knowing the physical and the hydrological properties of a watershed, WiMMed incorporates the meteorological inputs (rain, snow, solar radiation, wind, etc.) and simulates the water cycle and the generation and transport of sediment associated to it. The outputs of the model comprise a large amount of variables at different space and time scales. The current user-level version of WiMMed 2.0 includes all the functionalities for the simulation of every aspect related to water fluxes and hillslope sediment generation and transport. WIMMed is already calibrated for Sierra Nevada (Spain) for its present climate using the complete dataset of meteorological data, approximately available since 2000.

Results

We have developed a first version of the BBN (Fig. 33) and a preliminary spatial implementation of Sierra Nevada BBN in a watershed of Nevada (Fig. 34). As is described in the BBN schema, social variables as population structure (Diaz et al. 2011) and part-time business (Celio et al. 2014) influences the intention to farm. Likewise, topography variables determine the profitability of a plot to crop (Celio & Grêt-Regamey 2016, Spencer et al. 2014). Policies influence in actors´ decisions are very useful to explore in future scenarios. Other studies of land use change based on BBNs (Celio & Grêt-Regamey 2016, Lamarque et al. 2013) included such variables.

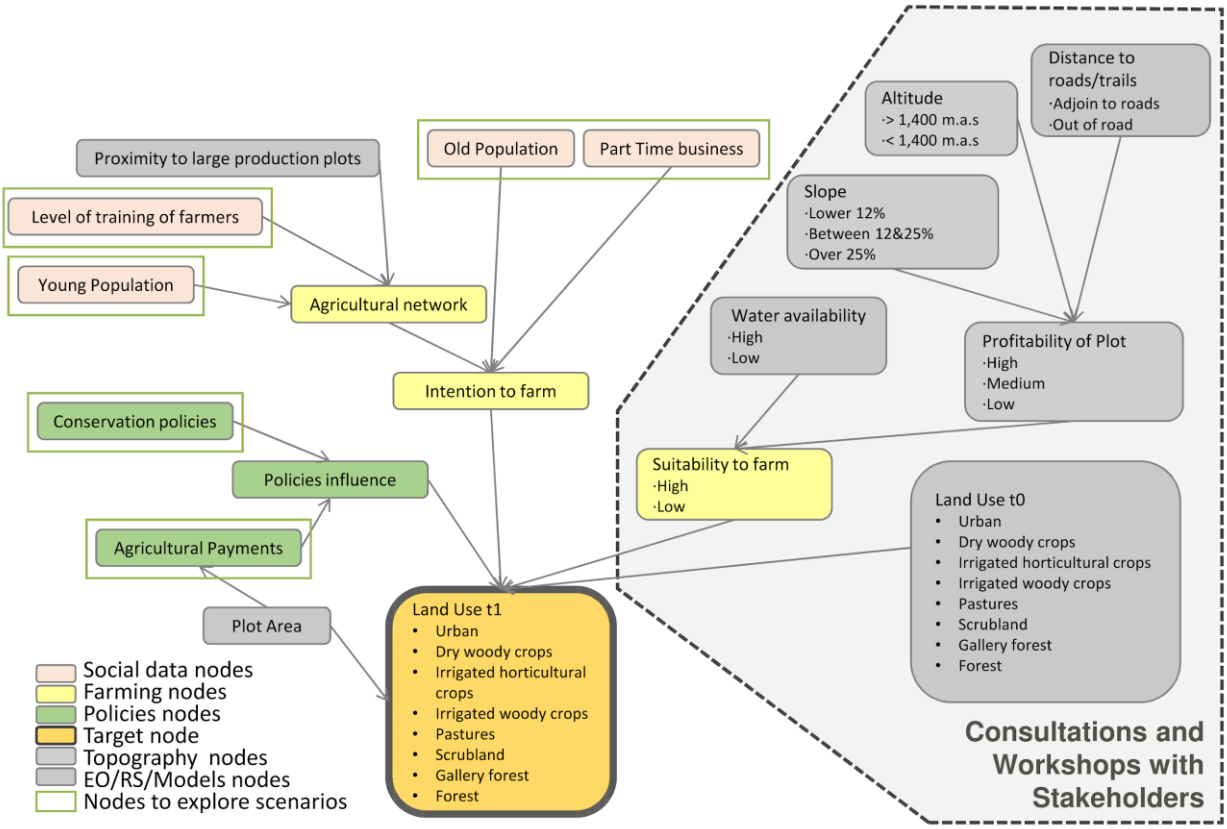

Figure 33: First version of the BBN to develop land use scenarios

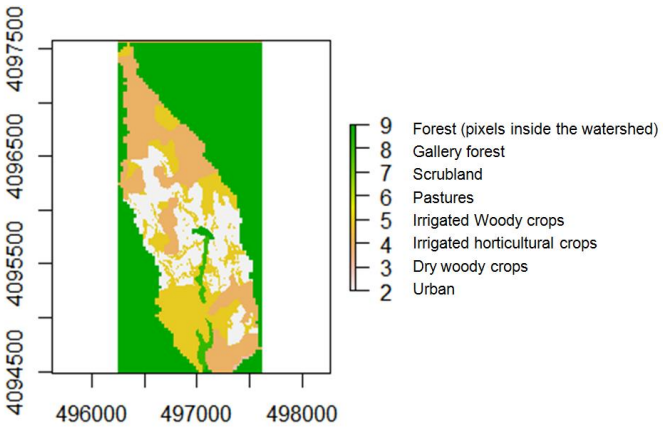

Figure 34: Preliminary implementation of Sierra Nevada BBN in a watershed of Nevada municipality. The map shows most likely class of land use.

In addition, we had some results assessing ESS as erosion prevention, pastures for livestock and crop production with WiMMed and other models, based on historical land use maps (Fig 35, 36 and 37).

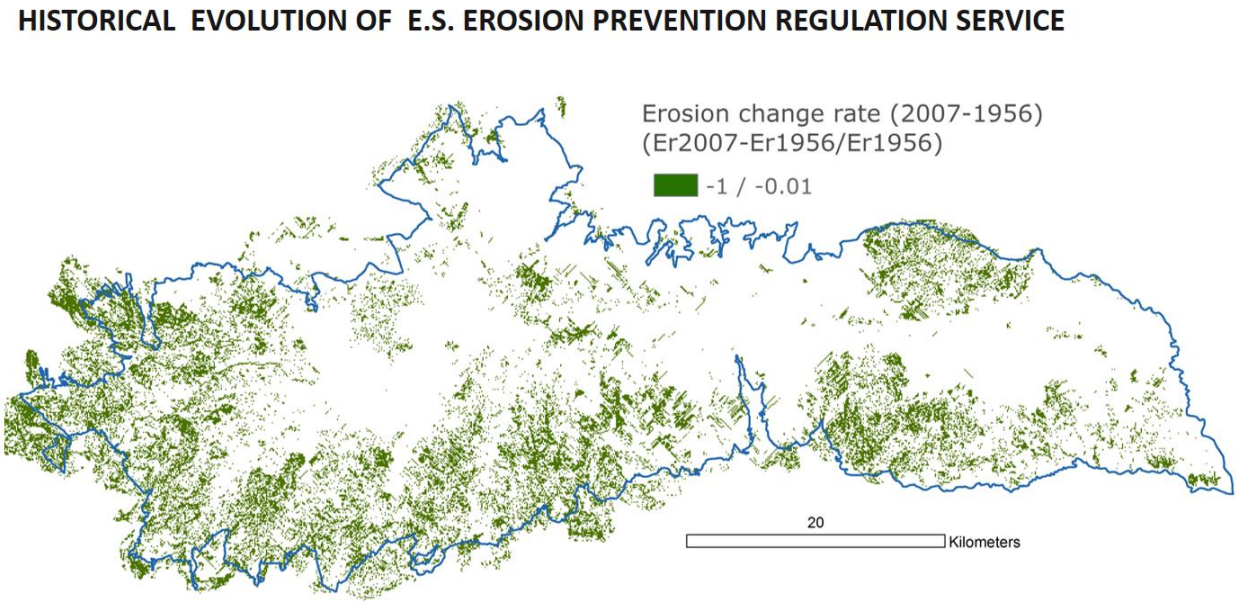

Figure 35: Decrease of erosion between 1956 and 2007 in Sierra Nevada.

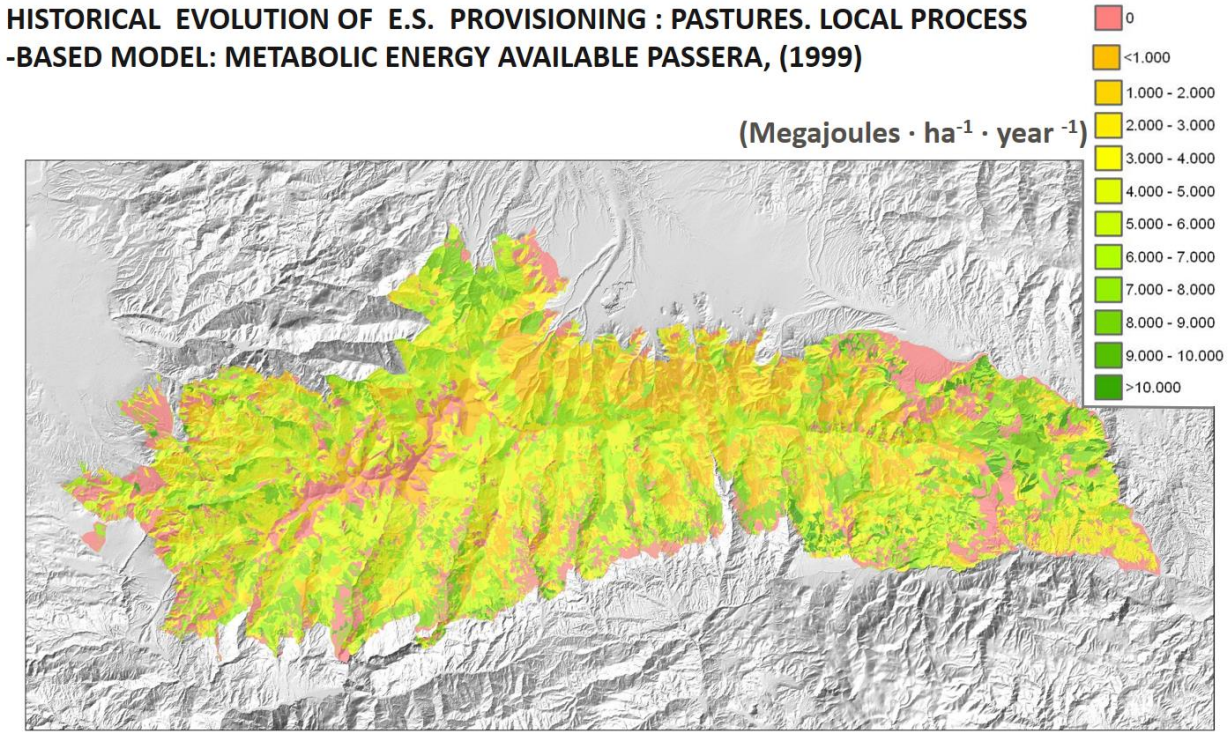

Figure 36: Pastures supply in Sierra Nevada (2007).

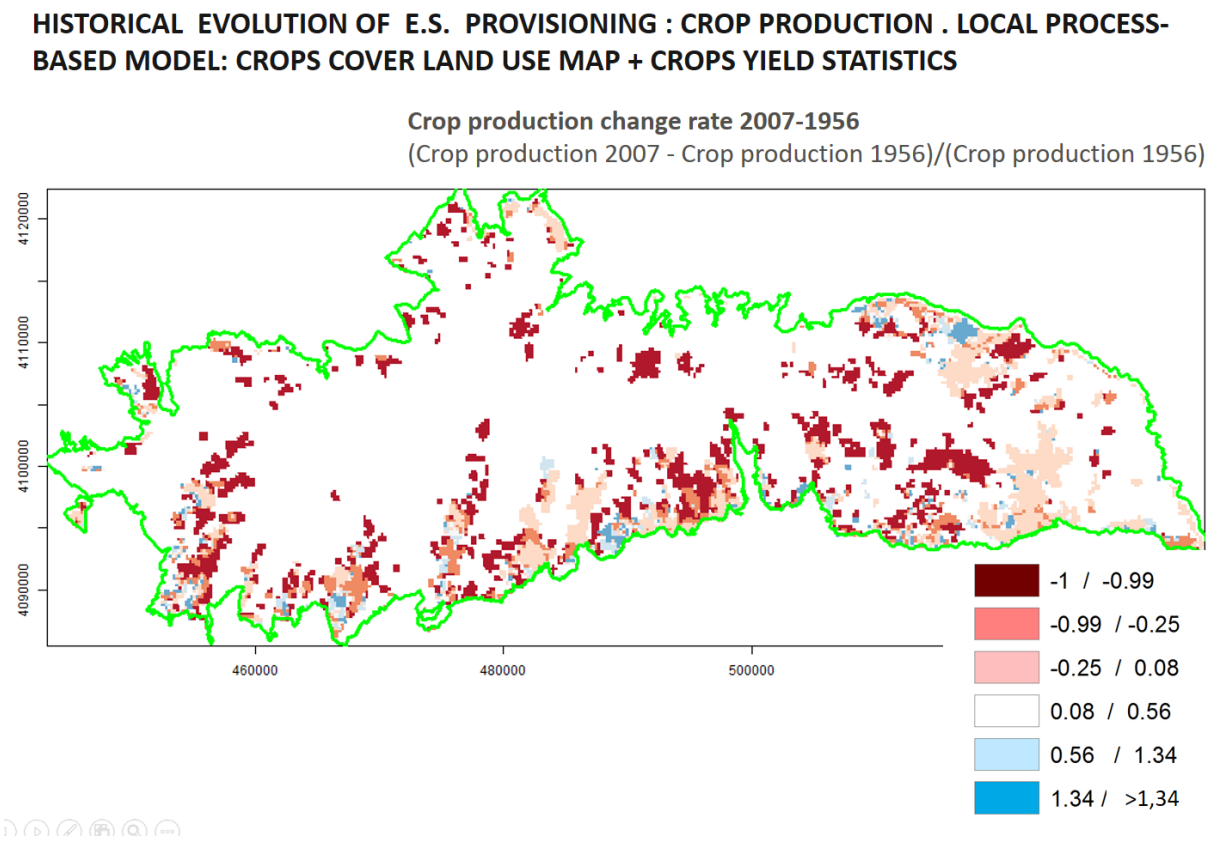

Figure 37: Decrease of crop production between 1956 and 2007 in Sierra Nevada.

Conclusion

In Sierra Nevada as a mountain region, climate and land use changes can condition the ecosystem services status. Future climate scenarios can be very useful as an input in our assessment of the effects of climate and land use changes on ecosystem services status in the future. Climate data plays an important role as an input data in the Bayesian Belief Network development and the ecosystem services assessment through models like WiMMed. All this information could help decision makers to understand how the key factors will affect ecosystem services in the future.

References

Aguilar (2008). Scale effects in hydrological processes. Application to the Guadalfeo river watershed (Granada). PhD Thesis. University of Córdoba, http://www. cuencaguadalfeo. com/archivos/Guadalfeo/Tesis/TesisCris en.

Bromley, J., Jackson, N. A., Clymer, O. J., Giacomello, A. M., Jensen, F. V. (2005). The use of Hugin® to develop Bayesian networks as an aid to integrated water resource planning. *Environmental Modelling & Software,* 20(2): 231-242.

Cain, J. (2001). Planning improvements in natural resources management. *Centre for Ecology and Hydrology, Wallingford, UK*, *124*: 1-123.

Celio, E., Koellner, T., Grêt-Regamey, A. (2014). Modeling land use decisions with Bayesian networks: Spatially explicit analysis of driving forces on land use change. *Environmental Modelling & Software*, *52*: 222-233.

Celio, E., Grêt-Regamey, A. (2016). Understanding farmers' influence on land-use change using a participatory Bayesian network approach in a pre-Alpine region in Switzerland. *Journal of environmental planning and management*, *59*(11): 2079-2101.

Díaz, S., Quétier, F., Cáceres, D. M., Trainor, S. F., Pérez-Harguindeguy, N., Bret-Harte, M. S., ... & Poorter, L. (2011). Linking functional diversity and social actor strategies in a framework for interdisciplinary analysis of nature's benefits to society. *Proceedings of the National Academy of Sciences*, 201017993.

Herrero, J., Polo, M. J., Moñino, A., Losada, M. A. (2009). An energy balance snowmelt model in a Mediterranean site. *Journal of hydrology*, *371*(1-4): 98-107.

Herrero, J., Aguilar, C., Polo, M. J., Losada, M. A. (2007). Mapping of meteorological variables for runoff generation forecast in distributed hydrological modeling. *Proceedings, Hydraulic Measurements and Experimental Methods*: 606-611.

Herrero, J., Millares, A., Aguilar, C., Egüen, M., Losada, M. A., & Polo, M. J. (2014). Coupling Spatial And Time Scales In The Hydrological Modelling Of Mediterranean Regions: WiMMed.

Lamarque, P., Artaux, A., Barnaud, C., Dobremez, L., Nettier, B., Lavorel, S. (2013). Taking into account farmers' decision making to map fine-scale land management adaptation to climate and socio-economic scenarios. *Landscape and Urban Planning*, *119*: 147-157.

Marcellus-Zamora, K. A., Gallagher, P. M., Spatari, S., Tanikawa, H. (2016). Estimating materials stocked by land-use type in historic urban buildings using spatio-temporal analytical tools. *Journal of Industrial Ecology*, *20*(5): 1025-1037.

Millares, A., Polo, M. J., Losada, M. A. (2009). The hydrological response of baseflow in fractured mountain areas. *Hydrology & Earth System Sciences Discussions*, *6*(2).

Spencer, J. L., Hughson, S. A., Levine, E. (2014). Insect resistance to crop rotation. In *Insect Resistance Management (Second Edition)* pp. 233-278.

Co-funded by the European Union

3. Future simulations on regional scales

3.1 Impact of climate change on Natura2000 sites across Europe

By Carl Beierkuhnlein and Samuel Hoffmann

Under climate change the climatic conditions inside protected areas will be altered, which will modify the species habitat within protected areas. To track suitable habitat, some species may emigrate from protected areas to unprotected surroundings. In order to inform conservationists about such climate-vulnerability of protected areas and species inside, we here identify and map climate change inside Natura2000 Species Areas of Conservation (SAC) and Special Protection Areas (SPA).

We used current and future climate data provided by Worldclim - Global Climate Data (Hijmans et al. 2005) representing projections from the global circulation model BCC-CSM1-1 for the representative concentration pathways RCP6.0 and 8.5, and time period 2061-2080. The spatial resolution of the climate raster data was 30 arc seconds. We first extracted for Europe, the EU and the entire Natura2000 network (EEA 2017) raster cells with climate information about mean annual temperature and annual precipitation. We then illustrated the climate niche, i.e. the climate space defined by these two climate variables, for Europe, the EU and the Natura2000 network considering two RCP scenarios 6.0 and 8.5 (Fig. 38 and 39).

We observe that parts of the future climate niches of Natura2000 sites (light red) will even exceed current climate conditions of Europe (light grey) and the EU (dark grey). These non-overlapping parts are particularly characterized by increasing temperature under future climate change. Under RCP8.5 the extent of these parts are larger than under RCP6.0.

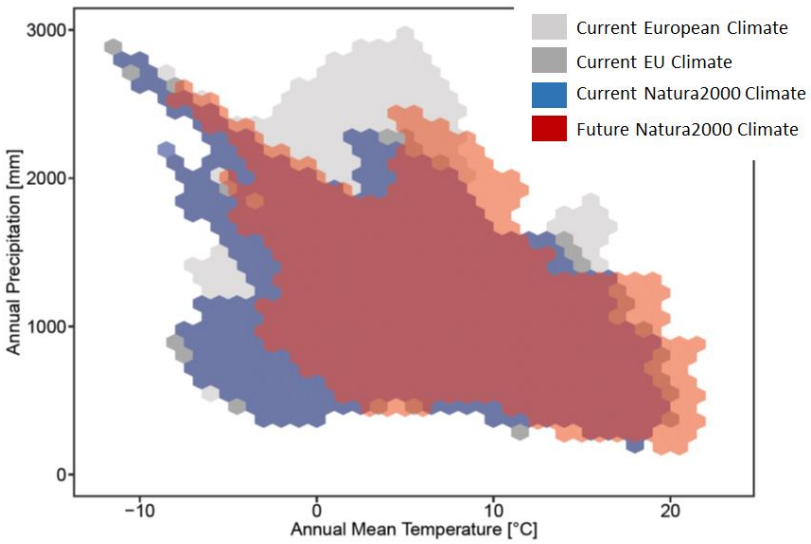

Figure 38: Climate niches of Europe, the EU and Natura2000 protected areas now and in future. The future climate data was provided by Worldclim (Hijmans et al. 2005) and represents projections from BCC-CSM1-1 for RCP6.0 and period 2061-2080. The spatial data resolution was 30 arc seconds.

Co-funded by the European Union

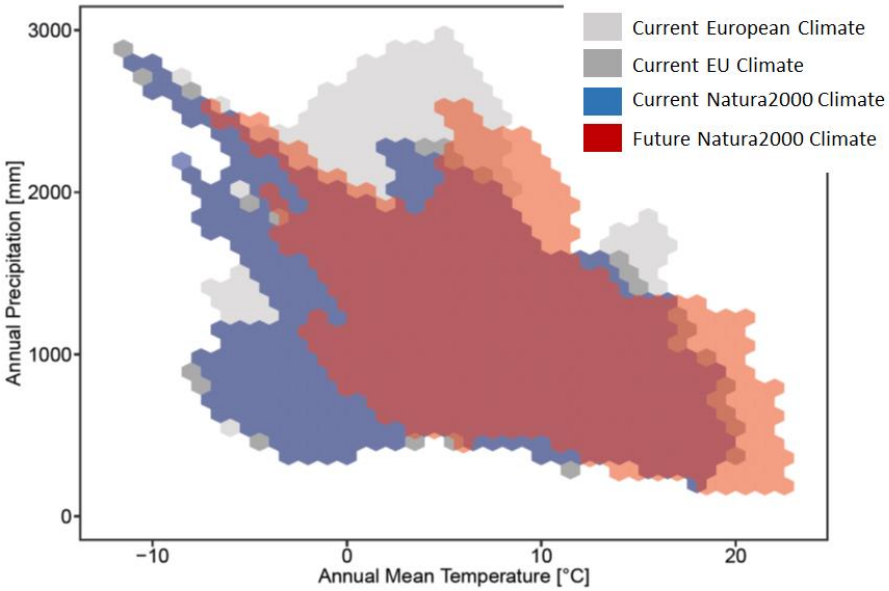

Figure 39: Climate niches of Europe, the EU and Natura2000 protected areas now and in future. The future climate data was provided by Worldclim (Hijmans et al. 2005) and represents projections from BCC-CSM1-1 for RCP8.5 and period 2061-2080. The spatial data resolution was 30 arc seconds.

We secondly conducted an individual climate change classification of raster cells inside each Natura2000 site. We here adapted a PCA-based climate change algorithm from Carroll et al. (2015), which assigns a climate class to each raster cell under current and future climate conditions (Fig. 40). By comparing the current and future climate classes of raster cells within individual protected areas, we derived a climate change cell classification as shown by Figure 41 and 42. Subsequently, we mapped these individual climate change cell classifications for each Natura2000 site (Fig. 43, 44 and 45).

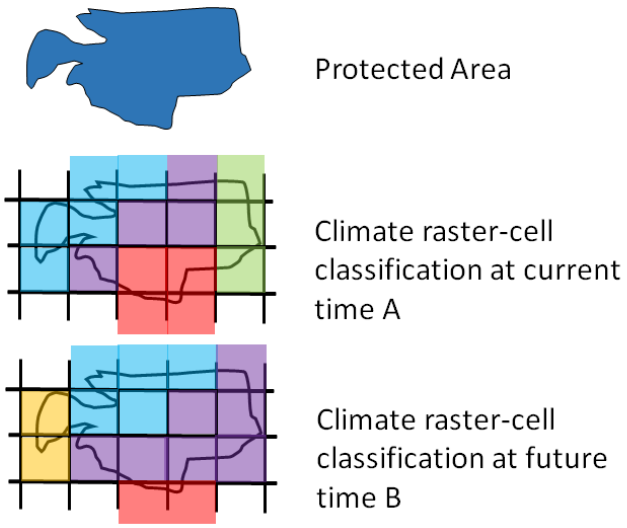

Figure 40: Climate cell classification of an individual protected area at current time A and future time B. the colours indicate different climate classes per raster cell.

Co-funded by the European Union

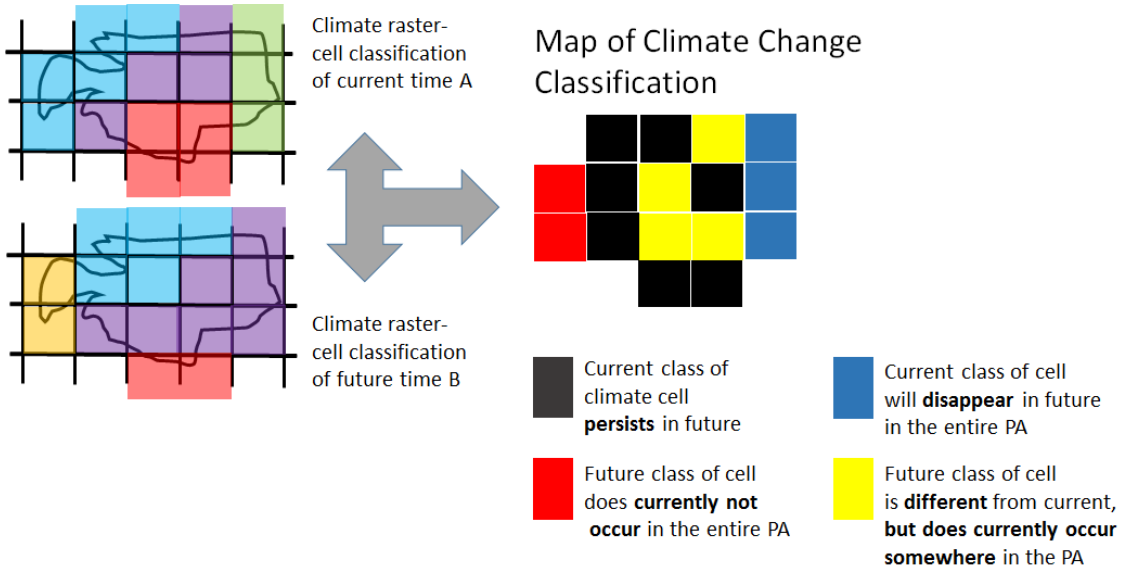

Figure 41: The comparison between current and future climate raster-cell classification of an individual protected area leads to a map of climate change classification. The colors indicate different climate classes per raster cell.

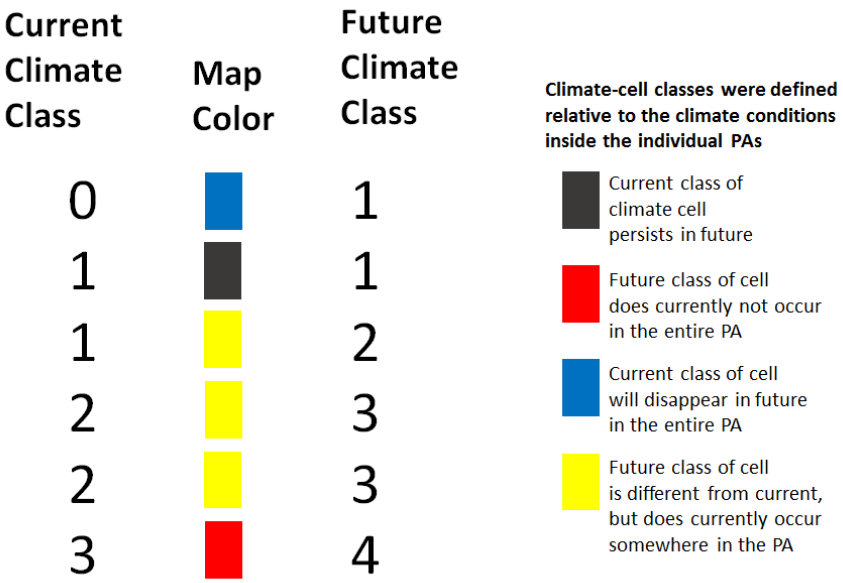

Figure 42: Example of a climate change classification for a single protected area covering six climate raster cells.

The red cells were dominant across Natura2000 sites in the EU; they reflect climate that does currently not appear in the entire single protected area (Fig. 43). The cells were mostly found in lowland regions with low topographic heterogeneity. In such protected areas the climate diversity is expected to be low, which means that climate conditions are likely to entirely change inside the individual protected area. In mountain regions, however, we found protected areas such as the Natura2000 site 'National Park Hohe Tauern' whose climate will not be entirely novel (Fig. 44). By contrast, the Natura2000 network of the Iberian Peninsula is particularly prone to novel climate conditions (Fig. 45).

Co-funded by the European Union

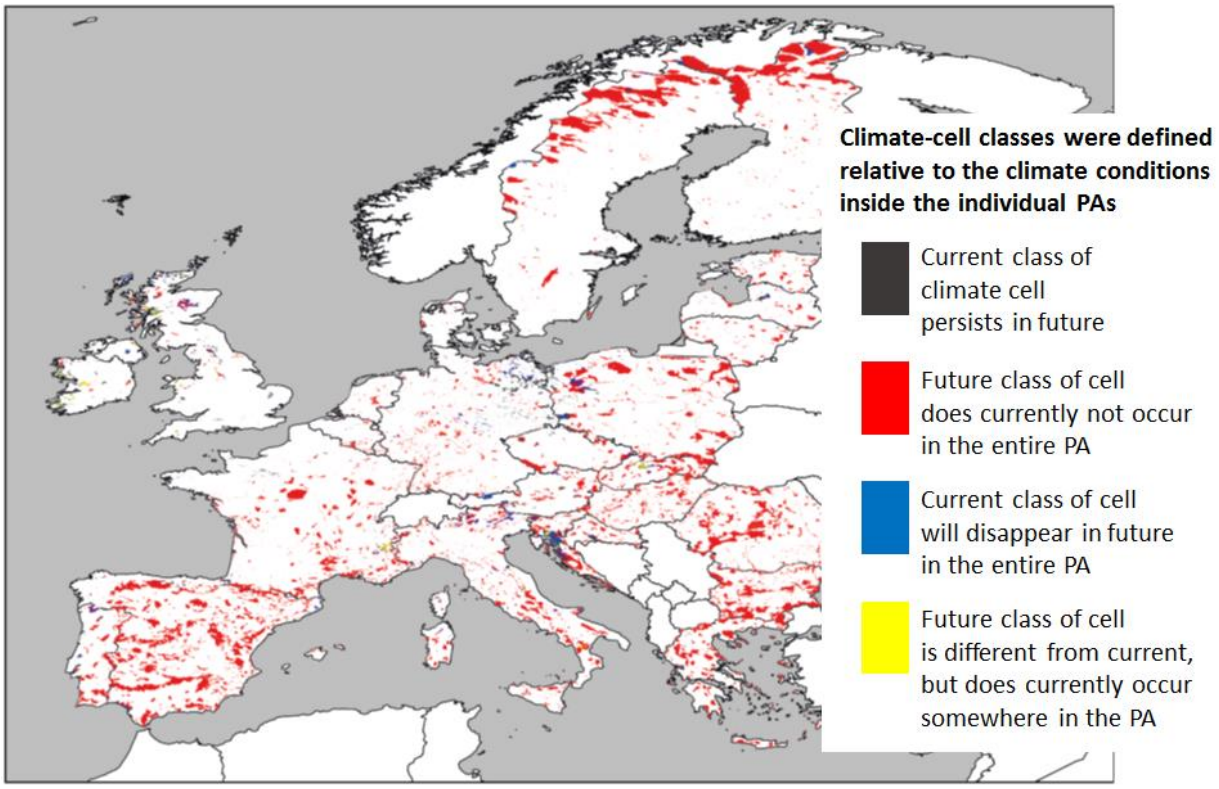

Figure 43: Climate change cell classification for Natura2000 protected areas (SAC and SPA); the extent of the EU. The future climate data was provided by Worldclim (Hijmans et al. 2005) and represents projections from BCC-CSM1-1 for RCP 6.0 and period 2061-2080. The spatial data resolution was 30 arc seconds.

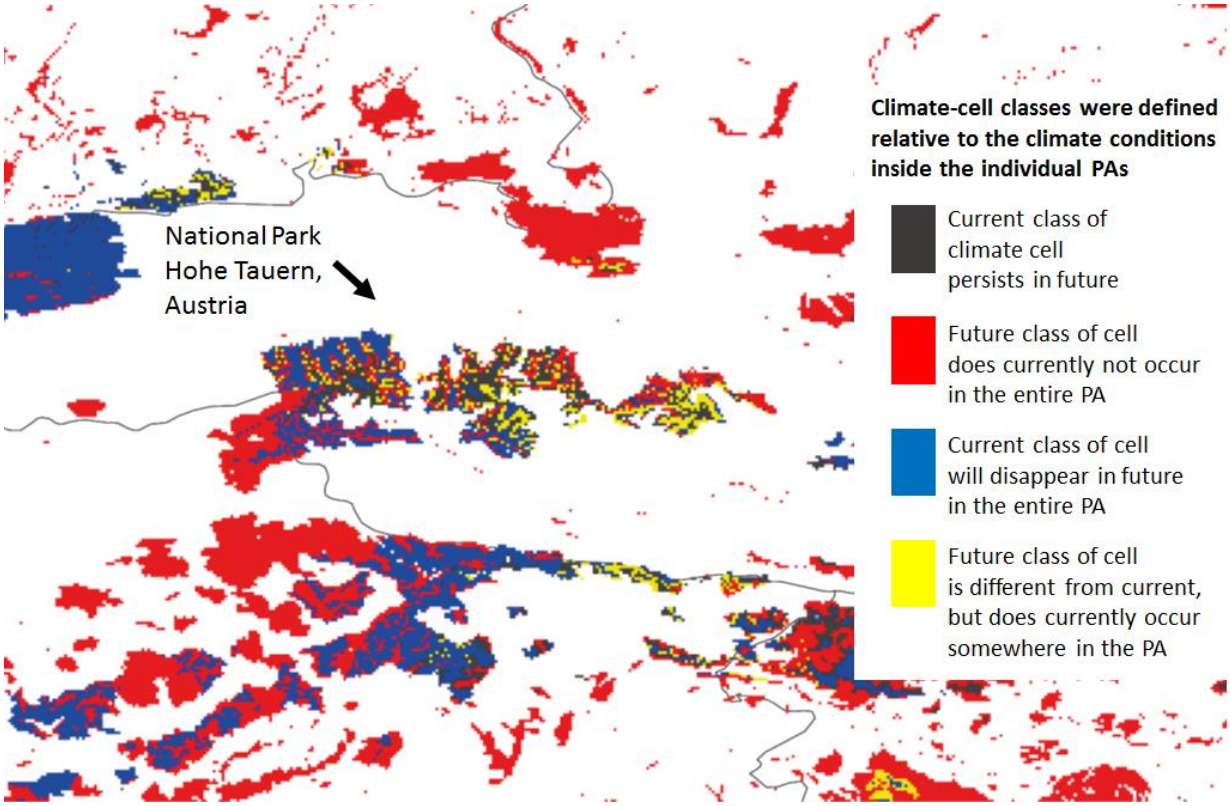

Figure 44: Climate change cell classification for Natura2000 protected areas (SAC and SPA); parts of the European Alps. The future climate data was provided by Worldclim (Hijmans et al. 2005) and represents projections from BCC-CSM1-1 for RCP 6.0 and period 2061--2080. The spatial data resolution was 30 arc seconds.

Co-funded by the European Union

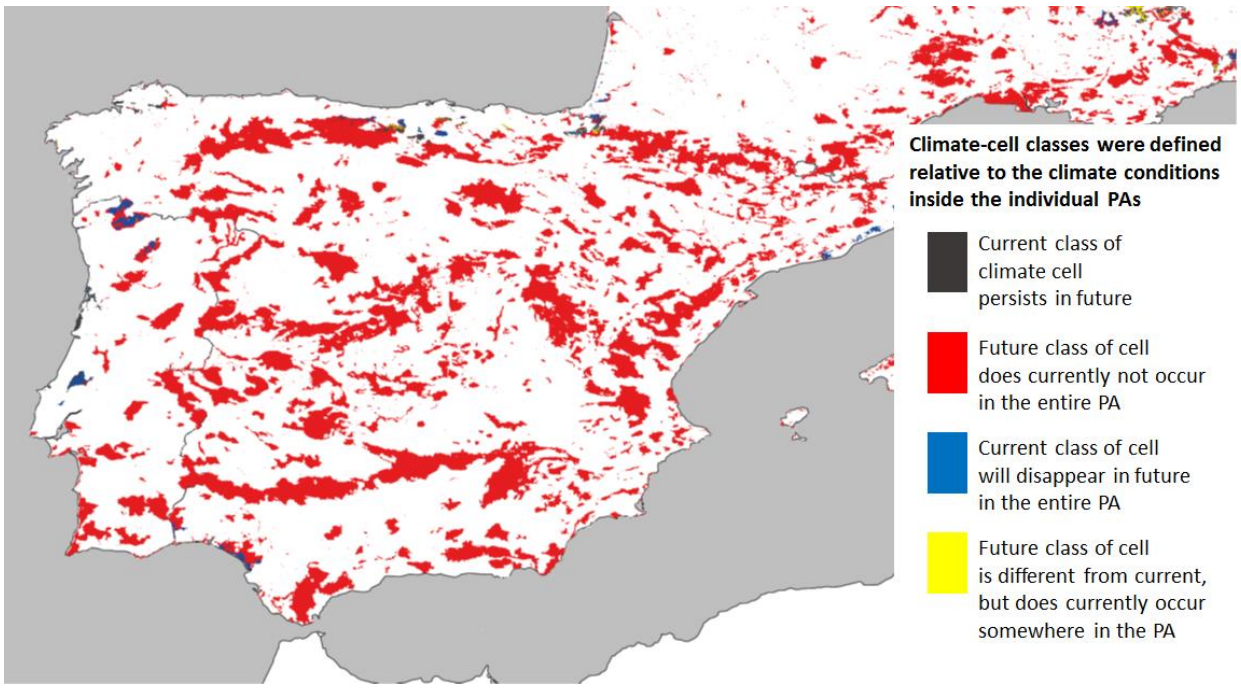

Figure 45: Climate change cell classification for Natura2000 protected areas (SAC and SPA); the Iberian Peninsula. The future climate data was provided by Worldclim (Hijmans et al. 2005) and represents projections from BCC-CSM1-1 for RCP 6.0 and period 2061-2080. The spatial data resolution was 30 arc seconds.

Conservationists must particularly pay attention to Natura2000 sites that experience a large proportion of novel climate conditions (red cells). Species inside such protected areas are expected to move out of the protected area to track suitable climate habitat, in case they are not able to adapt in-situ. In addition, new species may immigrate. Since dispersal ability is thereby crucial, invasive species may become dominant.

Since we here only apply a single GCM and RCP, we were not able to quantify uncertainty in climate projections. The results are thus a first estimate of climate change inside individual Natura2000 sites in the EU. Further investigations have to consider more GCMs and RCP to also quantify uncertainty in climate models.

References

Carroll, C., Lawler, J. J., Roberts, D. R., Hamann, A. (2015). Biotic and climatic velocity identify contrasting areas of vulnerability to climate change. *PLoS One*, *10*(10), e0140486.

EEA (2018). Natura 2000 data - the European network of protected sites. Available at https://www.eea.europa.eu/data-and-maps/data/natura-9.

Hijmans, R. J., Cameron, S. E., Parra, J. L., Jones, P. G., Jarvis, A. (2005). Very high resolution interpolated climate surfaces for global land areas. *International journal of climatology*, *25*(15): 1965-1978.

Co-funded by the European Union

3.2 Adaptation of natural forests to climate change in Europe

By Maik Billing, Kirsten Thonicke, Werner von Bloh, Boris Sakschewski and Ariane Walz

Introduction

By the end of the 21st century, temperature and precipitation will most likely undergo fundamental changes in Europe with strong impacts also on existing ecosystems. Field observations as well as experiments already indicate effects of these changes on woodlands (Peñuelas et al. 2001, Biegler et al. 2006), and for the end of the 21st century, numerous modelling studies show stress and decline of currently existing woodland ecosystems (Kurz et al. 2008, Sitch et al. 2008). At the same time, however, we expect adaption of the woodland ecosystems in place (Eilmann et al. 2009). One of the most investigated adaptation strategies is the shift in the extent and location of particular woodland ecosystems (Grace et al. 2002, Jump et al. 2006). More complex is a shift in their species composition due to new niches and competition under new environmental factors. On a more abstract level, this means a shift in the physiological traits of the ecosystem as a whole. Such shifts in the composition of physiological traits of woodland ecosystems have so far hardly been incorporated in Dynamic Global Vegetation Models (e.g. Sakschewski et al. 2014, Pavlick et al. 2013). Based on the newly adapted LPJmL-FIT model (Thonicke et al. In Prep), we can investigate the impact of climate change, the adaptation potential within single plant functional types and the role of functional diversity in buffering climate change impacts.

In this analysis, we thus aim at (1) estimating the impact of climate change on potential natural woodlands in Europe by the end of the 21st century and the effect that adaptation might have through shifts in the natural competition; (2) showing how individual traits adapt to a changing climate; and (3) relating initial trait diversity to simulated changes in the productivity of a woodland ecosystems under climate change.

Methods

We use the LPJmL-FIT (Thonicke et al. In Prep.) to simulate changes in biomass under a potential future climate until 2100. We then compare the carbon sequestrated in vegetation as an indicator for biomass with the results of standard LPJmL-4 (Schaphoff et al. 2018), which uses only one fixed value for plant traits. Furthermore, we show results for both adaptation strategies: the shifts in the location and extent of typical plant functional types over Europe, as well as shifts within the trait composition in the woodland ecosystems. Finally, we show how climate induced changes in productivity of woodland ecosystems relate to diversity of the initial ecosystem. We use carbon sequestrated in vegetation as an indicator for biomass, Specific Leaf Area (SLA) as an exemplary trait to demonstrate trait shift, and Gross Primary Production as an indicator for ecosystem productivity. Diversity is measured as functional richness based in traits of tree individuals as used in Schneider et al. (2017).

The LPJmL-FIT model

We used an adapted version for Europe of the LPJmL-FIT model (Sakschewski et al. 2015) which combines flexible individual traits with gap dynamics and plant physiology, hydrology and biogeochemistry. Being structured into seven vertical layers, trees compete for light and water as they grow in size. The trait combination of each tree determines its competitive strength under given climate conditions at a site, where several plant strategies can co-exist and form diverse communities in forest ecosystems. The interaction between competitiveness of individual trees through the suitability of their trait combinations to the given climate, spatial distribution of traits change with respective climatic gradients (Sakschewski et al. 2015). The recent adaptation of the model to European conditions (Thonicke et al. in Prep) include

- implementations of multiple, co-occurring PFTs that describe Mediterranean, temperate and boreal natural forests in Europe,

Co-funded by the European Union

- application of leaf and stem-economics spectrum approach of LPJmL-FIT for the four tree PFTs "broad-leaved summergreen" (BL-S), "broad-leaved evergreen" (BL-E), "temperate needle-leaved" (T-NL) and "boreal needle-leaved trees" (B-NL), with each PFT based on evaluated implementation of these PFTs in LPJmL-4 (Schaphoff et al. 2018a, Schaphoff et al. 2018b),
- replacement of fixed values to trait value ranges for each PFT for specific leaf area (SLA), leaf longevity (LL), leaf nitrogen content (Narea), the maximum carboxylation, rate of Rubisco per leaf area ($Vcmax_{area}$) and wood density (WD),
- establishment of empirical relations between traits values (e.g. higher Leaf Longevity-lower Specific Leaf Area, higher Wood Density-lower NPP) (see Thonicke et al. In prep. for more details)
- introduction of the phenological limitations of the PFTs, namely light, water and temperature stress (as provided by Forkel et al. 2015 and implemented in LPJmL-4)

The LPJmL-FIT has been successfully evaluated across the European continent using large-scale remote sensing products, on a local scale for single Protected Areas using remotely sensed data, trait data and FLUXNET data (Thonicke et al. In Prep.).

The LPJmL-4 model

LPJmL is a process-based ecosystem model designed to give a representation of global carbon and water fluxes (Sitch et al., 2003; Gerten et al. 2004) and is able to simulate natural vegetation as well as a variety of crops (Bondeau et al., 2007). The model is forced by environmental input variables such as climate and soil parameters and atmospheric CO_2 concentration on a 0.5 global grid. Vegetation dynamics in the model are driven by major processes such as growth, mortality, competition, and disturbances (mainly fire).

The model simulates photosynthesis, autotrophic and heterotrophic respiration as well as evapotranspiration, interception, percolation of water into the soil as well as runoff. The soil is divided into several soil layers of different sizes and the soil carbon accumulation in the soil from decomposing litter is vertically distributed. LPJmL has recently been updated to version 4.0 (Schaphoff et al. 2018a) to systematically describe, integrate and thoroughly validate (Schaphoff et al. 2018b) recent model developments which include an improved hydrology scheme, permafrost, river runoff scheme, plant phenology and process-based fire disturbance. Earlier versions of LPJmL have been applied in a wide variety of climate impacts studies globally and regionally (Schaphoff et al. 2018a). The model is driven by climate, atmospheric CO_2 concentration and soil texture and starts to simulate potential natural vegetation from bare-ground to bring vegetation and soil carbon pools intro equilibrium with climate.

Simulation protocol

We used the input of one Global Climate Model (HadGem2-ES) for two emission scenarios (RCP4.5 and RCP8.5), to drive simulations with both LPJmL-FIT and LPJml-4. The simulations start from bare-ground for a spin-up period of 500 years by recycling the first 30 years of the climate data set (1951-1980) to bring natural vegetation composition and all living and dead carbon pools into equilibrium with the spin-up climate. We then performed transient runs simulating potential natural vegetation until the end of 2099 (without land use). Both simulations run at a 0.5° grid over Europe. For the LPJmL-FIT simulations, 50 forest patches are being equivalent to 10 ha of forest area each are simulated in each grid cell where all patches receive the same climate data and the same soil data as model input. Respective model output is then aggregated over all these 50 stochastic realisations (patches) within a grid cell.

Quantifying diversity based on trait richness

Functional Richness is calculated as the hyper-volume of the trait space (Schneider et al. 2017), based on the following tree plant traits: Specific Leaf Area, Leaf Longevity and Wood Density. Function Richness - as calculated

here - is a combined index that incorporates diversity across plant functional types and within single plant functional types.

Results

The first simulation results show a strong decline of the overall biomass in Europe, with over 20 % of loss under RCP4.5 and over 40% under RCP8.5 (Fig. 46). The improved incorporation of the adaptive capacity of woodland ecosystems in LPJmL-FIT reduces the effect under both scenarios for 2100 substantially. Under RCP4.5 the LPJmL-FIT simulates loss by around 25 % opposed to 35% loss simulated by LPJmL-4, similarly the simulation results for 2100 of LPJmL-FIT under RCP8.5 are around 10 % higher than for LPJmL-4.

(A) Biomass under RCP4.5

(B) Biomass under RCP8.5

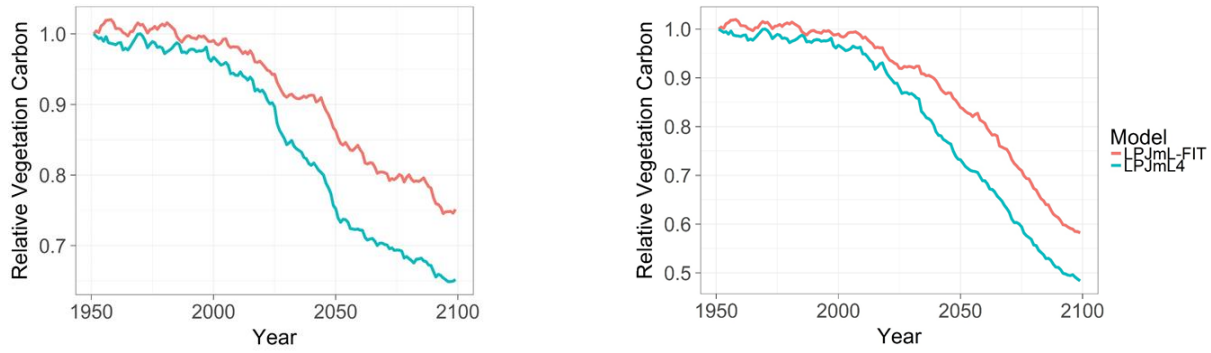

Figure 46: Relative changes in Vegetation Carbon under HadGEM_ES2, 1950-2100 overall cells and all plant functional types.

Simulation results show that Specific Leaf Area declines for BL-S, T-NL and B-NL trees, only the Specific Leaf Area of BL-E trees increases over the simulation period by around 3 % (Fig. 48). BL-E mainly occur in the Mediterranean, where the input climate data shows regular droughts in the second half of the century. There are two reasons that lead to this rise. First, BL-E in the Mediterranean suffer drought stress in the simulations. As a consequence, shorter leaf longevity becomes a competitive advantage, and in the simulation, trees with higher Leaf Longevity are more frequent among the BL-E trees. Second, higher temperatures in Central Europe allow BL-E to become more frequent, but seasonality in temperature favours again BL-E trees with shorter leaf longevity (Fig. 47). As Leaf Longevity is a negative exponential function of Specific Leaf Area (Sakschewski et al. 2015), the mean Specific Leaf Area of BL-E rises. At the same time, BL-S and, to a lesser extent also T-NL and B-NL, profit from a longer vegetation period due to increase temperatures, which leads to higher leaf longevity and a lowering of the Specific Leaf Area.

Co-funded by the European Union

(A) Coverage for each Plant Functional Types under RCP4.5 for 2004-2013 (top) and for 2090-2099 (bottom)

(B) Coverage for each Plant Functional Types under RCP8.5 for 2004-2013 (top) and for 2090-2099 (bottom)

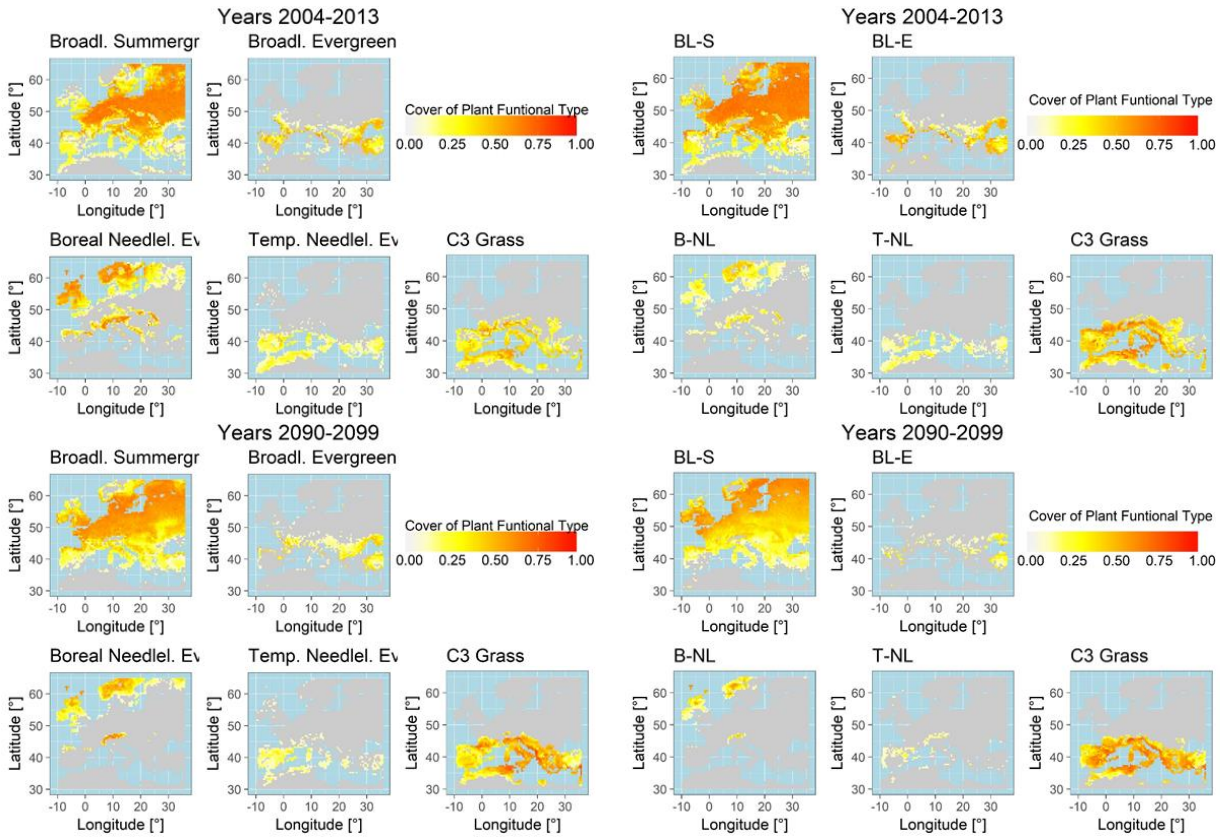

Figure 47: Mean coverage for each plant functional type under (A) RCP4.5 and (B) RCP 8.5.

(A) Specific Leaf Area under RCP4.5

(B) Specific Leaf Area under RCP8.5

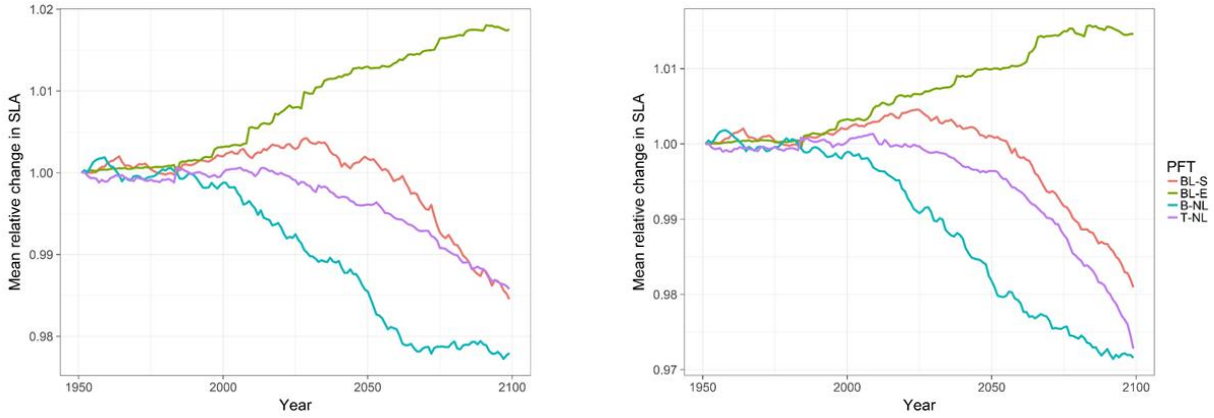

Figure 48: Mean Specific Leaf Areas over all cells for each plant functional type under (A) RCP4.5 and (B) RCP 8.5

Co-funded by the European Union

(A) Observed relation between simulated changes in Gross Primary Production (GPP), changes in potential evapotranspiration (PET) and Functional Richness (FRich) under RCP4.5

(B) Observed relation between simulated changes in Gross Primary Production (GPP), changes in potential evapotranspiration (PET) and Functional Richness (FRich) under RCP8.5

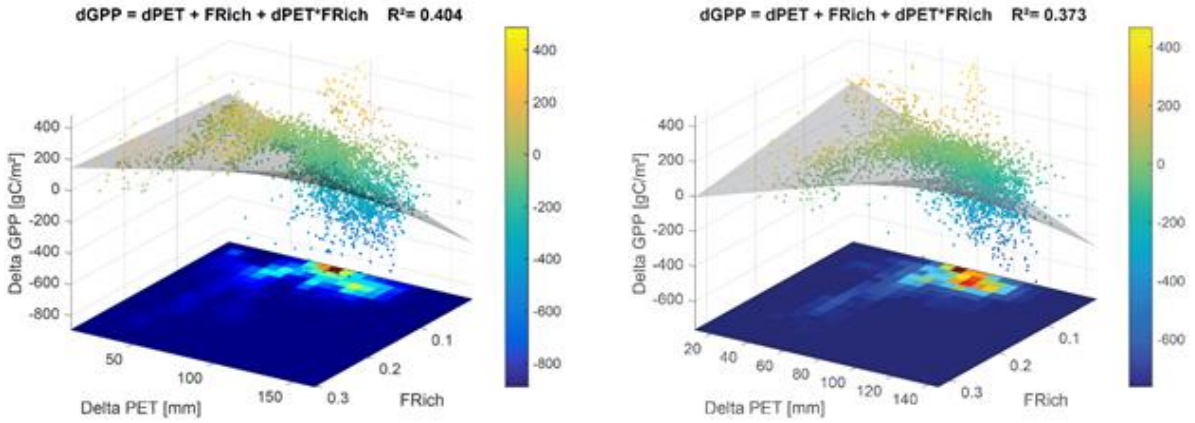

Figure 49: Observed relation between simulated changes in Gross Primary Production (GPP), changes in potential evapotranspiration (PET) and Functional Richness (FRich) under (A) RCP4.5 and (B) RCP 8.5 within each simulated cell.

Our simulations confirm that the effect of climate change on Gross Primary Production (GPP) is lowest where absolute change in Potential Evapotranspiration (PET) is small (Fig. 49). Here, present-climate functional richness has little influence on buffering GPP under climate change. With increasing shifts in Potential Evapotranspiration, changes in Gross Primary Production increase showing mainly a reduction, but also areas that profit from the changes in the climate inputs. Focus now on the effect of trait diversity of the initial ecosystem on the Gross Primary Production, it becomes obvious that functional richness (FRich) is negatively correlated to a stable Gross Primary Production, i.e. cells that showed initially high functional richness do show lesser change in Gross Primary Production, especially under high changes in Potential Evapotranspiration. A multiple regression underlines that Functional Richness becomes even more relevant if changes in Potential Evapotranspiration are high (compare Fig. 49A (RCP4.5) with Fig. 49B (RCP8.5)).

Discussion and conclusions

Our results highlight the role of functional diversity to buffer impacts of climate change on vegetation. Although our model builds on abstract woodland ecosystems and neither incorporates any aspects of the long land use history of European forest, nor concrete species prevailing there, our results confirm similar findings based on empirical data from four national forest inventories and extrapolates the effects both in time and in space (Madrigal-Gonzalez et al. 2016). From our results we draw two major conclusions: (1) The buffering effect of trait diversity on the impact of climate change on ecosystem productivity underlines the need for restoration of highly managed and to large parts widely uniform forests in Europe to increase their functional diversity to support their adaptation to changing climate conditions. (2) Our results further call for incorporating this adaptive potential also in vegetation models to improve our estimates of the climate change impact to these woodland ecosystems.

Our simulations show evidence of the principle sensitivities of the ecosystems. Although we use transient simulations based on climate inputs from the global climate model HadGem2-ES, we want to highlight the strongly explorative - and not predictive - character of this simulation work. One reason for this are the high uncertainties related to the outputs of long-term climate modelling, no matter whether we use one of them or an ensemble. Similarly, also the two RCPs only have an indicative character, which provides insight in the sensitivity of the model to variation in climate inputs.

A second reason is the level of abstraction in the vegetation that we simulate for Europe ignoring whether or not forest prevails in particular cells as well as any forest management. Current simulations show the impact and potential resistance of potential natural vegetation with higher plant-trait diversity in Europe. In this model setting, tree individuals of the same PFT can have different plant traits which aggregated over forest patches make up the trait space which is then extended by other co-occurring PFTs. Functional richness is higher, the more PFTs co-occur and the larger the trait space that is realized by all tree individuals. Competition for light and water dominate simulated forest composition and result from ecological sorting under given climate conditions. Adaptation of individual trees through plasticity is not captured as well as seed dispersal. For the latter, LPJmL-FIT assumes that enough seeds are available to allow for trait combinations to be drawn from observed trait ranges throughout the current and future climate simulation. Therefore, the ecological niches that PFTs cover at the end of the 21st century might be difficult to reach if dispersal rates are too low. In reality they might be even cut off due to widespread intensive land-use and urban areas.

Furthermore, we want to highlight that the presented simulations only show the potential for shifts in functional traits (between as well as within plant functional types). The results for the end of the simulation period represent only a snapshot. Even if we assumed the climate at the end of the 21st century would stabilise, woodland ecosystem would - in reality as well as in the model - require many more decades under these new stable conditions to potentially develop towards a new stable state.

References

Bigler, C., Bräker, O. U., Bugmann, H., Dobbertin, M., Rigling, A. (2006). Drought as an inciting mortality factor in Scots pine stands of the Valais, Switzerland. *Ecosystems*, *9*(3): 330-343.

Eilmann, B., Zweifel, R., Buchmann, N., Fonti, P., Rigling, A. (2009). Drought-induced adaptation of the xylem in Scots pine and pubescent oak. *Tree physiology*, *29*(8): 1011-1020.

Forkel, M., Carvalhais, N., Schaphoff, S., Bloh, W. V., Migliavacca, M., Thurner, M., Thonicke, K. (2014). Identifying environmental controls on vegetation greenness phenology through model-data integration. *Biogeosciences*, 11(23): 7025-7050.

Grace, J., Berninger, F., Nagy, L. (2002). Impacts of climate change on the tree line. *Annals of Botany*, *90*(4), 537-544.

Jump, A. S., Hunt, J. M., & Penuelas, J. (2006). Rapid climate change-related growth decline at the southern range edge of Fagus sylvatica. *Global Change Biology*, *12*(11): 2163-2174.

Kurz, W. A., Stinson, G., Rampley, G. J., Dymond, C. C., Neilson, E. T. (2008). Risk of natural disturbances makes future contribution of Canada's forests to the global carbon cycle highly uncertain. *Proceedings of the National Academy of Sciences*, *105*(5): 1551-1555.

Madrigal-González, J., Ruiz-Benito, P., Ratcliffe, S., Calatayud, J., Kändler, G., Lehtonen, A., Dahlgren, J., Wirth, C., Zavala, M. A. (2016). Complementarity effects on tree growth are contingent on tree size and climatic conditions across Europe. *Scientific reports,* 6: 32233.

Pavlick, R., Drewry, D. T., Bohn, K., Reu, B., Kleidon, A. (2013). The Jena Diversity-Dynamic Global Vegetation Model (JeDi-DGVM): a diverse approach to representing terrestrial biogeography and biogeochemistry based on plant functional trade-offs. *Biogeosciences*, *10*: 4137-4177.

Peñuelas, J., Lloret, F., Montoya, R. (2001). Severe drought effects on Mediterranean woody flora in Spain. *Forest Science,* 47(2): 214-218.

Sakschewski, B., von Bloh, W., Boit, A., Rammig, A., Kattge, J., Poorter, L., Penuelas, J., Thonicke, K. (2015). Leaf and stem economics spectra drive diversity of functional plant traits in a dynamic global vegetation model. *Global Change Biology*, 21: 2711-2725.

Schaphoff, S., Bloh, W.V., Rammig, A., Thonicke, K., Biemans, H., Forkel, M., Gerten, D., Heinke, J., Jägermeyr, J., Knauer, J., Langerwisch, F. (2018). LPJmL4–a dynamic global vegetation model with managed land–Part 1: Model description. *Geoscientific Model Development*, 11(4): 1343-1375.

Schaphoff, S, Forkel M, Müller C, Knauer J, von Bloh W, Gerten D, Jägermeyr J, Lucht W, Rammig A, Thonicke K, Waha K. (2018). LPJmL4 - a dynamic global vegetation model with managed land: Part II – Model evaluation, Geosci. Model Dev. Discuss.. *Geoscientific Model Development*, 11(4): 1377–1403.

Schneider, F.D., Morsdorf, F., Schmid, B., Petchey, O.L., Hueni, A., Schimel, D.S., Schaepman, M.E. (2017). Mapping functional diversity from remotely sensed morphological and physiological forest traits. *Nature communications*, 8(1): p.1441.

Sitch, S., Huntingford, C., Gedney, N., Levy, P. E., Lomas, M., Piao, S. L., ... & Jones, C. D. (2008). Evaluation of the terrestrial carbon cycle, future plant geography and climate-carbon cycle feedbacks using five Dynamic Global Vegetation Models (DGVMs). *Global Change Biology*, *14*(9): 2015-2039.

Co-funded by the European Union

3.3 Mapping pan-European current and future ecosystem services from species distribution models of 236 woody plants

By Yoni Gavish, Bill Kunin and Guy Ziv

Introduction

Mapping the supply and demand of various ecosystem services (ESS) is essential for effective planning. ESS maps provide valuable information on trade-offs and synergies between ESS, on the dependence of ESS on biodiversity, and on the future supply of multiple ESS under alternative future scenario. As such, mapping ESS is listed as one of the required steps according to Action 5 of the EU Biodiversity Strategy to 2020. Recently, Lavorel et al. (2017) distinguished between five types of mapping approaches including proxy models, phenomenological models, niche-based models, trait-based models and full-process models. The five approaches differ in their ESS provider (e.g., land-use cover, species, traits-based matrices and functional types), complexity (e.g., tier 1-3; Maes et al. 2014), scales and data requirement. As with other modelling techniques, each approach has its pros and cons and hybridization of approaches, taking the best from each, may further develop the field of ESS mapping.

One potential venue for such hybridization is between niche-based and trait-based models. Niche-based models rely on species as the ESS provider. The spatial distribution of species is extrapolated (and if needed, projected) using species-distribution models (SDM). In some cases, a single species known to provide a specific ESS is modelled. In other cases, SDMs of multiple species are aggregated to represent the total ESS supply by the entire (user-defined) community. In the trait-based approach different land-use or land-cover categories are linked to community-level trait values such as plant height or mineral concentration, which are known to relate directly or indirectly to the supply of certain ESS (Lavorel et al. 2011). The advantage of the SDMs based ESS map is in the relative ease by which SDMs can be projected to the future under various scenarios, the increasing availability of distribution data for model training and validation, and in the well-developed modelling tools. The limitation lies in the a-priori decision of which species constitute the community, and in assigning all species the same weight when aggregating, ignoring interspecific variability in ESS supply potential. On the other hand, trait-based models have the advantage of assigning different functional groups different ESS supply weights. However, the reliance of land-cover/land-use data, which is not easily projected (Titeux et al. 2016) limits the ability of the models in terms of comparing future scenarios.

In this analysis, we link niche-based and trait based ESS models. We integrated SDMs of 235 woody plant species with ecological and culturomic trait information on the ability of these species to supply seven ESS at a pan-European scale. We then explore the amount of ESS that located within protected area in current climate and several climate change scenarios.

Co-funded by the European Union

Methods

Study area, species distribution data and environmental predictors

We have focused the analysis on 38 European countries, overlaid with a 1×1 km2 INSPIRE compliant grid. We integrated distribution data for 352 woody plant species from two sources, the EU-Forest database (Mauri et al. 2017) and GBIF (GBIF.org 2017) and modelled 236 species that had at least 50 occurrences (a total of 2,643,377 records). We created 49 predictors based on topography (7), soil (7), and climate (35). For the topography, we used the 'GMTED2010' global digital elevation model (Danielson and Gesch 2011) with 30 arc-second resolution, which we re-projected and resampled to fit the 1×1 km2 INSPIRE grid. We prepared 7 soil predictors, using data from the European Soil Data Centre (ESDAC) (Panagos et al. 2012). We included current and future bioclimatic variables, based on the ClimateEU dataset, an ensemble of 15 CMIP5 models that performed well in Europe (ClimateEU 2013). We extracted 35 bioclimatic variables, for current and 3 future time periods, 2020 (2011-2040), 2050 (2041-2070) and 2080 (2071-2100), according to 2 emission scenarios (RCP4.5 and RCP8.5).

Species distribution models

We fitted MaxEnt models, which are best suited for presence-only data to the 236 species. We selected 150,000 background points, using a random selection process that accounted for sampling bias. We then optimized the choice of MaxEnt parameter following a model-selection based parameter sweep covering 48 combinations of eight feature class sets and six regularization multipliers. Depending on the amount of occurrences, we divided the data to several spatial or non-spatial cross-validation sets and fitted a MaxEnt model with the optimal parameters to each set. For each fitted model we predicted for all current and future climatic scenarios. We averaged the predicted relative likelihoods (RL) over all cross-validation sets, ensuring the usage of test data only. We repeated this entire procedure 6 times for each species (each time selecting different background points) and took the average predicted RL over all runs. We assessed the performance of the models with AUC adapted for presence-only data.

Trait-based weights for seven ESS

We conducted a thorough literature review to assign all the species values according to 7 different ESS including:

1. Timber – we aggregated information from 2 sources and gave each species an initial score between 0 and 1 based on it being mentioned or not in the two sources. We further corrected the weights based on the growth form of the species with weights for trees > tree/shrubs > shrubs.

2. Pollination – We quantified the pollination weights using the multiplication of two traits from the TRY database: a) The pollination syndrome (TraitID 29), standardized to three levels: Animal = 1, mixed = 0.5 and wind = 0. b) The amount of nectar (traitID 205): Nectar none = 1, Nectar little = 2, Nectar Present = 3 and Nectar Plenty = 4. If the data of any of the traits was unavailable for a given species we took the mean value of the closest taxonomic level (genus, family, order, class and phylum at this order).

3. Medicinal usage – quantifying medicinal weights is not straightforward, as most species are listed as having at least some medicinal value in traditional medicine and there is considerable confusion between common and scientific names. It was beyond the scope of this paper and the expertise of the authors to validate each source and common name. Instead we took a culturomics approach, based on Kew Gardens' Medicinal Plant Names Services database. The database aggregated more than 530,000 data records with scientific pharmaceutical and common names of medicinal plants from 143 sources. We assumed that if a species is mentioned in many sources it is either used extensively in the pharmacological and/or traditional medicine or it has been explored extensively in that regards. We took the number of sources each species was mentioned in as the weights.

Co-funded by the European Union

4. Edibility – We integrated information from multiple sources, giving higher emphasis to FAO publications, to the EU pesticide database and to 12 volume series covering a large number of edible plants. We assigned species to 4 levels: a) Species with global commercial value as edible food source (weight: 5). b) Species with a more local commercial value as edible food source (weight: 3.5). c) Species is edible and is used in traditional cuisine (weight: 1.5). d) Species with anecdotal or no documented usage as food source (weight: 0.5).

5. Cultural value – We relied on culturomics methods to assign species cultural value weights (see webpanel1 in: Ladle et al. 2016). We searched for the species scientific name in 5 online platforms: a) Google Chrome (number of results). b) Microsoft Bing – (number of results), c) YouTube (number of results), d) Flicker – (number of pictures tagged with scientific name), e) Google Books Ngram Viewer (mean number of results over the years 1970-2000). We then ranked species in each platform and took the mean rank as the weight.

6. Carbon storage potential – We integrated multiple sources for diameter (6 sources, 2,121,052 observations), height (7 sources, 259,046 observations) and wood density (5 sources, 870 observations) to estimate per-capita Above Ground Biomass (AGB) as a proxy for species' carbon storage potential. We relied on Paul et al. (2016) allometric equations to transform diameter measured at different heights above ground to AGB. Plant height data was used in two ways, first to fill in gaps in diameter measurement by exploring the relation between height and diameter with 9 non-linear regression models. Second, along with wood density to identify the most appropriate allometric equation for each species: Shrubs (height ≤ 2 m), Other-L (height > 2 m, wood density ≤ 0.5 g/cm^3), Other-H (height >2 m, wood density ≥ 0.57 g/cm^3) and Universal (all other cases).

7. Soil fertility - We used leaf nitrogen concentration (mg/g) as a proxy for the soil fertility, since species with higher leaf nitrogen usually have higher nutrient cycling rates, resulting with more fertile soils (van Bodegom and Price 2015). We extracted data on Leaf nitrogen concentration from the TRY database and took the mean value for each species, covering 181 species. For the remaining 55 species we took the mean value of the closest taxonomic level.

We explored the ESS weights for all species using nMDS analysis based on Gower distances.

Mapping ESS

Prior to stacking RL we transformed the values of each cell as:

$$X_{n,s,es} = \frac{RL_{n,s}}{\sum_{n=1}^{N} RL_{ns}} \cdot \frac{V_{s,es}}{\sum_{s=1}^{S} V_{s,es}} \cdot G \qquad \text{Eq.1}$$

With RLn,s being the relative likelihood value of species s in cell n, N the total number of cells, S the total number of species, Vs,es the overall value of species *s* to ecosystem service *es* and G a value to which $\sum_{s=1}^{S}\sum_{n=1}^{N}(X_{n,s,ES})$ should equal. Eq. 1 is comprised of three terms. The first term ensures that all species contribute the same total value when summed over all cells prior to weighting by the *es* value. The second term weigh species total contribution relative to their ability to provide various ESS. The third term is a standardization value ensuring that the sum over all species and cells of the ESS map would be comparable to other ESS maps. If all ESS are constructed from the same number of species, G can be set to S (as we have done here), and thus the units of any aggregated subset of $X_{n,s}$ is measured in units of 'species'.

The first standardization term $RL_{n,s}/\sum_{n=1}^{N} RL_{ns}$ is an extension of a commonly used index 'endemism-richness' to the probabilistic output of SDM. Usually, 'endemism-richness' is calculated for each cell as the proportion of the species total range size found within the cell giving equal contribution of 1/RangeSize to all occupied cells. It is interpreted as the specific contribution of the species and cell to global biodiversity and can be summed over multiple species and/or cells to represent the overall contribution of an area to global biodiversity. When using the

Co-funded by the European Union

probabilities of SDMs for standardization, cells that differ in their RL very in their contribution. The standardized value may be interpreted as the specific contribution of the species and cell to the potential distribution of global biodiversity. However, when projecting SDMs to the future there is an inherent trade-off between two standardization methods. In the first one, $\sum_{n=1}^{N} RL_{ns}$ is done for each climate separately, while in the second $\sum_{n=1}^{N} RL_{ns}$ is summed over all climates together. In the first approach, each species contribute a total of 1 to each climate, but the generated maps ignore overall trends in RL with time. In the second approach, each species contribute a total of 1 to all climates together, and the proportion assigned to each climate may differ between species. However, in the second approach trends in RL are conserved and accounted for, making the ESS of various climates scenarios more comparable. Although unexplored, we suggest using the first approach if the main question focuses on trade-off and synergies between various ESS in given time, and the second approach if comparison of future scenarios is the main focus. Here, we focus on both multiple ES and multiple future scenarios, thus we used the second standardization method (unless stated otherwise).

The second term $V_{s,es}/\sum_{s=1}^{S} V_{s,es}$ standardize the overall value of the species contribution to a certain ESS, relative to all other species. We note here that for the standardization to make sense, $V_{s,es}$ should reflect the overall value of the species and not the per-capita value of the species. This is true here for the cultural value ESS, but for the other six ESS we added an additional weight to the equation, accounting for the prevalence of the species and allowing more common species to contribute more than rarer species

$$X_{n,s,es} = \frac{RL_{n,s}}{\sum_{n=1}^{N} RL_{ns}} \cdot \frac{V_{s,es} \cdot \sum_{n=1}^{N} RL_{n,s} \,/\, \sum_{s=1}^{S}\sum_{n=1}^{N} RL_{ns}}{\sum_{s=1}^{S}\left[V_{s,es} \cdot \sum_{n=1}^{N} RL_{ns} \,/\, \sum_{s=1}^{S}\sum_{n=1}^{N} RL_{ns}\right]} \cdot G \qquad \text{Eq.2}$$

After weighting each species by the $V_{s,es}/\sum_{s=1}^{S} V_{s,es}$ term, the index may be interpreted as the specific contribution of the species and cell to the potential distribution of the ecosystem services. When stacked over all species for a given cell, the index measures the contribution of the cell to the potential distribution of the ecosystem service. Finally, when aggregating multiple cells, the index measures the the potential ESS that is found within the aggregated area.

Additional analysis

After creating the seven ESS maps for the current and each of the future scenarios, we aggregated the values spatially, to identify biodiversity hotspots and trend in total ESS with time. To aggregate, we superimposed a 32x32 km grid on the entire extent and summed the ESS values in each 32x32 cell over all 7 ES. We also summed the amount of ESS found with protected area networks (PAN). We used the Natura2000 network, the CDDA network and the combination of both as PAN. We compared the observed values to a null model which reflect the amount of ESS that is expected to be found within each PAN if ESS is randomly distributed in space and time: $C_{PAN} \cdot 235 / 7$ with C_{PAN} being the proportion cover of the PAN, 235 being G from Eq. 1 and Eq. 2 and 7 being the number of climates to which the data was standardized.

Results

The mean AUC (over all runs for a given species) was in the range 0.820-0.999, with mean value of 0.939, for all species except one that failed to converge, leaving 235 species for ESS mapping. The nMDS of the species ESS weights revealed a first separation between cultural value and edibility/timber value, and a second separation between pollination value and carbon storage values (Fig. 50). For all ESS, we found a similar trend of total ESS with time, with a slight increase in the amount of ESS potential ESS in 2020, followed by a decrease for 2050 and 2080. The degree of decrease in total ESS was greater for RCP8.5 than for RCP4.5 (Fig. 51). ESS hotspots were identified in south Sweden, Britain and Western Europe, with additional hotspot on the Mediterranean coast of Spain. ESS hotspots followed a similar trajectory as the ESS themselves, with Western Europe losing much of its potential to

Co-funded by the European Union

support multiple ESS under the RCP8.5 scenario. Finally, we found that the Natura2000 PAN support less ESS then expected by a null model both currently and in future scenarios (Fig. 53). On the other hand, the CDDA PAN network support more ESS than expected by chance in all future scenario other than RCP8.5 for the year 2080. When considering both PANs, the network support more than expected by chance for the RCP4.5, but less than expected by chance for RCP8.5.

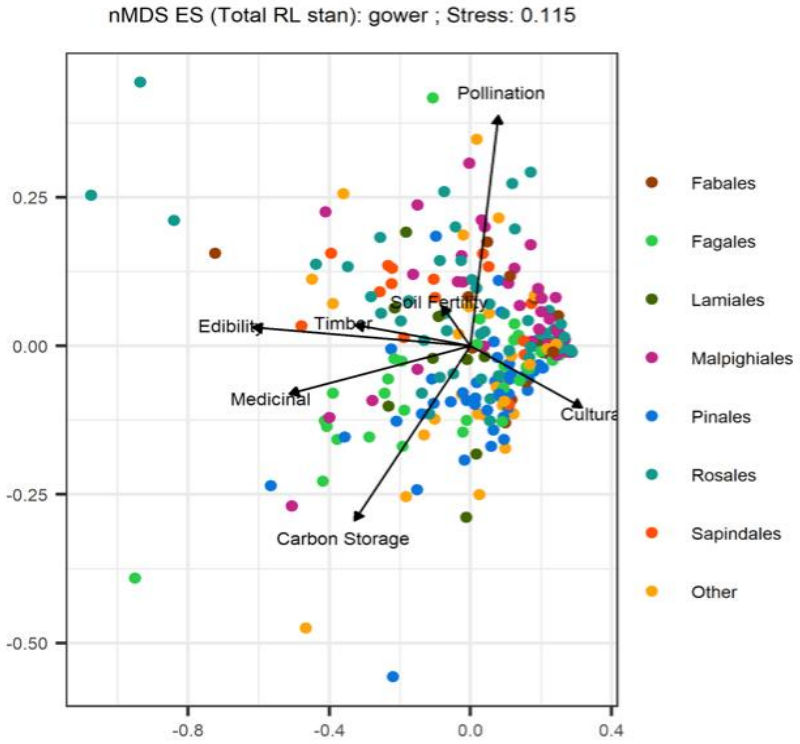

Figure 50: nMDS of the per-species ESS weights for the 235 species (points). Taxonomic orders with at least 10 species are labelled with different colours.

Co-funded by the European Union

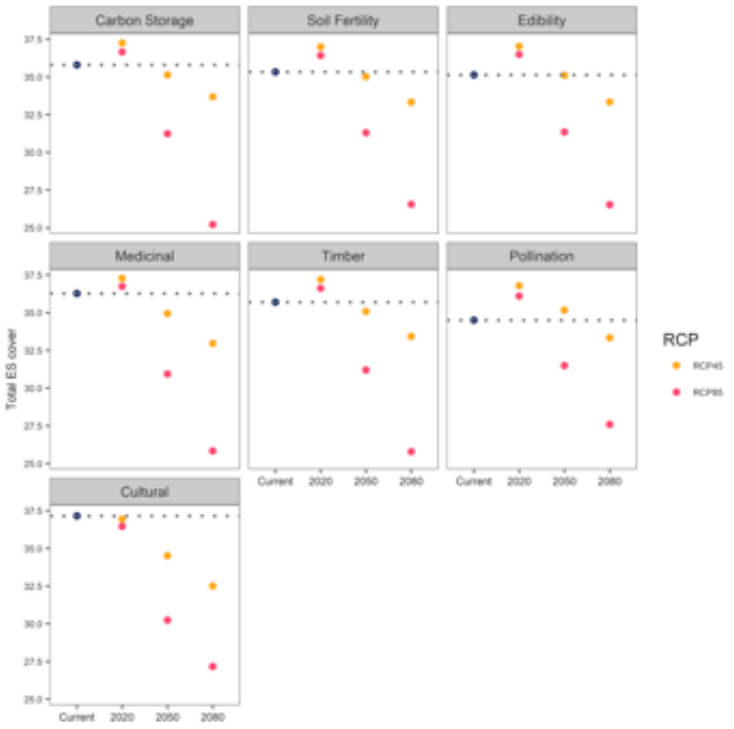

Figure 51: Change in total ESS with time and climate scenario relative to current cover of ESS (blue point and dashed line). Total ESS is measured in units of species and the sum of all values in each panel should equal 235. The expected value according to a null model is 235/7 = 33.57.

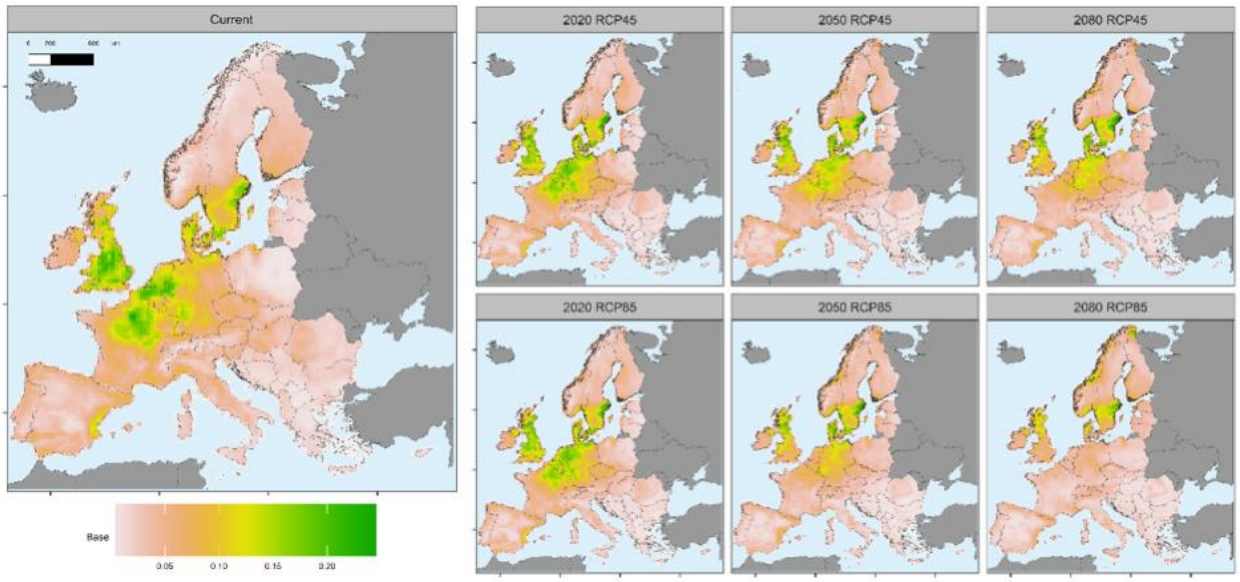

Figure 52: The current and future spatial distribution of total ESS, when summing all seven ES in each location. Values are aggregated to 32×32 km grid for clarity.

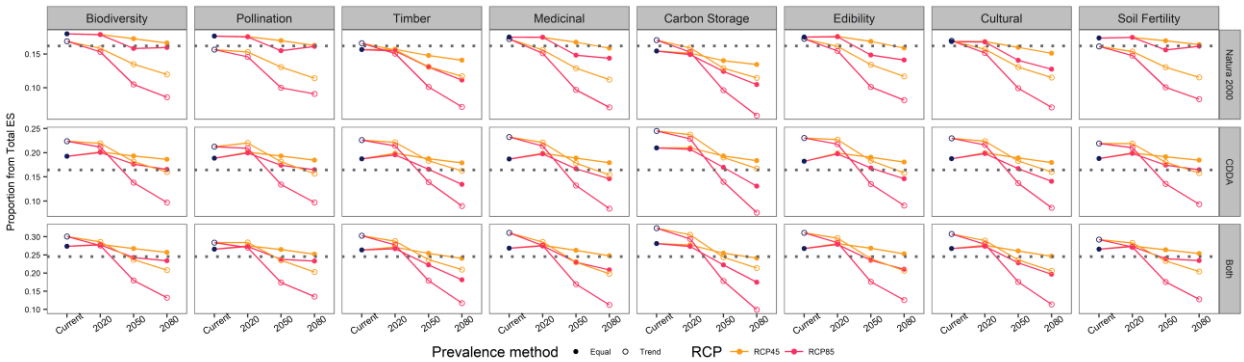

Figure 53: Change in the proportion of ESS found with the NATURA2000, CDDA and both protected area network, according to each climatic scenario. Dashed line is the expected value under an area-based null model.

Discussion and conclusions

Our results show the potential hybridization of SDMs and trait-based weights for mapping the current and future distribution of the supply of multiple ESS. As far as we know, this is the first time such an attempt is done. We found an overall decline in most ESS with time and climate change. Although more species are declining in total RL than increasing (RCP4.5: 136 declining and 99 increasing; RCP8.5: 153 declining and 82 increasing), the difference does not seem to be large enough to dominate the patterns. In other words, the declining species are also those that have larger weight for at least some ESS, especially since many species only slightly changed their total RL with climate change. Since all ESS maps are eventually based on similar SDMs, it is not surprising they exhibit similar overall distribution patterns. However, out trait analysis reveal potential trade-off between ESS (Fig. 50) that may translate to fine scale differences in ESS distribution which are beyond the scope of this report. Finally, we found a contrasting pattern in relation to Natura2000 and CDDA, with the first supporting less ESS than expected by chance and the second more than expected by chance (Fig. 53). On the other hand, when considering biodiversity per-se (as richness or IUCN based weights), the Natura2000 network support more than expected by chance (results not shown here), suggesting the PAN may do what it is designed to do – protect biodiversity, but cannot capture the species that provide the highest value for various ESS. We note, that this analysis is currently being finalized for publication and advice the readers to search for more detailed results and discussion later this year.

References

ClimateEU. (2013). Climate data has been generated with the ClimateEU v4.63 softwarepackage, available at http://tinyurl.com/ClimateEU, based on methodology described by Hamann et al. (2013).

Danielson, J. J., and D. B. Gesch. (2011). Global multi-resolution terrain elevation data 2010 (GMTED2010): U.S. Geological Survey Open-File Report 2011–1073.1-23. GBIF.org. 2017. GBIF Home Page. Available from: http://gbif.org [3rd November 2016].

Ladle, R. J., R. A. Correia, Y. Do, G. J. Joo, A. C. M. Malhado, R. Proulx, J. M. Roberge, and P. Jepson. (2016). Conservation culturomics. Frontiers in Ecology and the Environment 14:269-275.

Lavorel, S., A. Bayer, A. Bondeau, S. Lautenbach, A. Ruiz-Frau, N. Schulp, R. Seppelt, P. Verburg, A. v. Teeffelen, C. Vannier, A. Arneth, W. Cramer, and N. Marba. (2017). Pathways to bridge the biophysical realism gap in ecosystem services mapping approaches. Ecological Indicators 74:241-260.

Lavorel, S., K. Grigulis, P. Lamarque, M.-P. Colace, D. Garden, J. Girel, G. Pellet, and R. Douzet. (2011). Using plant functional traits to understand the landscape distribution of multiple ecosystem services. Journal of Ecology 99:135-147.

Maes, J., A. Teller, M. Erhard, P. Murphy, M. L. Paracchini, J. I. Barredo, B. Grizzetti, A. Cardoso, F. Somma, J.-E. Petersen, A. Meiner, E. R. Gelabert, N. Zal, P. Kristensen, A. Bastrup-Birk, K. Biala, C. Romao, C. Piroddi, B. Egoh, C. Fiorina, F. Santos, V. Naruševičius, J. Verboven, H. M. Pereira, J. Bengtsson, K. Gocheva, C. Marta-Pedroso11, T. Snäll, C. Estreguil, J. S. Miguel, L. Braat, A. Grêt-Regamey, M. Perez-Soba, P. Degeorges, G. Beaufaron, A. Lillebø, D. A. Malak, C. Liquete, S. Condé, J. Moen, H. Östergård, B. Czúcz, E. G. Drakou, G. Zulian, C. Lavalle. (2014). Mapping and Assessment of Ecosystems and their Services. Indicators for ecosystem assessments under Action 5 of the EU Biodiversity Strategy to 2020. Publications office of the European Union, Luxembourg.

Mauri, A., Strona, G., San-Miguel-Ayanz. J. (2017). EU-Forest, a high-resolution tree occurrence dataset for Europe. *Scientific Data* 4:160123.

Panagos, P., Van Liedekerke, M., Jones, A., Montanarella, L. (2012). European Soil Data Centre: Response to European policy support and public data requirements. *Land Use Policy* 29: 329-338.

Paul, K. I., S. H. Roxburgh, J. Chave, J. R. England, A. Zerihun, A. Specht, T. Lewis, L. T. Bennett, T. G. Baker, M. A. Adams, D. Huxtable, K. D. Montagu, D. S. Falster, M. Feller, S. Sochacki, P. Ritson, G. Bastin, J. Bartle, D. Inildy, T. Hobbs, J. L. Armour, R. Waterworth, H. T. L. Stewart, J. Jonsonf, D. I. Forrester, G. Applegate, D. Mendhan, M. Bradford, A. O'Grady, D. Green, R. Sudmeyer, S. J. Rance, J. Turner, C. Barton, E. H. Wenk, T. Grove, P. M. Attiwill, E. Pinkard, D. Butler, K. Brooksbank, B. Spencer, P. Snowdon, N. O'Brien, M. Battaglia, D. M. Cameron, S. Hamilton, G. McAuthur, A. Sinclair. (2016). Testing the generality of above-ground biomass allometry across plant functional types at the continent scale. Global Change Biology 22:2106-2124.

Titeux, N., K. Henle, J.-B. Mihoub, A. Regos, I. R. Geijzendorffer, W. Cramer, P. H. Verburg, L. Brotons. (2016). Biodiversity scenarios neglect future land-use changes. *Global Change Biology,* 22: 2505-2515.

van Bodegom, P. J. H., Price, T. (2015). A traits-based approach to quantifying ecosystem services. Pages 40-64 *in* J. A. Bouma and P. J. H. van Beukering, editors. Ecosystem Services: From Concept to Practice. Cambridge University Press, Cambridge, UK.

Co-funded by the European Union

3.4 Impact of climate change on Mediterranean wetlands

by Brigitte Poulin, Gaetan Lefebvre et al., TdV

Introduction

The Mediterranean basin is a biodiversity and climate change hotspot home to ecologically and economically important semi-permanent wetlands. The region's overall negative water balance results in the formation of semi-permanent marshes along the coast of the basin, which dry-up in summer and refill with water over winter. They are characterised by aquatic emergent vegetation whose productivity is far greater compared to terrestrial ecosystems in the region. They provide food and habitat for animal species which are endemic, endangered and of heritage interest. Biodiversity and the services provided by these wetlands (provision of food, building materials, recreational activities, etc.) rely on the seasonal flooding patterns. Most climate models predict a pronounced warming, reduction in precipitation and increased inter-annual variability for all parts of the Mediterranean in the 21st century. The impacts will be spread over a very heterogeneous zone where the current water deficits are very different according to the regions; for example, Trieste, Italy has an average annual precipitation of 1,203 mm and evapotranspiration of 1,602 mm, whereas, Ksar El Boukhari, Algeria, has a much greater water deficit with 381 mm average annual precipitation and 2,030 mm evapotranspiration. Further, evapotranspiration on dry soil is much lower than on flooded soil. Accordingly, if an increase in summer drought coincides with the natural period of drying up there will be lesser impact. However, if it doesn't, it will lead to a decrease in the flooding period which entails a loss of functionality, a significant degradation or the disappearance of this type of habitat. This makes it difficult to predict the extent of hydrological changes and how they will differ for different areas. To predict the hydrological functioning of semi-permanent wetlands under climatic change we used two greenhouse gas concentration projections emissions, RCP 4.5 and RCP 8.5, for the years 2050 and 2100 and simulated evolution of the water balance, wetland habitat changes and water volumes necessary for maintenance of semi-permanent wetlands in 229 localities around the Mediterranean basin.

Methods

Study area: semi-permanent Mediterranean wetlands

The wetlands modelled naturally flood and dry each year; their good development and functioning are directly associated with the duration of flooded and dry periods. Where flooding is deepest, the marshes are typically colonized by tall emergent vegetation such as tall club-rushes and bulrushes (e.g. Schoenoplectus lacustris, Schoenoplectus litoralis and Thypa spp.). In the zone in-between these species and the edges of marshes, sea club-rush (Scirpus maritimus) and common reed are found (Phragmites australis). If the dry period is too long, vegetative growth is low, which results in a loss of biodiversity (e.g. reed passerines, reed-nesting herons and ducks) and ecosystem services (e.g. provision of building materials, water purification and breeding habitats for fish and ducks). If flooding periods are very short, tall emergents are replaced by smaller emergents, such as sedges (Cyperaceae), sea club-rush and species with annual growth (e.g. Salicornia spp.). Over several years of prolonged dry seasons, the habitat is replaced by temporary ponds with a procession of completely different plant and animal species, such as pteridophytes (Isoetes, Marsilea, Pilularia), water-starwort (Callitriche) and Lythrum. Lastly, if the flooding periods of temporary ponds are too limited, the growth of typical wetland vegetation ceases and more terrestrial species develop.

Climate model

Climate simulations were performed with the Rossby Centre regional atmospheric model, RCA4 (*SMHI-RCA4*). It included five complete sets of runs driven by five different Coupled Model Intercomparison Project Phase 5 (CMIP5)

Co-funded by the European Union

global climate models (GCMs): EC-Earth, CNRM-CM5, IPSL-CM5A-MR, HadGEM2-ES and MPI-ESM-LR. All five members of the model were included and focused on the recent climate (1981-2000), and on two future timeframes: mid- (2031-2050) and late (2081-2100) 21st century, at the highest available spatial resolution of 0.11° (approximately 12 km). For the future projections, two different RCP scenarios were considered: RCP 4.5 and RCP 8.5. Total precipitation and potential evapotranspiration were considered for all models, time periods and scenarios at 3-hour and daily temporal resolution, respectively.

To quantify RCA4 biases over the Mediterranean region, the mean daily precipitation of each RCA4 member was compared to that of the observational gridded dataset, E-OBS. To account for biases, the GCM-RCA4 model data were adjusted by applying a constant, multiplicative factor to the daily data in such a way that the model's long-term climatology is the same as in the E-OBS reference data. For all Regional Climate Models (RCMs), the potential evapotranspiration values were transformed into evapotranspiration for a large emergent marsh. The timing of wet and dry periods is essential to this study and it was important that the selected model reproduces the seasonal variation in precipitation and evapotranspiration as accurately as possible. Therefore, the data were further corrected by multiplying the data set by a coefficient to match the mean values during the critical period of the year. For each factor and site, paired t-tests were used to compare monthly values of historical data with contemporary predicted data to choose the best RCM for each factor. The selected precipitation and evapotranspiration patterns were incorporated into simulation software (Mar-O-Sel). For each site, a correction coefficient was applied to all modelled data to match the annual averages of the actual historical data to those predicted for the contemporary period.

Mar-O-Sel

The simulation tool Mar-O-Sel was used to investigate how much water level change can be expected under climate change projections, with comparison to contemporary levels. Mar-O-Sel integrates marsh parameters, hydrological data and management strategies to predict monthly water levels and water volumes needed to achieve any management strategy inputted. Historical precipitation data, evapotranspiration data and greenhouse gas projection scenarios, RCP 4.5 and RCP 8.5, for the years 2050 and 2100, for 242 localities in 21 Mediterranean countries, are used for simulations. The localities are 1 degree in size and trapezium in shape. Up to 10 consecutive years can be simulated using one of the six datasets.

To calculate the conditions necessary for a semi-permanent wetland to be maintained at each locality, catchment area size, overflow level and water table depth needed were estimated. Using these parameters, 200 simulations (20 runs of 10 years using monthly values) of historical and contemporary simulated climatic data for each locality (242) were run and checked to ensure the simulated data fit the historical. Localities that did not fit were eliminated, leaving 229 localities for analyses. For these localities, 300 simulations were run using RCP 4.5 and RCP 8.5 greenhouse gas concentration projections for 2050 and 2100. The simulations were performed in three sets of 100; the first set simulated a permanent watering of 10cm to estimate the evolution of water deficit; the second set had no human intervention, in order to estimate the maintenance and evolution of semi-permanent marshes; the third set maintained 10 cm of water from November through April and -5 cm in July and August to estimate the water volumes managers would need to input during each month.

Results

Evolution of water stress

The contemporary water balance is negative for all localities and there is no clear geographical pattern, aside from higher deficits at the eastern edge of the basin (Fig. 54). The water deficits increase at most localities in 2050 with

Co-funded by the European Union

similar amplitude in changes between both RCP scenarios, whereas in 2100 under RCP 8.5 all localities will be affected and more strongly so than RCP 4.5 (Fig. 55). A geographical pattern emerges in the future scenarios with lower water deficits in the centre of the basin and higher deficits in Northern Africa, Spain and at the eastern edge of the basin (Fig. 56).

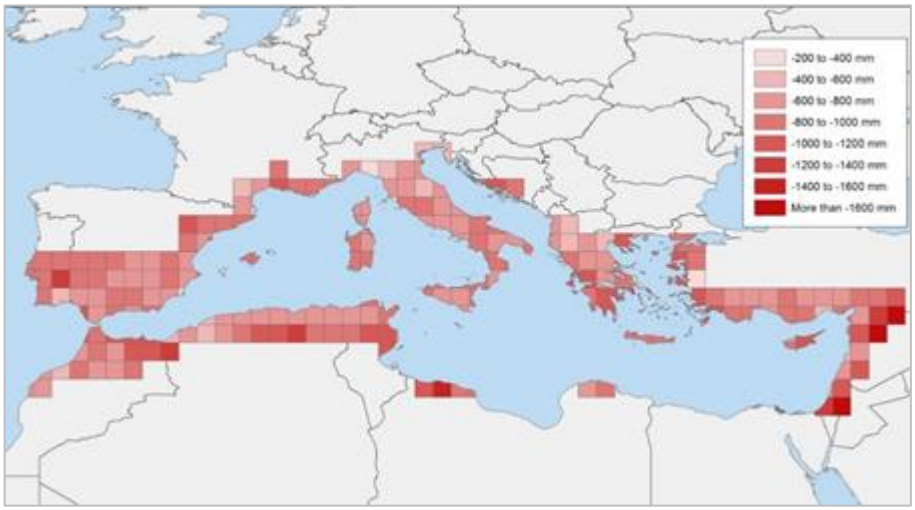

Figure 54: Contemporary annual water balance (precipitation minus evapotranspiration) for each of the 229 localities under constant flood conditions.

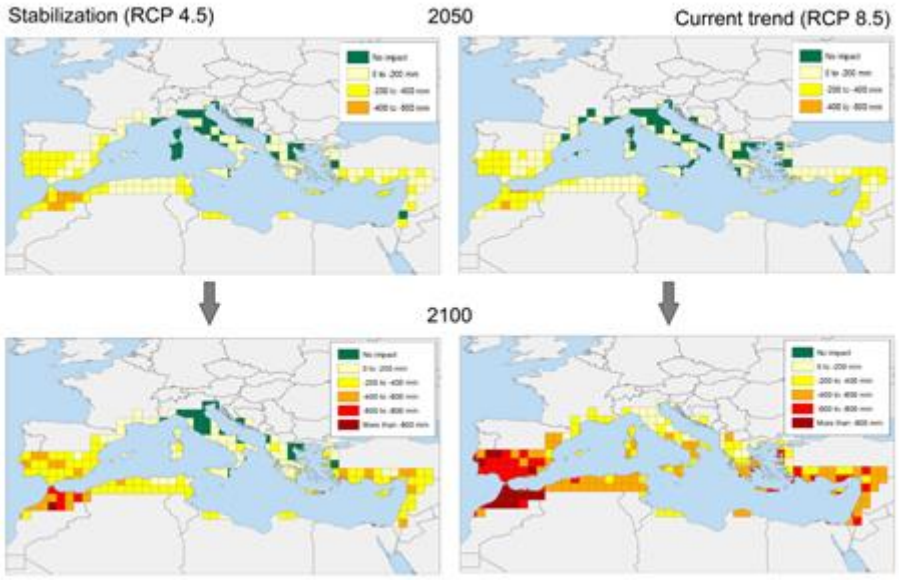

Figure 55: The change in annual water balance, under constant flooding conditions, for each locality under the RCP 4.5 (stabilization) or RCP 8.5 (steady increase) scenarios of greenhouse gas emissions for 2050 and 2100.

Evolution of vegetation types

Under contemporary simulated conditions, 97 % of localities can have wetland habitats in good condition (Fig. 56). By 2050, however, this proportion will decrease to 81 % and 68 % under the RCP4.5 and RCP8.5 scenarios, respectively, these proportions decreasing further to 52 % and 27 % by 2100. The RCP8.5 scenario shows a more dramatic degradation of habitat, both in degree of degradation and number of localities affected in 2100. Countries at highest risk of wetland degradation and loss are Algeria, Morocco, Portugal and Spain while the centre of the basin experiences less habitat change, particularly France and the northern regions of Italy and Greece. In many

Co-funded by the European Union

cases, water deficits are increasing without affecting habitat conditions, suggesting wetlands can cope with -200 to -400 mm decrease in annual precipitation.

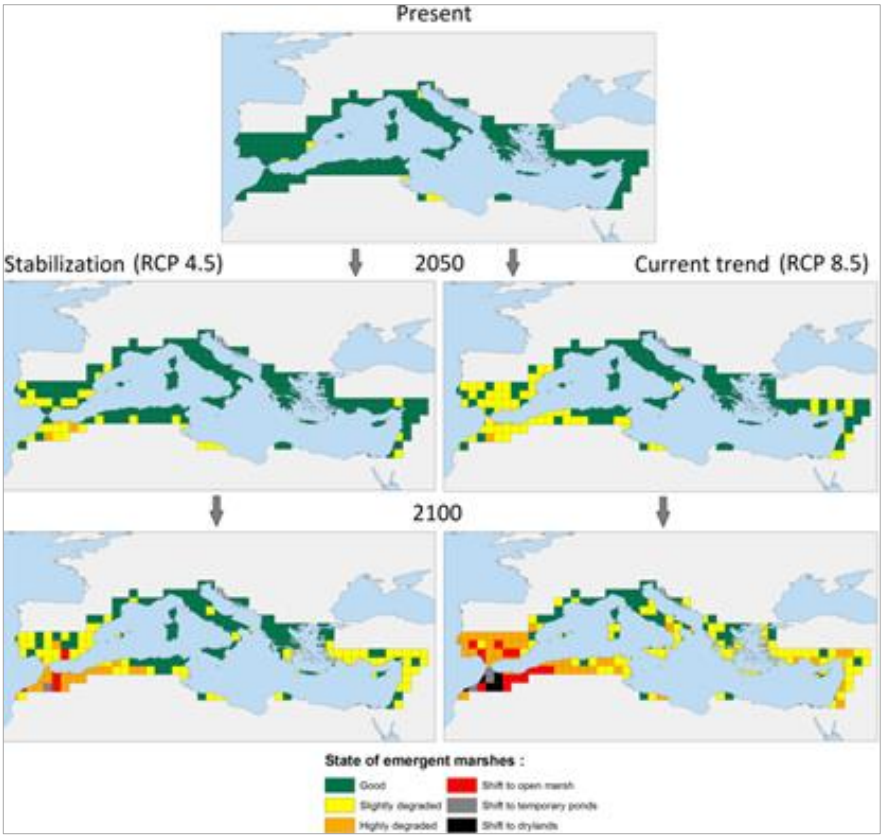

Figure 56: The expected habitat change of semi-permanent marshes under the greenhouse emission scenarios RCP 4.5 (stabilization) and RCP 8.5 (steady increase) for the years 2050 and 2100.

Water inputs

The mean water contributions needed to maintain the full functionality of wetlands for each stage of degradation are: slightly degraded habitats 1055 m^3/ha, highly degraded 1722 m^3/ha, shift to open marsh 2263 m^3/ha, shift to temporary ponds 2857 m^3/ha and shift to drylands 3537 m^3/ha.

4. Discussion of major findings and uncertainties

4.1 Main findings across studies

The Deliverable 8.4 presents the results of 12 ECOPOTENTIAL future simulation studies (which are in some cases still preliminary). These studies cover several biological scales from the individual population to the biome. The following Table 6 gives a summary overview of their main results.

Table 6: Main results for future states of ecosystems from ecological modelling.

No.	Name of Study	Biological scale (Bellard et al.2012)	Main results	Summary of modelled trends
Chapter 2: PA-scale studies				
2.1	Gran Paradiso NP: Chamois population	population	· Predicted stabilization or increase in population under RCP4.5 until 2100 throughout the majority of unstructured models, RCP8.5 prediction suggests a stable increase, especially in male and kid population · Differing /conflicting results with structured population models	↗ Overall pop ↗ Males ↘ Females Kids
2.2	Gran Paradiso NP: Topographic effects on metapopulation	meta-population	· Predicted different elevation-dependent fates decrease in species occupancy, and a decrease in species diversity under climate change	↘ species diversity
2.3	Pelagos: Fin whale distribution	population	· Predicted decline in population distribution · High uncertainty in results	↘ population density
2.4	Negev: Plant composition	ecosystem	· Predicted decline in vegetation cover of 50 % and 60 % until 2100 in RCP4.5 and RCP8.5, respectively, indicating an increased desertification towards the end of the century. · Fundamental differences between GCMs	↗ desertification ↘ precipitation ↘ vegetation cover
2.5	Peneda Geres: Hydrological impacts	ecosystem	· Predicted increase in precipitation during winter, slight decrease in summer on both RCP4.5 and RCP8.5 (even more pronounced) · Possible increase in flood events, heavy precipitation events and soil erosion · Fundamental between RCPs and GCMs	↗ precipitation seasonality ↗ extreme events ↗ soil erosion
2.6	Curonian Lagoon: Physical parameters	ecosystem	· Predicted decrease in salinity values, salinity fluxes and salt water intrusions	↗ water temp. → renewal time ↘ salinity values ↘ salinity fluxes intrusions
2.7	Wadden Sea: Physical parameters	ecosystem	· Predicted increase in water temperature over the years 2040, 2070, 2090 under RCP4.5 · Diverging results for salinity and chlorophyll-a concentrations depending on station	↗ water temp. ↕ salinity ↕ chlorophyll-a
2.8	Sierra Nevada: Land use changes	ecosystem	· Most likely classes of land use types are irrigated woody and horticultural crops	
Chapter 3: large-scale studies				
3.1	Climate Niches of N2000	ecosystems/ biome	· Future climate niches of Natura2000 sites predicted to even exceed current climate conditions of Europe · Different predicted responses of Natura2000 sites across EU, with wide spread predicted alterations of local climate conditions	↗ change in climate conditions
3.2	Adaptation of traits in European Woodlands	biome	· Gradual difference between RCPs, · Richness of trait values reduce GPP loss	↘ trait richness

3.3	European woody plant distribution and ESS	biome	· Predicted slight increase in the amount of ESS potential ESS in 2020, followed by a decrease for 2050 and 2080 with a greater predicted decline under RCP8.5 · Predicted decreasing trend in species abundance across all species, but abundance increases for some species · in future: NATURA2000 supporting less ESS than expected by chance, while CDDA more ESS than expected by chance	↘ long term ESS potential ↘ overall species abundance
3.4	Water balance and habitats of Mediterranean Wetlands	biome	· Predicted negative water balance in all localities, higher deficits and habitat impacts under RCP8.5 with increasing discrepancy until 2100	↗ Water deficits

The individual studies cover different spatial scopes - from PA-level to pan-European level - and predict future states of different abiotic elements (e.g. hydrological response) and biotic ecosystem elements (e.g. population dynamics) as well as their provision of ecosystems services, until the end of the 21st century.

On PA-scale results on abiotic and climate conditions of ecosystems generally indicate strong impacts of increasing extreme climate events. Our PA-scale studies show flooding (e.g. Peneda Geres, Portugal), soil erosion (e.g. Peneda Geres, Portugal), altered seasonality of precipitation (e.g. Peneda Geres, Portugal), negative water balances (e.g. water balance and habitats of Mediterranean wetlands), drought (e.g. Northern parts of the Negev), and continued desertification (e.g. Northern parts of the Negev). These results are consistent with our pan-European studies in the larger picture, and the results of IPCC AR5 for Europe (2013) as well as the IPCC SREX report (2012).

Changes in the climate conditions have been explored for their biotic impact at different scales, too. Simulated population dynamics of fin whales in the Pelagos or the chamois in Gran Paradiso NP revealed changing patterns in population composition and distribution, possibly leading to horizontal and vertical spatial displacements of populations. Additional results on marine salinity and chlorophyll-a distributions impose possible indirect effects on native species, as indicated in the study of the Curonian Lagoon and the Wadden Sea. A further decline of plant diversity was found in the Negev desert, where especially the shrubs and perennials are predicted to decline. From an overall large-scale perspective, almost all Natura2000 sites are likely to undergo substantial changes in climate conditions, with potential impacts on their ecosystem composition and habitats. For the terrestrial European biome, total biomass is expected to decline, and we are likely to see a shift in plant functional types and their prevailing trait distribution. The study on terrestrial ecosystem services predicts an overall reduction in ES provisioning in the face of climate change, namely for timber, pollination, edibility, medical supply, cultural value, carbon storage and soil fertility. It further shows that Natura2000 is less efficient than CDDA in capturing the supply of these ecosystem services in future.

In nature, social-ecological processes interact heavily between each other, creating a complex system of interdependencies. These are also called cross-scale interactions (CSI), when the cause-and-effect relationships of the drivers of ecosystems changes and their response variables operate on different temporal and spatial scales (Soranno et al. 2014). In model settings, these indirect driver of change are often not sufficiently accounted for, mainly due to the essential global connectivity between subsystems and the nearly infinite number of parameters and required data. In most cases a comprehensive knowledge on all spatial non-linearities, threshold behaviours, and cascading effects is non-existent (Peters et al. 2004). For an increased holistic understanding and the prediction of environmental changes, however, a consideration of at least the main identifiable sociocultural, geophysical or ecological cross-interactions would be an additional advance to reduce uncertainties. As already many different scales are covered in this study, an ideal next step could therefore include an increased focus of local- and macroscale interactions and the modelling of such CSI. One future example for the implementation of such CSI will

Co-funded by the European Union

relate fin whale population at Pelagos to international agreements in the adaptations of marine traffic routes in the Mediterranean Sea. The CSI quantification by Soranno et al. (2014) including multi-thematic, multi-scaled databases as well as Bayesian hierarchical models can be used as a reference methodology for this as well as for more follow-up CSI studies. To elaborate further on potential uncertainties in future simulations, the following section will reflect on the findings on the different types of uncertainties, their diverse handling within the studies as well as on suggestions for best practices of uncertainty assessments.

4.2 Handling of uncertainties

The handling of uncertainties in the different future simulation studies of ECOPOTENTIAL varies strongly. Hence, the collection of the presented studies allows us to summarise common practices. Table 4 differentiates between internal modelling (e.g. processes (not) accounted for, comparison of models, sensitivity to calibration data, ...), input data for simulation runs (e.g. quantitative consistency analysis with observed data, number of GCMs and RCMs used/compared, choices in selection of GCMs and RCMs, ...) and scenario uncertainty (e.g. multiple RCPs used to indicate the level of uncertainty of future emission), which are also further explained in the introduction. The degrees of addressing these uncertainties have been accounted for by the differentiation of mentioned, discussed, aggregated and quantified. “Mentioned” refers to the recognition of the uncertainty, “discussed” to explained choices and their potential implications. “Aggregated” has been used only for uncertainties related to climate input data and refers to the use of several models, without a reference to the range of climates and climate impacts covered. This occurs if several GCMs are used for simulations, but the results are shown as mean over all GCMs, or by using products that already provide a mean climate input from a number of GCMs (e.g. ClimateEU, see Hamann et al. 2013). “Quantified”, finally, refers to a quantitative assessment describing the uncertainty, either by simple comparison of values, or by more elaborate statistics (e.g. root mean square errors over several parameters and GCMs). Most importantly, this also includes the quantitative comparison between modelled climate data and observed data for a period in the past.

Co-funded by the European Union

Table 7: Handling and reflection of uncertainties.

No.	Name of Study	Handling of uncertainties Mentioned (M), Discussed (D), Aggregated (A), Quantified (Q)		
		Internal model uncertainty	Input data uncertainty	Scenario uncertainty
Chapter 2: PA-scale studies				
2.1	Gran Paradiso NP: Chamois population	Q: comparison of structured and unstructured population models	Q: Shows and quantifies range between 5 downscaled GCMs	Q: Comparison between two RCPs
2.2	Gran Paradiso NP: Topographic effects on metapopulation	Q: Quantified from stochastic model simulations	n/a	n/a
2.3	Pelagos: Fin whale distribution	Q: Comparison of performance of two species distribution modelling methods: GLM and MaxEnt Q: Comparison of performance of different folds of occurrence data for both model types Q: Standard deviation in both the current and future climate model ensembles D: Reflection on the high variation in response curves between the algorithms	Q: five-fold subsampling of input and validation data and comparison of resulting models and model performances	M: one RCP only
2.4	Negev: Plant composition	Q: Validation of vegetation cover with remote-sensed reference data M: limitation to three plant functional types M: no erosion included	Q: Comparison of 4 downscaled GCMs Q: Consistency of modelled climate data with locally observed precipitation data	Q: Comparison between two RCPs
2.5	Peneda Geres: Hydrological impacts		Q: Comparison of 4 downscaled GCMs	Q: Comparison between two RCPs
2.6	Curonian Lagoon: Physical parameters		Q: Scaled RMS error as percentage error of all meteorological parameters of the 5 downscaled GCMs A: Results of 5 downscaled GCMs presented as mean	Q: Comparison between two RCPs
2.7	Wadden Sea: Physical parameters		D: Explanation why only one downscaled GCMs Elaboration has been used (equal likelihood of their occurrence)	D: Explanation of the decision to show results only for one RCP
2.8	Sierra Nevada: Land use changes		n/a	n/a
Chapter 3: large-scale studies				
3.1	Climate Niches of N2000		M: Availability and need for further include more GCMs	M: Availability and need to further include more RCPs
3.2	Adaptation of traits in European Woodlands	Q: Comparison of results from models that include different mechanisms of adaptation to climate change D: Explanation for the reductionist view of trees D: lack of forest management	M: Mentioned, but focus of study on mechanism of trait shift, not prediction.	Q: Comparison between two RCPs
3.3	European woody plant distribution and ESS	Q: Calculation of the averaged predicted relative likelihoods (RL) of occurrence for plant species over all cross-validation sets Q: Repeat background point selection process multiple times per species.	A: Use a data product with mean of 15 GCMs as input to simulation	Q: Comparison between two RCPs
3.4	Water balance and habitats of Mediterranean Wetlands		A: Results of 5 GCMs to a mean impact on annual water balance and habitat change	Q: Comparison between two RCPs

In total, we identified 36 uncertainties that explicitly referred to in the presented studies, which are nearly equally distributed between the three types of uncertainties. 22 of these 36 uncertainties were quantified, and the remaining uncertainties were at least explicitly mentioned. Quantification for each of the three types of uncertainty ranges between 50 % and 70 % for the scenario uncertainty (see Fig. 57), which is mostly based on simple

Co-funded by the European Union

comparison between RCPs. Consistency assessment between observed climate data and modelled climate data has been conducted in several studies, such as Negev (2.4), and Curonian Lagoon (2.6).

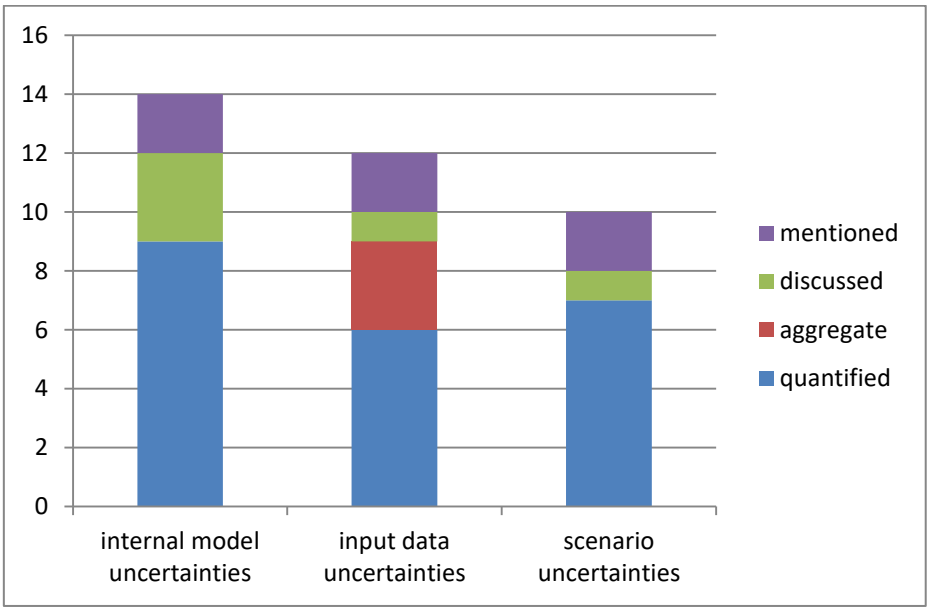

Figure 57: Handling of different types of uncertainties in future simulations in the presented ECOPOTENTIAL studies.

Overall, the distribution of quantitative assessments between uncertainty types is very heterogeneous between the studies, depending on their individual focus. For instance, some studies investigate explicitly the behaviour and sensitivity of their model, and thus strongly focus on the internal model uncertainties, whereas others have a focus on estimating the impact of future climate, here the full range of climate inputs generated by GCMs and RCPs is intensively used, compared and discussed.

The distribution of quantitative assessments within our set of studies indicates no systematic bias towards different handling of uncertainties at different biological or spatial scales. We find quantitative assessments of uncertainties across biological scales and in both PA-scale and large-scale studies, for all types of uncertainty.

Although the collection of presented studies is neither comprehensive nor representative, we can identify three profoundly different strategies how ECOPOTENTIAL studies handled uncertainties in future simulations and climate change impact studies for ecosystems. Two of these strategies directly deal with uncertainties inherent to the ecological models and focus on modelled ecosystem behaviour (1-A and 1-B), and one addresses uncertainties in the climate input data for concrete climate impact assessment (2).

1-A: Focus on uncertainties in ecological models themselves, with respect to different processes, explanatory variables, model types (e.g. Chamois population in Gran Paradiso NP; fin whales at Pelagos; adaptation of vegetation traits in Europe)

These studies mainly test the effects that particular processes (for process-based physical models) and explanatory variables (for empirical models) have in explaining the current functioning and its implications for the ecosystem behaviour under climate change. They, hence, reflect uncertainties that occur with the selection of a particular model, as well as the processes and factors included. For instance, the results of unstructured and structured empirical modelling of the chamois population at Gran Paradiso NP leads to qualitatively different results, with one

Co-funded by the European Union

indicating stability and the other an increase in the population with climate change. Similarly the role of individual environmental factor in GLM and MaxEnt based species distribution models on Fin whales in the Pelagos differs between both model types (as well as for different parts of the original sample data, see below 1-B). Likewise, the comparison between different versions of process-based models can reveal the effect of particular processes, such as the potential to adapt plant traits with changing climate in the study on European woodland ecosystems.
These three studies therefore underpin very clearly, that all models represent a reductionist view of the systems, and each of them has its limitations. Inherently, there is always a strong uncertainty. This uncertainty is even larger, when these models are used to predict ecosystem behaviour under future climatic conditions with potential shifts in the role of single processes and factors. These studies very clearly highlight that testing several models and comparing their outcomes in ecosystem behaviour reveals these uncertainties and allows making them explicit. This, however, does not reduce the uncertainty per se.

1-B: Focus on uncertainties in empirical models due to data selection and availability (e.g. fin whales at Pelagos, and European-wide plant distributions and impacts on ESS)

Here, we also deal with uncertainties internal to ecological model, and more specifically we deal with the uncertainty introduced through the limited representation of reality through data. This addresses, firstly, the random characteristics of the data we use to develop (in case of empirical models), calibrate (in case of process based models) and validate models. The study on fin whales in the Pelagos demonstrates very clearly that different folds of data lead to different statistical models which perform not equally well in the validation. In this study, highlighting this effect was possible, as the dataset was stratified and a number of models were deduced from different parts of the same dataset. None of these models is wrong, but as different parts of the dataset are used, they lead to different models. This reflects the diversity of our data as well as the lack of harmonisation and interoperationalisation of different monitoring and modelling approaches to systematically capture variability of ecosystems, both over space and time at various scales. Although this uncertainty cannot be solved fundamentally in principle, some statistical methods directly account for this problem. For instance, bootstrapping datasets to draw many random samples from them has been used widely to reduce such effects. Although most often the limited representation of the real ecosystem by our data cannot so be revealed with all its variability, and associated uncertainties not quantified, the study nicely demonstrates these effects. This holds true for both in-situ data, as well as remote sensing data, although regular observation and large spatial coverage might suggest a fundamental improvement with better availability of remote sensing data.
Secondly, it also addresses the choice of parameters we use to describe the modelled ecosystem. For the representation of vegetation, we could choose, for instance, between parameters such as biomass, aboveground biomass, composition or soil coverage for communities, plant functional types or single species (see study in Negev, and pan-European studies on trait adaptation, and on ecosystem services). Similar choices are made for the abiotic environment (e.g. salinity, temperature, water exchange, see studies on Curian Lagoon and Wadden Sea) and fauna (e.g. population, meta-populations, parts of a population, habitat suitability, see studies on chamois at Gran Paradiso NP or on fin whales in Pelagos).

2: Focus on uncertainties in GCM inputs (e.g. chamois population in Gran Paradiso NP; shifts in vegetation composition, Negev; Curonian Lagoon)

Simulating future climate impacts is particularly difficult, as these studies rely directly on the highly controversial climate inputs (e.g. Frigg et al. 2015). Several of the presented studies address these uncertainties related to future climate data which by themselves are the results of global climate modelling and further refinement in space and

time (by regional climate models or for smaller spatial and temporal resolution by stochastic downscaling) with all their uncertainties (Murphy et al. 2004, Provenzale & Palazzi 2015). For instance, a consistency check between the modelled climate and observed meteorological data for a past period has become a standard. Further, it has become a standard to use several GCM and downscaling products, and then show the range of simulated ecosystem impacts. These impacts can considerably vary, but often show the same qualitative results. However, given the large range in the input data provided by GCMs ecosystem behaviour can also be qualitatively inconsistent over the range of climate inputs. This is then more difficult to interpret, as discussed in the study on vegetation change in the transition zone at Northern Negev.

Out of the twelve ECOPOTENTIAL future simulation studies, three studies do not explicitly report such an uncertainty assessment. Although they discuss uncertainties, mainly due to future climates, results from a quantitative uncertainty assessment are not part of their study. Reasons for that are either to keep the overall complexity of the study to a communicable level (e.g. in the case of the multi-step analysis on the impacts on ESS provision from future plant species distribution), or to at least include some first, preliminary results in this report at this stage of the project although the final uncertainty assessment is not yet performed (e.g. the study on the Wadden Sea, and the Climate Niches of N2000). Both reasons highlight the need for additional technical and computational efforts to conduct uncertainty assessments and to communicate them appropriately.
The decision to avoid these additional efforts is partly because working with the individual GCM requires expertise that is not always available among ecologists and therefore some ecologists prefer using ready products like WorldClim or ClimateEU. Additionally, repeating the entire modelling procedure for each GCM can be computationally demanding, (e.g. running the SDMs just for one climate inputs but for the 235 species took 2 month on an high performance computer cluster (10 nodes with 128 GB each) in the study on impacts on ESS provision; repeating the analysis for each of the 15 GCM separately would take 2.5 years, not including all the post SDMs analyses). Problems in communicating of uncertainties have been recognised in the late 1990s and early 2000s. Especially the IPCC has strongly advanced the methods and standards of communication (Swart et al. 2009). With the systematic Guidance Notes for Lead Authors of Assessment Report Four on Addressing Uncertainties (IPCC 2005), the IPCC laid the foundation to communicate uncertainty in “calibrated language” including the quality of the evidence base and the agreement between different scientific studies. Despite this progress in setting communication standards, the multiple dimensions of uncertainties in climate impact assessments need careful thinking for the elaboration of unambiguous graphs, tables and statistics in individual study.

Finally, we want to address the use of distinct RCPs in the analyses. These RCPs (representative concentration pathways) represent the fundamental uncertainty in estimating the amount of climate relevant treehouse gases in future. The RCPs are externally set and might be realised by different combinations of climate mitigation policies, economic development, technical advances and last but not least by global demographics. They refer to an uncertainty that exceeds methodological and data-induced biases, but indicates the fundamental lack of knowledge on humanity's future development.

Basics for comprehensive uncertainty assessment in climate impact studies

By Leonard A. Smith

Effective Uncertainty Quantification in climate science is challenging. The problem is one of extrapolation, and the time and spatial scales of interest to ECOPOTENTIAL are “virtually never” resolved explicitly by today’s climate models - whatever the ultimate fidelity of these models actually is. In this context, tracking uncertainty is complex

Co-funded by the European Union

even when one stays in model-land. ECOPOTENTIAL practitioners, however, aim to act on our insights in making decisions in the real-world. Part of the problem arises from the wide variety of decisions different practitioners face, and from the various different types of uncertainty that confront them (Smith and Stern 2011). In ECOPOTENTIAL, the focus is on statistical (including those arising from the physics) uncertainty and the notions of Uncertainty Quantification and Uncertainty Guidance giving useful but imperfect simulation models (Berger and Smith 2018). As shown in Figure 57, information is provided on each of the three types of uncertainty included: internal model uncertainty including structural model error, uncertainties in the inputs, and uncertainty in the future scenarios as approximations for principle pathways of how human society might evolve over the next century. For each of these uncertainty types we have data from at least 50% of the ECOPOTENTIAL studies, at most 88%. This is significant progress beyond many studies in the past.

Besides internal uncertainties in the ecological models, climate inputs and scenarios (including technical implementation through different GCMs, downscaling procedures and socio-demographically motivated RCPs) are a major source of uncertainties in climate impact studies. Due to the high availability and use of such data, we provide the basics again to pay respect to their limitations. This becomes particularly important if scientific studies aim to support real-world decision making.

THREE TASK MINIMUM PROGRAMME TO ASSESS UNCERTAINTY

It is important to acknowledge that traditional good practice tools for Uncertainty Quantification in measurement and laboratory science are not appropriate for climate science, as many of those tools simply cannot be applied to the questions being asked in climate science (Berger and Smith 2018). That said, there are three tasks that yield relevant insights and are well doable and applicable for climate impact research.

(1) Give time scales on which the results are likely to be reliable or to fail. Example: “these assumptions are expected to hold quantitatively until 2050, but are expected to fail, making the analysis misleading, well before 2100”. Such a simple statement of the confidence the scientists have in their quantitative results is a crucial start to communicate them to decision makers. Stressing the probability of a “Big Surprise” further helps to make additional uncertainty clear to decision makers.

(2) Test internal consistency of climate input data with the level of consistency stated in clear, intuitive terms. Consider for example a RCM used to downscale GCM output, for each GCM grid point we can compute the total precipitation by summing over relevant RCM grid points. If the mismatch is huge, this can be easily communicated. This is not a question of detailed matching, but rather one of identifying significant mismatches and potential drivers of feedbacks that will limit the distance into the future where the processed model output will be consistent with the driving GCM.

(3) ommunicate the extent to which the levels of uncertainty expressed by the IPCC itself in the AR5, affects the individual climate impact study.

BASICS OF COMMUNICATING UNCERTAINTY

Uncertainty can often be reduced significantly with clearer, systematic writing conventions.

- Make clear, at each use, whether a value corresponds to the outcome of a measurement (an observation, a real-word value) or corresponds to some calculation based on simulation model outputs (a model-value).
- State some form of confidence range for each value provided. Confidence in a calculation is communicated more effectively when it is clearly stated (1) which potential consistency checks have and have not been done,

and/or (2) what magnitude of uncertainty has been suggested by those which have been done (expressed in the units relevant to the current study).

- Discuss the Relevant Dominate Uncertainty (Smith and Peterson, 2099) and the time scales on which it makes the reported simulations/predictions misleading.
- Provide expert opinion on magnitude and timescales on Known Neglects and Known Unknowns. Known Neglects are phenomena of boundary conditions known to be important, but not included in the models for practical (usually computational) reasons. Known Unknowns are factors that are known to exist but not quantifiable for simulation (Curry and Weber 2011). Ideally, the experimental design of the simulations would allow information on the potential impacts of these phenomena, to inform the experts interpreting it from model-land into the real-world. When lacking information on model diversity, expert opinion becomes an even more critical component for informed decision-making.

References

Berger, J. and Smith, L.A. (2018). *Uncertainty quantification.* Annual Review of Statistics and Its Application. ISSN 2326-8298 (In Press).

Curry, J. A., and Webster, P. J. (2011). Climate science and the uncertainty monster. *Bulletin of the American Meteorological Society,* 92(12), 1667-1682. doi: 10.1175/2011BAMS3139.1

Smith, L.A. and Petersen, A. (2014). Variations on reliability: connecting climate predictions to climate policy. In: Boumans, Marcel and Petersen, Arthur and Hon, Giora, (eds.) Error and uncertainty in scientific practice. History and philosophy of technoscience (1). Pickering & Chatto Publishers, London, UK, 137-156. ISBN 978184893416

Smith, L. A., & Stern, N. (2011). Uncertainty in science and its role in climate policy. *Phil. Trans. R. Soc. A*, *369*(1956): 4818-4841.

References

Donges, J.F., Heitzig, J., Barfuss, W., Kassel, J.A., Kittel, T., Kolb, J.J., Kolster, T., Müller-Hansen, F., Otto, I.M., Wiedermann, M. and Zimmerer, K.B. (2018). Earth system modelling with complex dynamic human societies: the copan: CORE World-Earth modeling framework. *Earth System Dynamics Discussions*, pp.1-27.

Frigg, R., Smith, L.A. and Stainforth, D.A. (2015). An assessment of the foundational assumptions inhigh-resolution climate projections: the case of UKCP09 Synthese, 192 (12). 3979-4008. ISSN 1573-0964.

Hamann, A. and Wang, T., Spittlehouse, D.L., and Murdock, T.Q. (2013). A comprehensive, high-resolution database of historical and projected climate surfaces for western North America. *Bulletin of the American Meteorological Society* 94: 1307–1309. (ClimateEU available under: https://sites.ualberta.ca/~ahamann/data/climateeu.html).

Hassol, S.J., 2008. Improving how scientists communicate about climate change. *Eos, Transactions American Geophysical Union*, *89*(11): 106-107.

IPCC (2005). Guidance note for lead authors of AR5 on addressing uncertainties: http://www.ipcc-wg2.awi.de/guidancepaper/uncertainty-guidance-note.pdf

IPCC (2013). Climate Change (2013). The Physical Science Basis. Contribution of Working Group I to the Fifth Assessment Report of the Intergovernmental Panel on Climate Change [Stocker, T.F., D. Qin, G.-K. Plattner, M. Tignor, S.K. Allen, J. Boschung, A. Nauels, Y. Xia, V. Bex and P.M. Midgley (eds.)]. Cambridge University Press, Cambridge, United Kingdom and New York, NY, 1535 pp.

IPCC (2012). Managing the Risks of Extreme Events and Disasters to Advance Climate Change Adaptation. A Special Report of Working Groups I and II of the Intergovernmental Panel on Climate Change [Field, C.B., V. Barros, T.F. Stocker, D. Qin, D.J. Dokken, K.L. Ebi, M.D. Mastrandrea, K.J. Mach, G.-K. Plattner, S.K. Allen, M. Tignor, and P.M. Midgley (eds.)]. Cambridge University Press, Cambridge, UK, and New York, NY, USA, 582 pp.

Murphy, J.M., Sexton, D.M., Barnett, D.N., Jones, G.S., Webb, M.J., Collins, M. and Stainforth, D.A. (2004). Quantification of modelling uncertainties in a large ensemble of climate change simulations. *Nature*, *430*(7001): 768.

Provenzale, A. and Palazzi, E., (2015). Assessing climate change risks under uncertain conditions. In *Engineering Geology for Society and Territory-Volume 1*: 1-5. Springer, Cham.

Peters, D. P., Pielke, R. A., Bestelmeyer, B. T., Allen, C. D., Munson-McGee, S., Havstad, K. M. (2004). Cross-scale interactions, nonlinearities, and forecasting catastrophic events. *Proceedings of the National Academy of Sciences*, *101*(42): 15130-15135.

Soranno, P. A., Cheruvelil, K. S., Bissell, E. G., Bremigan, M. T., Downing, J. A., Fergus, C. E., Filstrup, C.T., Henry, E.N., Lottig, N.R., Stanley E.H., Stow, C. A., Tan, P.-N., Wagner, T., Webster, K.E. (2014). Cross-scale interactions: quantifying multi-scaled cause–effect relationships in macrosystems. *Frontiers in Ecology and the Environment*, *12*(1), 65-73.

Swart, R., Bernstein, L., Ha-Duong, M. and Petersen, A. (2009). Agreeing to disagree: uncertainty management in assessing climate change, impacts and responses by the IPCC. *Climatic change*, *92*(1-2): 1-29.

Co-funded by the European Union

5. Conclusion

Questions on how climate change will impact species distributions, habitat compositions or the provision of ESS are not only relevant for scientific purposes but also are urged to be answered for practical adaptation measures.

This documentation of selected ECOPOTENITAL studies reflects not only on the diverse outputs in simulating these future ecological processes, but furthermore focuses on the technical realities behind these analyses. For one, the studies demonstrate nicely, how the impacts of climate change are highly heterogeneous depending on the regarded biological and spatial scale as well as on the biogeographical region. Secondly, the documentation also shows that the studies are aware of the divers uncertainties that are inherent in climate-based future simulations of complex systems. With a common modelling protocol, ECOPOTENTIAL laid out a frame for their study implementations. However, realities show that this standardisation cannot always be met, e.g. due to computational limitations in accounting for the entire GCM Ensemble.

To provide decisive answers on future ecological states therefore is a highly sensitive topic. Depending on the question, appropriate scales and a sound methodological approach have to be defined to get meaningful results. But even with the incorporation of these requirements and a comprehensive uncertainty quantification, uncertainties persist – either through existing model simplifications or the (climate) input data and scenario choice. Here, modellers can only go so far as to thoroughly check the completeness, consistency and plausibility of the input datasets. For subsequent communication purposes and potential practical decision-making the scientists lastly have to transparently elaborate on the remaining uncertainties and the limitations of the result interpretation. With our basic guidance on this topic we provide minimum requirements for acknowledging and communicating these uncertainties.

Keeping this in mind, ecological models are an essential tool to simulate possible future ecosystem states, or to provide insights on the availability of ESS that are essential for human wellbeing. Furthermore, consistent ecological modelling can provide valuable information for the monitoring of ecosystem or land cover changes, adding to monitoring conducted by remote sensing or in-situ assessments. This topic will be further discussed in the upcoming Deliverable 8.5.

Co-funded by the European Union

6. Appendix

A5.1: Common modelling protocol (as explained in detail in Deliverable 8.1)

GCMs	RCM	Downscaled by CNR	RCPs	Time period
EC-Earth, CNRM-CM5, IPSL-CM5A-MR, HadGEM2-ES, MPI-ESM-LR (CMIP5)	RCA4 (Euro-CORDEX)	Precipitation: stochastically downscaled using RainFARM Temperature: downscaling based on orographic correction (using the atmospheric temperature lapse rate)	RCP4.5 RCP8.5	1970-2100